Characterizing the role of Stromal Cell Derived Factor 2 Like-1 (SDF2L1) in Pancreatic β-Cells

by

Akansha Tiwari

A thesis submitted in conformity with the requirements

for the degree of Master of Science

Department of Physiology

University of Toronto

ABSTRACT

Akansha Tiwari

Master of Science (2011)

Graduate Department of Physiology

University of Toronto

CHARACTERIZING THE ROLE OF STROMAL CELL DERIVED FACTOR 2 LIKE-1 (SDF2L1) IN PANCREATIC β-CELLS

Type 2 diabetes is characterized by insulin resistance and pancreatic β-cell failure. Insulin resistance leads to increased insulin demand, which can lead to increased proinsulin misfolding in the endoplasmic reticulum (ER). The accumulation of the misfolded proteins in the ER can cause ER stress, which can lead to pancreatic β-cell dysfunction. Cells respond to ER stress by the unfolded protein response (UPR), which increases protein folding capacity and causes degradation of misfolded proteins. Using a pancreatic β-cell model of induced misfolded proinsulin expression (proinsulin-C96Y tagged with GFP) we discovered that one of the most highly induced genes was stromal cell-derived factor 2 like 1 (SDF2L1). SDF2L1 is an ER localized soluble protein with an as yet unknown function. In this thesis I examined the potential role of SDF2L1 in pancreatic β-cells in ER stress conditions.

ACKNOWLEDGMENTS

First and foremost, I would like to thank my supervisor, Dr. Allen Volchuk, for his guidance, support, and confidence during my two years as a Master of Science student. His constant motivation and constructive criticism has allowed me to mature as a researcher and his efforts have strengthened my knowledge and interest in the field of diabetes. Furthermore, Dr. Volchuk has served as a role model with his professionalism, knowledge, and ability to balance his responsibilities as a scientist and a teacher. These are attributes I hope to also achieve in my career. I would also like to thank my supervisory committee members, Dr. William Trimble and Dr. Adria Giacca, for their valuable insight and direction. The success of my project could not have been possible without their critical evaluations and insightful suggestions.

I would like to thank past and present members of the Volchuk lab for all their support and assistance: Liling Zhang, Ravi Vellanki, Irmgard Schuiki, Tracy Teodoro, Taila Hartley, and Madura Siva. Liling, thank you for always being very patient with me when I showered you with endless questions about lab techniques. Ravi, thank you for all your advice and lectures, which helped me stay on track with my experiments. Irmgard, you are an amazing person and I have learned to be very calm and collected in stress situations from you. Tracy, thank you for exposing me to the finer things in life and always keeping me on my toes. Madura, thank you for always being so full of life and being my fellow herbivore. You are crazy and I miss you. I also want to thank Kathrin Dettman for all her help and inspiration. Thanks to all of you for making my graduate studies memorable. I also want to thank the other members of the floor, and all my friends for their love and support. Lastly, I am thankful to my family, Mama, Papa, Mini, Vyom and Akshat for their patience and tireless efforts to provide moral support. Love you guys!

TABLE OF CONTENTS

LIST OF PUBLICATIONS AND PRESENTATIONS

(i) Project Specific Publications

- Tiwari, A., Schuiki, I., and Volchuk, A. Stromal Cell Derived Factor 2-Like 1 in involved in mutant proinsulin degradation in pancreatic β-cells. *Manuscript in preparation.*

(ii) Project Specific Poster Presentations

"Elucidating the Role of SDF2L1 in ER Stress in Pancreatic β-cells" poster presented at:

- Banting and Best Diabetes Centre Scientific Day on May 13, 2011, at The Old Mill Inn, Toronto
- Canada Research Chairs Conference on November 25-25, 2010, in Metro Toronto Convention Centre, Toronto
- 5th Annual Canadian Society of Life Science Research conference on August 13-15, 2010, in Montreal
- Banting and Best Diabetes Centre Scientific Day on May 13, 2010, at The Old Mill Inn, Toronto

(iii) Project Specific Oral Presentations

- "Elucidating the Role of SDF2L1 in ER Stress in Pancreatic β-cells" presented at Frontiers in Physiology on April 8, 2011, at Medical Sciences Building, University of Toronto
- "The Role of SDF2L1 in Pancreatic β-cells" presented at Frontiers in Physiology on April 15, 2010, at Medical Sciences Building, University of Toronto

LIST OF FIGURES

CHAPTER 6. APPENDIX

LIST OF ABBREVIATIONS

AAA+	ATPases Associated With Diverse Cellular Activities +
ANOVA	Analysis Of Variance
ATF4, ATF6	Activating Transcription Factor 3,4,6
ATP	Adenosine Triphosphate
ATZ	3-Amino-1,2,4-Triazole
ASK1	Apoptosis Signal Regulating Kinase-1
Bak	Bcl-2 Homologous Antagonist/ Killer
Bax	Bcl-2 Associated X-Protein
BiP	Immunoglobulin Heavy Chain Binding Protein Zip
BPTI	Bovine Pancreatic Trypsin Inhibitor
Ca2+	Calcium
CC3	Cleaved Caspase 3
CC12	Cleaved Caspase 12
cDNA	Complementary Deoxyribonucleic Acid
CFTR	Cystic Fibrosis Transmembrane Conductance Regulator
CHOP	CAAT/Enhancer Binding Protein (C/EBP) Homologous Protein
chx	Cycloheximide
cnx	Calnexin
CPY	Carboxypeptidase Y
CRT	Calreticulin
CSSR	Core Stress Sensing Region
Derlin-1	Degradation In Endoplasmic Reticulum Protein 1
Dox	Doxycyline
DMEM	Dulbecco's Modified Eagle Medium
DSP	Dithiobis(Succinimidyl Propionate)
DTT	Dithiothreitol
EGFP	Enhanced Green Fluorescent Protein
EDEM	ER Degradation Enhancing Mannosidase Like Protein
eIF2α	Eukaryotic Translation Initiation Factor 2 A
ER	Endoplasmic Reticulum
ERAD -C,-L, -M	Endoplasmic Reticulum Associated Degradation - (Cytosolic, Luminal, Membrane-Spanning Domain)
Ero 1	ER Oxidoreductin 1
FBS	Fetal Bovine Serum
FFA	Free Fatty Acid
G418	Geneticin
GADD34	Growth Arrest And DNA Damage 34
GFP	Green Fluorescent Protein
GRP78	Glucose-Regulated Protein 78
GRP94	Glucose-Regulated Protein 94
GRP170	Glucose-Regulated Protein 170
GRP194	Glucose-Regulated Protein 194
HEK	Human Embryonic Kidney
HEPES	4-(2-Hydroxyethyl)-1-Piperazineethanesulfonic Acid

HERP	Homocysteine-Responsive ER-Resident Protein
HeLa	Henrietta Lacks (HELA) Immortal Cells
Hrd1	HMG-Coa Reductase Degradation Protein 1
Hsp70, HSP 40	Heat Shock Protein 70, 40
IAP	Inhibitor Of Apoptosis
IGF1	Insulin-Like Growth Factor 1
IgG	Immunoglobulin G
IP	Immunoprecipitation
IP_3	Inositol 1,4,5-Trisphosphate
IRE1	Inositol Requiring Enzyme 1
JNK	C-Jun N-Terminal Kinases
KD	Knock-Down
KRBH	Krebs-Ringer Bicarbonate With HEPES
LSC	Liquid Scintillation Counting
MHC	Major Histocompatibility Complex
MIR	Mannosyltransferases, Inositol 1,4,5-Trisphosphate Receptors And Ryanodine Receptors
mRNA	Messenger RNA
NEFA	Non-Esterified Free Fatty Acid
Npl4	Nuclear Protein Localization Protein 4
OST	Oligosaccharyltransferase
P97/VCP	P97/ Valosin Containgin Protein
PBS	Phosphate Buffered Saline
PCR	Polymerase Chain Reaction
PDI	Protein Disulfide Isomerase
PERK	Protein Kinase RNA (PKR)-Like ER Kinase
PFA	Paraformaldehyde
POFUT1	Protein O-Fucosyltransferase 1
POMTs	Protein O-Mannosyltransferases
PPI	Peptidyl-Propyl Cis-Trans Isomerases
PP1c	Protein Phosphotase (PP) 1c
RIA	Rat Insulin Radioimmunoassay
ROS	Reactive Oxygen Species
RRP1B	Ribosomal RNA Processing 1 Homolog B
RPMI	Roswell Park Memorial Institute Medium
Ryr	Ryanodine Receptor
S1P, S2P	Site 1 Protease, Site 2 Protease
SDF2L1	Stromal Cell Derived Factor 2 Like 1
SDS-PAGE	Sodium Dodecyl Sulfate-Polyacrylamide Gel Electrophoresis
Ser	Serine
SERCA	Sarco/Endoplasmic Reticulum Ca2+-ATPase
siRNA	Short Interfering RNA
Stau	Staurosporin
Tg	Thapsigargin
Thr	Threonine
Tm	Tunicamycin

TNF	Tumor Necrosis Factor
TRAF2	Tumor Necrosis Factor (TNF) Receptor-Associated Factor 2
UBL	Ubiquitin-Like Domain
UBX	Ubiquitin Regulatory X Domain
Ufd1	Ubiquitin-Fusion Degradation-1
UGGT	UDP-Glc:Glycoprotein Glucosyltransferase
UPR	Unfolded Protein Response
UPS	Ubiquitin Proteasome System
VIMP	Valosin-Containing Protein-Interacting Membrane Protein
VSVG	Vesicular Stomatitis Virus Glycoprotein
WFS 1	Wolfram Syndrome 1
WRS	Wolcott-Rallison Syndrome
XBP 1	X-Box Binding Protein-1

CHAPTER 1. INTRODUCTION

This thesis will focus on elucidating the role of Stromal Cell-Derived Factor 2 Like-1 (SDF2L1) in pancreatic β-cells. This chapter will provide a basic introduction to ER function under normal and stressed conditions, the cell-survival pathways involved in the management of ER-stress, ER-associated degradation (ERAD) and apoptosis resulting from chronic ER stress. A brief overview of ER-stress induced β-cell dysfunction and its relation to type II diabetes will also be provided. Finally, a detailed review of current literature available on SDF2L1 will be discussed.

1.01 The Endoplasmic Reticulum

The Endoplasmic Reticulum (ER) is a cellular organelle responsible for lipid and protein production, calcium storage and signaling (Berridge 2002). About one-third of all cellular proteins (both membrane and secretory proteins) are translated on ER bound ribosomes. During synthesis secretory proteins are translocated into the ER lumen, where they are post-translationally modified and folded (Kaufman 2010). Protein modification includes N-glycosylation and disulfide bond formation, which assists in the formation of a properly folded state (Pilon 1998). These reactions are mediated by ER-resident proteins, which include protein folding chaperones (discussed in section **1.02**), which maintain proteins in a folding-competent state (Kaufman 1999). In addition, the ER provides an oxidizing environment that allows disulfide bond formation (Gething 1992). Disulphide bonds are formed by protein disulphide isomarases (PDI), which are oxidized by Ero1 and other molecules (Jessop 2009). Only proteins that are properly folded and modified can exit the ER and those that do not are targeted for ER-Associated Degradation (ERAD) (discussed in section **1.04**) (Ellgaard 2003; Schröder 2005; Brodsky 2007).

In addition to protein folding, the ER is also responsible for signal transduction via calcium release. The SERCA calcium ATPase maintains a calcium gradient in the resting ER by continuously pumping calcium from the cytosol into the ER lumen, while IP_3 and ryanodine receptors allow for calcium release from the ER (Berridge 2002). Due to the ability of the ER to store and secrete Ca^{2+}, it is responsible for several cellular functions including organogenesis, transcription, stress responses, and apoptosis. The relatively high ER lumen Ca^{2+} levels (100-500μM) are also necessary for efficient function of protein folding chaperones in the ER. Many chaperone proteins such as calnexin (cnx), calreticulin (crt), GRP78/BiP, among others are calcium binding proteins, which is essential for their function. Thus a decline in luminal Ca^{2+} levels can lead to the accumulation of misfolded and unfolded proteins (Berridge 2002; Schröder 2005). An increase in misfolded or unfolded proteins can also result from disruption of ER redox state, protein mutations or inhibition of protein glycosylation (Kaufman 1999). If the levels of unfolded polypeptides exceed the folding capacity of the ER, this creates a state of ER stress. This leads to activation of the unfolded protein response (UPR) (**Figure 1.1**) to compensate for the reduced folding capacity (Ron 2007).

The UPR alleviates ER stress by three distinct effects; 1) a transient translational attenuation to reduce overall ER protein folding demand; 2) increased transcription of UPR genes including ER chaperones to increase the folding capacity of the ER, and 3) an increase in ERAD components and ERAD capacity to remove irreversibly misfolded proteins from the ER lumen. If the cell protective changes of the UPR are not sufficient to reduce the levels of misfolded, unfolded or aggregated proteins, then apoptosis is activated leading to cell death. ER stress and the UPR will be discussed further in Section **1.03**.

1.02 Molecular Chaperones of the ER

1.02.1 Calnexin and Calreticulin

The Calnexin (cnx) and Calreticulin (crt) chaperones are responsible for interacting with and assisting the folding of glycosylated proteins. As polypeptides are cotranslationally translocated into the ER, they are glycosylated with the preassembled $Glc_3Man_9GlcNAc_2$ at the Asn residue of Asn-X-Ser(Thr) sequence by oligosaccharyltransferase (OST). The oligosaccharides are further processed by glucosidase I and II, which remove the terminal glucoses generating a $GlcMan_9GlcNAc_2$ moiety in the folding substrate that is recognized by lectin proteins crt and cnx. Crt (an ER lumen protein) is a calcium-binding protein that also functions as a chaperone for glycosylated proteins. Cnx (a type 1 membrane protein) is a lectin protein homologous to crt, which also binds nascent glycosylated proteins to insure their proper folding. If the protein is adequately folded, the terminal glucose in the substrate can be cleaved by glucosidase II removing the cnx/crt binding site (Trombetta 1992). If, however, the protein folds incorrectly, ER-resident UDP-Glc:glycoprotein glucosyltransferase (UGGT) binds unfolded regions of nascent glycoproteins and adds a single glucose from UDP-glucose to the deglucosylated glycan at the N-linked Man9-GlcNAc2 glycan (Määttänen 2010). This provides the binding site for chaperone proteins cnx/crt and allows further attempts at the substrate folding (Taylor 2003). If the glycoprotein folds appropriately, the protein is secreted. If, however, the proteins fails to fold the cycle repeats till the protein is able to fold or is targeted for degradation (Meunier 2002).

Proteins that cannot be efficiently folded by cnx/ crt, are processed by ER-mannosidase (Mns1) and get degraded by the ERAD machinery. This will be discussed in detail in section **1.04**.

1.02.2 GRP78/BiP

GRP78/BiP was identified as an ER-localized protein that bound to immunoglobulin heavy-chains in the absence of a light chain in pre-B lymphocytes thereby inhibiting the secretion of misfolded immunoglobulins (Haas 1983). It was also independently identified as a glucose-deprivation induced protein in virally transformed cells, and thus categorized as a glucose-regulated protein (GRP) (Lee 1987).

GRP78/BiP, an HSP70 molecular chaperone located in the ER lumen, binds newly-synthesized proteins and maintains them in a state competent for subsequent folding and oligomerization. GRP78/BiP contains an N-terminal ATPase and a C-terminal substrate binding domain (Määttänen 2010). In the ATP bound form, GRP78/BiP binds substrates with low affinity. However, substrate binding stimulates the ATPase activity and allows high affinity binding capacity of GRP78/BiP (Gething 1999). ATP hydrolysis causes a conformational change of the ADP-bound GRP78/BiP and leads to release of substrate (Meunier 2002). The ATP hydrolysis is regulated by co-chaperones such as the DNAJ domain-containing proteins (Walsh 2004; Schröder 2005). GRP78/BiP associates with nascent peptides transiently and immediately, however, it has prolonged association with misfolded proteins (Hammond 1994). It preferentially binds peptides containing a subset of aromatic and hydrophobic amino acids in alternating positions in folding intermediates (Blond-Elguindi 1993). The ATPase activity of GRP78/BiP is stimulated by hydrophobic amino acids (Blond-Elguindi 1993). It interacts with hydrophobic patches on folding intermediates and maintains them in a folding-competent state.

GRP78/BiP allows the solubilization of aberrant proteins by retaining them in the ER and maintaining them in a retrotranslocation-competent state since GRP78/BiP deletion leads to stabilization and aggregation of mutant pro-alpha-factor and carboxypeptidase Y (Nishikawa

2001). In addition, GRP78/BiP is important in immunoglobulin folding and thus IgGs are an excellent model for studying the chaperone's activity. GRP78/BiP remains bound to the heavy chain in the absence of light chain synthesis since heavy chains do not fold until light chains have folded and are released from GRP78/BiP. Upon release form GRP78/BiP, the heavy chain folds rapidly and forms disulfide bonds. Misfolded L-chain immunoglobulin, when artificially retained in the ER, does not get degraded suggesting the importance of GRP78/BiP recognition and solubilization of folding intermediates and misfolded proteins (Knittler 1995).

GRP78/BiP is found in complex with several other ER-resident proteins including foldases such as PDIs and peptidyl-propyl cis-trans isomerases (discussed below), and may work in coordination with other chaperones such as cnx/ crt (Mayer 2000). In the 2002 study by Meunier *et al*, 35S-methionine trans-labeling and DSP cross-linking was used to demonstrate that various chaperones are part of the heavy chain-GRP78/BiP complex, including GRP94, PDIs, Hsp40 co-chaperones, GRP170, ERp72, cyclophilin B, UGGT and SDF2L1. However, cnx and crt were absent from this complex or only present in small quantities. It is possible that the two chaperone systems (cnx/crt and GRP78/Hsp40) may have a spatial separation accounting for their temporal interactions with misfolded glycoproteins as observed in some studies discussed in the following section (Meunier 2002). GRP78/BiP is also induced by ER-stress as part of the UPR, which will be discussed in section **1.03**.

1.02.3 Other chaperones and Protein Disulfide Isomerases

As previously mentioned, chaperones are often found in complexes and the two chaperone systems may work together for glycosylated protein folding. GRP78/BiP and cnx can both fold non-glycosylated proteins efficiently *in vitro* (Stronge 2001). In fact, some cnx/crt

substrates are initially bound to GRP78/BiP when N-linked glycosylation is blocked (Meunier 2002). However, cnx is more efficient at folding glycosylated proteins than GRP78/BiP due to its lectin site. In the 1994 study by Hammond and Helenius, biosynthetic labeling was used to study the interactions of GRP78/BiP and cnx with vesicular stomatitis virus (VSV) glycoprotein (G protein). In that study, GRP78/BiP was found to interact with early folding intermediates of VSV G protein, while cnx was required for the efficient folding and retention of the functional protein (Hammond 1994). Furthermore, in the 2003 study by Caramelo *et al*, it was demonstrated that GRP78/BiP recognizes linear glycoproteins, while UGGT preferentially binds globule-like structures (Caramelo 2003). Therefore, it is possible that the two chaperone systems recognize folding intermediates at different stages of folding, thus working together to fold both glycosylated and non-glycosylated proteins.

Other chaperones and co-chaperones in the ER are also found in complex with GRP78/BiP. GRP94 associates with folding intermediates through its N-terminus peptide-binding site and is likely regulated by co-chaperones through ATP hydrolysis (Wearsch 1997). Meanwhile, peptidyl-propyl cis-trans isomerases (PPIs) allow cis-trans isomerization of proline residues thereby expediting the protein folding process. For example, cyclophilin B is a PPI that allows IgG folding in vivo in COS-1 cells (Feige 2009).

Protein Disulphide Isomerases (PDIs) are one of the most abundant ER proteins which function to oxidize, reduce and isomerize disulfide bonds. PDIs are part of a protein family containing 20 related proteins with ER retention motifs and thioredoxin-like domains (Määttänen 2010). PDIs have substrate specific binding domains, which allow them to function specifically as oxidases, reductases, isomerases and/or chaperones (Jessop 2009). PDIs work together with GRP78/BiP thereby allowing proper folding of substrate proteins. GRP78/BiP and PDI act

synergistically in the *in vitro* folding of the denatured and reduced F_{ab} fragment (Mayer 2000). GRP78/BiP binds the unfolded polypeptide chains and keeps them in a conformation in which the cysteine residues are accessible for PDI for disulfide bond formation. PDIs are also necessary for maintaining ER homeostasis. Disruption of disulfide bonds with reducing agents such as dithiothreitol (DTT) leads to an accumulation of misfolded proteins and an induction of the ER stress response.

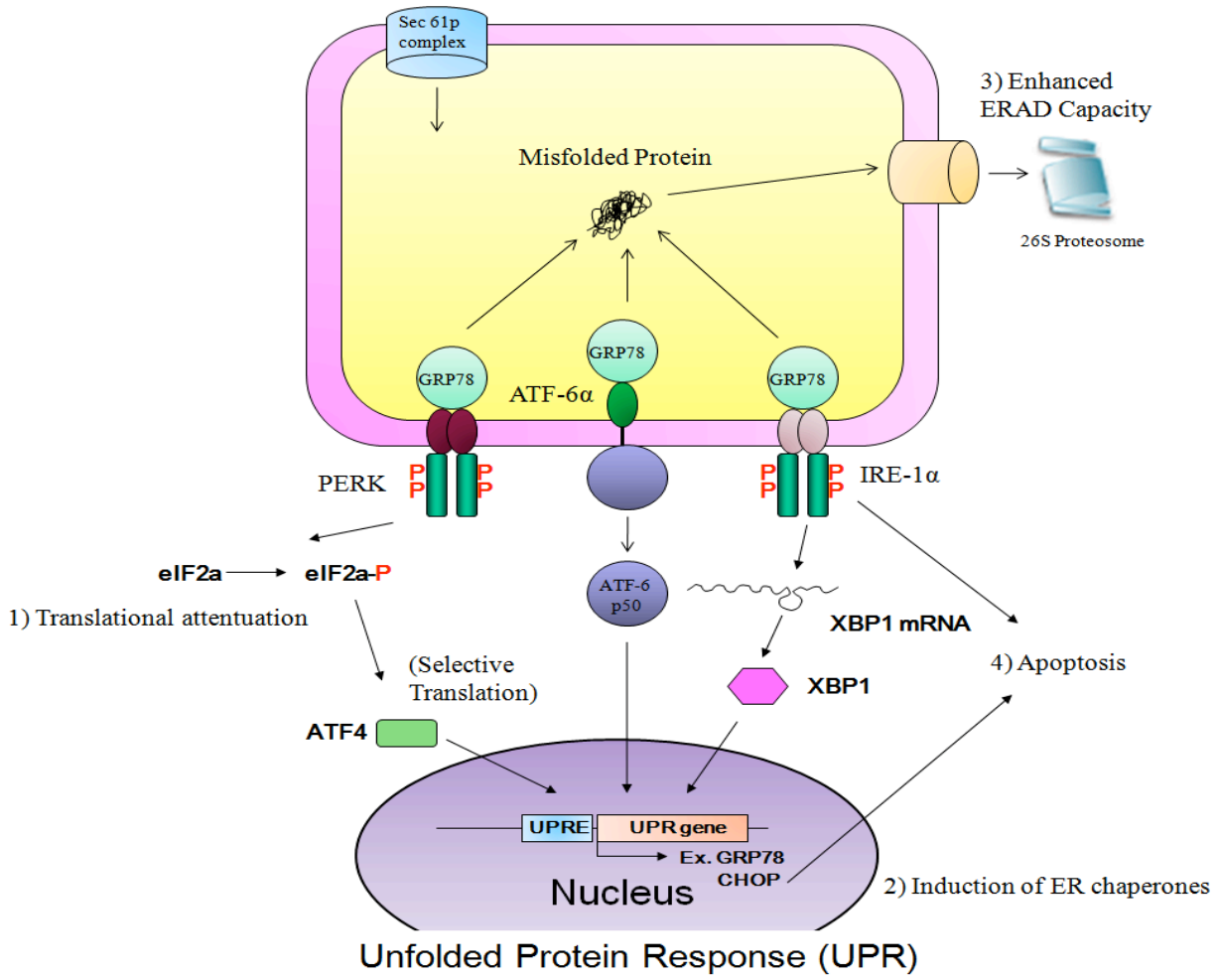

L,Figure 1.1: The Unfolded Protein Response (UPR). As misfolded/unfolded or aggregated proteins accumulate in the ER lumen causing ER stress, three transmembrane signal transducer proteins, IRE-1, PERK and ATF-6, activate the unfolded protein response (UPR). The UPR aims to alleviate ER-stress through 3 distinct effects: 1) translational attenuation, 2) transcriptional induction of various genes such as chaperones, and 3) increased ER Associated Degradation (ERAD) capacity to eliminate misfolded proteins. If however, ER-stress persists apoptosis 4) is induced. Upon release from GRP78/BiP and subsequent association with misfolded proteins, PERK and IRE-1 oligomerize and trans-autophosphorylate. Activated PERK phosphorylates eIF2α, leading to translational attenuation and reduced transcriptional load in the ER. The ATF-4 mRNA, however, is selectively translated and activates the UPR target genes including CHOP. Activated IRE-1 cleaves XBP-1mRNA, which gets translated and acts as a transcription factor for activating UPR target genes including ERAD genes. ATF-6 upon release from GRP78/BiP is trafficked to the Golgi where its cytosolic fragment is cleaved. The cleaved p50 fragment acts as a transcription factor to further activate the UPR responsive genes including chaperones. If chronic and severe ER stress persists, the UPR signal can result in apoptosis. Figure adapted from Oyadomari S, Koizumi A, Takeda K, Gotoh T, Akira S, Araki E, Mori M. (2002). Targeted disruption of the Chop gene delays endoplasmic reticulum stress-mediated diabetes. *J Clin Invest.*; **109**(4):525-32.

1.03 ER Stress and the Unfolded Protein Response (UPR)

When the concentration of chaperones in the ER is insufficient to fold and process secretory proteins, unfolded and misfolded proteins accumulate in the ER, creating a state of ER-stress and leading to the activation of the UPR (**Figure 1.1**) (Nishikawa 2005). The UPR decreases ongoing protein synthesis, and upregulates key chaperones that attempt to improve the protein folding and degradative capacity of the ER. If the homeostasis is not re-established then cell death pathways are triggered. The UPR is defined by 3 distinct arms represented by the ER-stress sensor proteins inositol-requiring protein-1 (IRE-1), activating transcription factor-6 (ATF-6) and protein kinase RNA (PKR)-like ER kinase (PERK) (Ron 2007).

1.03.1 IRE-1

IRE-1α was initially identified in yeast by a screen for mutations that block the activation of the UPR (Ron 2007). There are two isoforms of IRE-1 in mammals; IRE-1α is expressed in most cells, while IRE-1β expression is restricted to intestinal epithelial cells (Eizrik 2008). IRE-1α is an ER resident type 1 transmembrane protein with Ser/Thr kinase activity in the cytoplamic domain.

Under ER stress conditions, IRE-1α can be activated by unfolded proteins directly and/or by release of chaperone GRP78/BiP from the luminal portion of the protein causing it to oligomerize and trans-autophosphorylate (Määttänen 2010). In yeast, it has been shown that GRP78/BiP release from the IRE-1α luminal domain leads to its partial activation, while the binding of misfolded protein to the core stress sensing region (CSSR) of IRE-1α allows a conformational change in its cytosolic domains leading to its complete activation (Kimata 2007).

Autophosphorylation activates the endoribonuclease activity of IRE-1α leading to the cleavage of 26 nucleotides from the X-Box Binding Protein-1 (XBP-1) mRNA. The spliced form of XBP-1 mRNA is translated and translocates to the nucleus where it acts as a transcription factor for UPR target genes. The unspliced form of XBP-1 is also translated and acts as an inhibitor of the spliced form thereby reducing the activation of the UPR genes. It may function as a negative regulator of spliced XBP-1 (Ron 2007).

IRE-1α may also degrade ER-client mRNAs thereby decreasing the ER translational load (Eizrik 2008). Recent research has shown IRE-1α mediated degradation of ER-associated mRNAs in an XBP-1 independent manner (Ron 2006). ER stress was induced using DTT in Drosophila S2 cells depleted of either IRE-1α or XBP-1 by RNA interference. The expression profile of approximately 5000 genes was performed using microarray analysis. The findings suggested a significant overlap between the IRE-1α and XBP-1 knock down (KD) conditions in the expression of genes related to ER protein folding, glycosylation, protein-trafficking and lipid metabolism. However, a cluster of genes was observed which were repressed only with IRE-1α and not with XBP-1 KD. Repression was mainly observed for genes related to secretory proteins and plasma membrane proteins. The IRE-1α mediated cleavage of mRNAs that are not required for ER function, in conjunction with the PERK pathways discussed below, acts as the initial mechanism to reduce ER transcriptional load and releases the translational machinery for subsequent up-regulation of other UPR target genes (Hollien 2006).

IRE-1α can also activate the stress-induced c Jun N-terminal kinase (JNK) protein and interacts with components of the cell-death machinery such as cleaved caspase 12 independently of RNase activity (Ron 2007). In ER stress conditions, IRE-1α senses ER-stress through its

luminal domain and recruits TRAF 2 to the ER membrane (Nishitoh 1998; Urano 2000). The IRE-1α-TRAF 2 complex activates apoptosis signal regulating kinase-1 (ASK-1), which allows JNK activation (Nishitoh 1998). Upon activation, JNK phosphorylates transcription factors cJUN or activation protein-1 family and eventually initiates apoptosis (Yoneda 2001). Alternatively, in ER stress conditions, the IRE 1-TRAF 2 complex also interacts with procaspase 12, and allows their clustering and activation (Nakagawa 2000; Morishima 2004). Cleaved caspase 12 in turn activates caspase 9, and consequently activates a caspase cascade resulting in apoptosis (Rao 2002).

1.03.2 PERK

PERK, like IRE-1, is an ER-resident type 1 transmembrane protein with luminal sensing domains and cytosolic kinase domains (Ron 2007). Upon activation by release from chaperone protein GRP78/BiP or possibly by binding to unfolded/ misfolded proteins directly, PERK oligomerizes and trans-autophosphorylates. This leads to PERK mediated phosphorylation of the α subunit of eukaryotic translation initiation factor 2 (eIF2α) at Ser51, resulting in translational attenuation (Scheuner 2001). PERK mediated phosphorylation of eIF2α inhibits the 80S ribosome assembly and protein translation thereby decreasing the ER protein load. The activation of PERK, however, is tightly controlled in ER stress conditions since PERK de-phosphorylation occurs within minutes of restored ER homeostasis (Bertolotti 2000).

Phosphorylation of eIF2α promotes general translational repression, but under such conditions the translation of the ATF-4 mRNA is enhanced. ATF-4 is a transcription factor that induces various genes as part of the UPR (Harding 2003). ATF-4 regulates genes involved in amino-acid transport, glutathionine biosynthesis and resistance to oxidative stress. ATF-4 also

induces the expression of the transcription factor CAAT/Enhancer binding protein (C/EBP) homologous protein (CHOP/ GADD153) (Scheuner 2001). ATF-4 mediated activation of CHOP leads to the transcription of growth arrest and DNA damage 34 (GADD34) protein, which interacts with the catalytic subunit of protein phosphotase (PP) 1c to de-phosphorylate eIF2α (Eizrik 2008). This results in the regulation of the PERK/eIF2α/ATF-4 by a negative feedback loop.

CHOP is also a transcriptional repressor that can inhibit the expression of pro-survival Bcl-2, thereby inducing mitochondrial death signaling cascade leading to cell death (Alberts 2002; Rao 2004). Thus, under unresolvable ER stress CHOP can contribute to ER stress-induced cell apoptosis.

1.03.3 ATF-6

ATF-6 was identified as a protein bound to the UPR activated promoter element (Haze 1999). There are two isoforms of ATF-6, ATF-6α and ATF-6β, which are ubiquitously expressed type II transmembrane proteins. Most ER-stress related studies have focused on ATF-6α, which will be further discussed here. ATF-6α is a 90kDa bZIP glycoprotein with a central hydrophobic stretch. The cytosolic N-terminal domain contains a basic leucine zipper motif and transcriptional activation domains. ATF-6α is activated upon the release of GRP78/BiP under ER-stress conditions and by post-translational modifications such as disulphide bond reduction. ATF-6α activation leads to its translocation to the Golgi where it is cleaved by site 1 protease (S1P) and site 2 protease (S2P) to release a 50kDa protein (Eizrik 2008). This cytosolic DNA binding N-terminal fragment (ATF-6 p50) translocates to the nucleus and binds the ER stress response element CCAAT(N)9CCACG in genes encoding molecular chaperones, thereby

increasing the folding capacity of the ER in cooperation with spliced XBP-1 (Ron 2007). The target genes of ATF-6α include chaperones such as GRP78/BiP, GRP94 and cnx/crt, and foldases such as PDI, ERP57 and ERP72.

The three arms of the UPR work in coordination with each other. For instance, phosphorylated eIF2α causes the dissociation of mRNAs from ribosomes and translation factors. These mRNAs may be degraded by IRE-1α, thereby reducing ER translational load (Hollien 2006). There is also functional redundancy between the IRE-1α/ XBP-1 arm and the ATF-6α arm as XBP-1 is transcriptionally activated by ATF-6α and PERK signaling (Ron 2007).

UPR activation also leads to transcriptional induction of genes involved in ER-associated Degradation (ERAD). ERAD allows for the clearance of misfolded/ unfolded proteins from ER lumen by their retro-translocation to the cytosol for proteosomal degradation. In addition, the cell may also resort to autophagy for degradation of misfolded protein aggregates in the ER in order to reduce ER stress (Nair 2005).

1.04 Endoplasmic Reticulum Associated Degradation (ERAD)

If the chaperone-mediated repair of misfolded proteins is ineffective, the aberrant proteins are cleared by ER Associated degradation (ERAD) (**Figure 1.2**). In this process, the misfolded/ unfolded proteins are retrotranslocated to the cytosol and degraded by the ubiquitin-proteosome system (UPS) (Nishikawa 2005; Hoseki 2010). The molecular details of this complex process are described below.

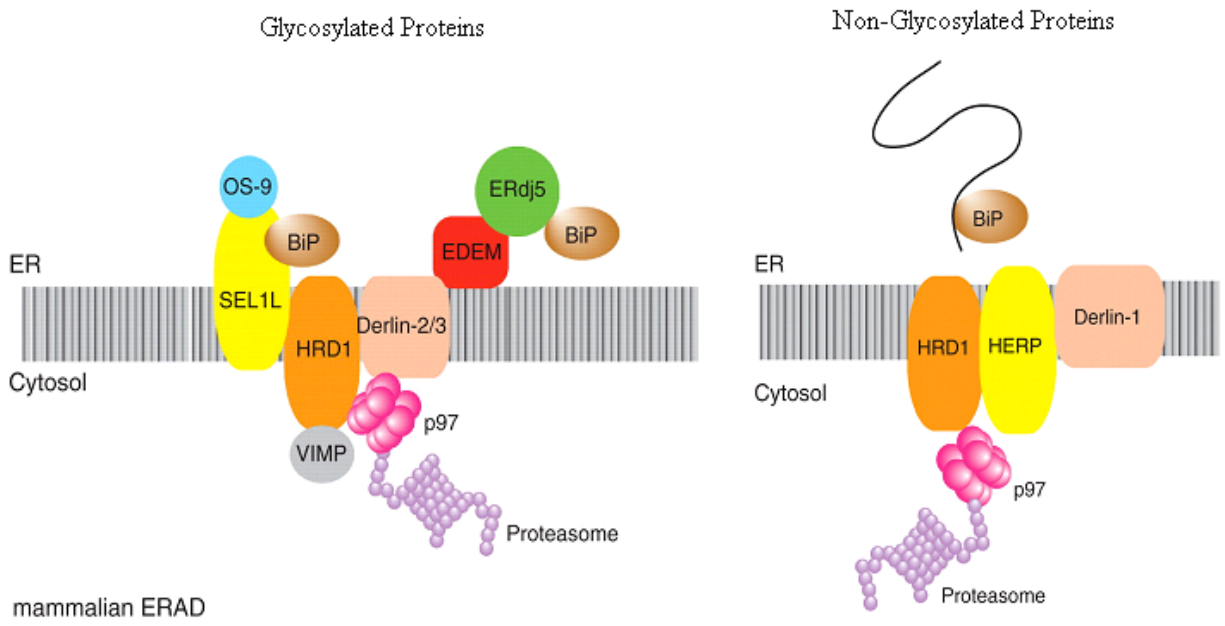

Figure 1.2: Mammalian Endoplasmic Reticulum Associated Degradation (ERAD) of glycosylated and non-glycoylated proteins. Misfolded glycosylated proteins are recognized by chaperone and co-chaperone complexes such as GRP78/BiP and lectin chaperones calnexin/ calreticulin. If the substrate is not capable of folding properly, it is modified by mannose trimming and recognized by EDEM proteins which bring the substrate to the ERAD machinery. ERdj5 interacts with EDEM and GRP78/BiP and allows dislocation of the substrate by reducing their incorrect disulfide bonds. Members of the ERAD complex include E3 ubiquitin ligases such as Hrd-1 and Derlin-2/3, which retrotranslocate and polyubiquitinate the substrate in the cytosol. The valosin containing protein (VCP)/p97 is a AAA+ protein that allows ATP-dependent extraction of the polyubiquitinated ERAD substrate to the cytosolic side and translocates it to the 26S proteosome for degradation. Non-glycosylated proteins are similarly recognized by chaperones and chaperone complexes and transferred to the ERAD machinery for polyubiquitination by E3 ubiquitin ligases such as Hrd-1, HERP and Derlin-1, retrotranslocated and subsequently degraded by the 26S proteosome. Figure obtained from Hoseki, J. (2010). "Mechanism and components of endoplasmic reticulum-associated degradation." J Biochem **147**(1): 19-25.

1.04.1 Chaperone Mediated ERAD Substrate Selection

Chaperones allow for substrate selection for ERAD (Schmitz 1995). Cnx/crt recognize specific N-linked glycosylations which form in slow folding, unfolded or misfolded glycoproteins. If, however, the substrate retention in the ER is prolonged due to improper folding, it may be modified by mannosidases thereby targeting the protein for ERAD (Fagioli 2001). A single mannose is trimmed by ER α1,2-mannosidase I and the Man8 moiety is recognized by EDEM (Hosokawa 2001). EDEM (ER degradation enhancing α-mannosidase-like protein) is a type II transmembrane protein belonging to the Class I α1,2-mannosidase family (glycosylhydrolase family 47). EDEM proteins are ER stress inducible and have been shown to enhance ERAD. The 2003 study by Molinari *et al* showed that over-expression of EDEM leads to faster release of misfolded substrates from the cnx cycle and earlier degradation, while down-regulation of EDEM leads to prolonged cnx mediated folding and delayed degradation (Molinari 2003).

This mannose trimming permits recognition and sorting of terminally misfolded proteins for ERAD. In the 2010 study by Hosokawa *et al*, it was demonstrated that overexpression of EDEM1 trims mannose from the C branch of N-glycans and produces Glc(1)Man(8)GlcNAc(2) isomer C on terminally misfolded null Hong Kong alpha1-antitrypsin (NHK) *in vivo* (Hosokawa 2010). Thus EDEM proteins have α 1,2-mannosidase activity and accelerate glycoprotein ERAD *in vivo* (Hirao 2006). The substrate is then transferred from cnx/crt to EDEM, which then transfers the substrate to the ERAD translocon ((Kanehara 2007; Hosokawa 2010).

GRP78/BiP recognizes hydrophobic regions of misfolded and/or unfolded proteins and binds them in an ATP-dependent manner, allowing their proper folding. In the 1995 study by Schmitz *et al*, the researchers used peroxidase mediated iodination of tyrosine residues which are

located internally in the mature proinsulin, but exposed in folding intermediates and misfolded proinsulin. This was a mechanism to monitor exposure of internal domains of proinsulin during protein folding. The addition of GRP78/BiP led to inhibition of iodination, which suggested that the exposed internal domains represent the signal for protein degradation in the ER (Schmitz 1995). GRP78/BiP KD leads to the release of substrates such as mutated bovine pancreatic trypsin inhibitor (BPTI) from the ERAD machinery (Coughlan 2004). This further implicates the role of GRP78/BiP in ERAD substrate selection. However, GRP78/BiP does not bring the ERAD substrate to the retrotranslocon; instead, EDEM and PDI bring the substrate to the ERAD machinery (Nishikawa 2005). PDI functions in tandem with cnx/crt and GRP78/BiP to allow retrotranslocation of aberrant glycosylated and non-glycosylated proteins for ERAD (Molinari 2002).

It is possible that the solubilization of the aberrant peptide due to high affinity interaction with GRP78/BiP, targets the protein for ERAD (Nishikawa 2005). ERdj co-chaperones stimulate hydrolysis of ATP by GRP78/BiP thereby allowing higher affinity binding to the substrate (Otero 2010). The ERdj co-chaperones may be primarily recognizing the substrates and directing GRP78/BiP activity, thereby allowing it to determine if a protein is bound for folding or for degradation. The co-chaperones ERdj 3 and 6 are mainly involved in protein folding while ERdj 4 and 5 have a greater role in ERAD (Määttänen 2010). Co-chaperone ERdj5 has reductase activity, through which it cleaves disulfide bonds of misfolded proteins and accelerates ERAD through its associations with EDEM and GRP78/BiP. The ERdj5-GRP78/BiP-EDEM triad functions in the ERAD of several substrates including null Hong Kong variant of human α 1-antitrypsin and the j chain of mouse immunoglobulin M (Ushioda 2008).

1.04.2 Retrotranslocation and Polyubiquitination

Soluble ERAD substrates are selected and transported to the ERAD machinery for retotranslocation, polyubiquitinated and subsequent degradation by 26S proteosome (Schulze 2005). ER membrane bound proteins are dislocated or removed from the membrane lipid bilayer before being targeted for degradation (Goeckeler 2010).

Proteins are polyubiquitinated by the actions of E1, E2, E3 and in some cases E4, which is a ubiquitin-chain-extension enzyme (Nakatsukasa 2008). E1 (ubiquitin activating enzyme) hydrolyses ATP and forms a thioester-linked complex between ubiquitin and itself. E2 (ubiquitin conjugating enzyme) receives ubiquitin from E1 and forms a similar intermediate with ubiquitin. E3 (ubiquitin ligase) binds E2 and the ERAD substrate and catalyzes the transfer of ubiquitin onto the substrate. E4 allows multiubiquitin chain assembly (Richly 2005). These molecules add at least 4 ubiquitins in series onto the polypeptide which is then recognized by a series of ubiquitin receptors present on the proteosome (Goeckeler 2010). HSP70 and co-chaperones HSP40 allow association of mutant protein ste6p* to E3 ubiquitin ligase (Nakatsukasa 2008).

There are several candidate channel proteins for ERAD substrate retrotranslocation. Homocysteine-responsive ER-resident protein (HERP) may act as a receptor and a retrotranslocation channel for non-glycosylated GRP78/BiP substrates. HERP contains ubiquitin-like domain (UDP) and is ER-stress inducible. HERP co-immunoprecipitates with other candidates for retrotranslocation channels such as Hrd-1 and Derlin-1, and also with polyubiquitinated ERAD substrates, p97/VCP and 26S proteosome (Okuda-Shimizu 2007). Hrd-1 is also shown to interact with chaperones, EDEM, other E3 ligases and cytoplasmic factors that drive substrate extraction (Gauss 2006; Kanehara 2007). EDEM-1 associates with Derlin-2 and Derlin-3, which are also retrotranslocation candidates (Vembar 2008). Derlin-1 is also an

important factor for extraction of certain misfolded proteins from the mammalian ER (Lilley 2004). In fact, Sec61 may have the dual role of translocation and retrotranslocation as it interacts with the ERAD substrates and ERAD machinery (Scott 2008). In the 2005 study by Schulze *et al*, interaction between Hrd-1 and HERP, Hrd-1 and Derlin-1, Hrd-1 and p97, Derlin-1 and p97, and p97 and VIMP were determined through binding assays (Schulze 2005). This data suggests that the retrotranslocon might form transiently from one or more candidate channel proteins (Goeckeler 2010).

1.04.3 Cdc48/p97 Complex Mediated Dislocation of ERAD Substrates

The ATPase p97/ Valosin containing protein (VCP), also known as cdc48 in yeast, belongs to a family of ATPases associated with diverse cellular activities (AAA proteins). This family of proteins is composed of conserved domains called AAA cassettes, which contain Walker A and Walker B motifs that allow ATP binding and hydrolysis, respectively (Ye 2003). Proteins being retrotranslocated are polyubiquitinated as they emerge in the cytosolic side. The polyubiquitinated substrates are subsequently recognized by cdc48/p97, which extracts them to the cytosol (Ye 2004). The cdc48/p97 protein interacts with substrate-recruitment cofactors Ufd-1 (ubiquitin-fusion degradation) and Np14, forming a complex which binds ubiquitinated substrates and couples ATP hydrolysis to retrotranslocation (Richly 2005; Goeckeler 2010). cdc48/p97 contains two ATPase domains (D1 and D2). The D1 domain when bound to ATP interacts with the polyubiquitinated or unmodified peptides emerging from the ER membrane, while the N-terminal domain interacts with the ER membrane. The D1 and D2 domains alternate in ATP hydrolysis, which allows the movement of the misfolded polypeptide to the cytosol (Ye 2003).

The specificity of cdc48/p97 activity depends on its cofactors Ufd-1 and Npl4 as well as ER membrane UBX proteins. UBX proteins contain a ubiquitin regulatory X (UBX) domain which allows it to bind cdc48/p97. UBX proteins are part of the ER membrane and recruit cdc48/p97 and Ufd1 to ERAD substrates and ERAD components such as Doa10, Hrd1 and Der-1 (Schuberth 2005). cdc48/p97 also associates with membrane proteins Derlin-1 and VIMP (VCP-interacting membrane protein), however, the exact mechanism of extraction is unclear (Ye 2004; Schulze 2005). Derlin-1 is an ER transmembrane protein spanning the membrane four times with the C and N-terminal in the cytosol. VIMP spans the ER membrane once and contains a short luminal and a longer cytoplasmic domain. VIMP recruits cdc48/p97 to Derlin-1 and together the complex allows misfolded protein retrotranslocation from the ER (Ye 2004). The Lysine 48 linkage of ubiquitin chains is required as a recognition site for cdc48/p97-Ufd1-Npl4 complex mediated detection of polyubiquitinated substrate. However, polyubuitination acts as a recognition site only and does not serve as a ratcheting molecule which keeps the substrate in the cytosol (Flierman 2003).

In yeast, depending on the location of the lesion in the aberrant protein, it is targeted to different ERAD pathways. A lesion in the cytoplasmic domain (C) leads to the ERAD-C pathway, which requires Doa 10 ubiquitin ligase for substrate polyubiquitination. Meanwhile, lesions in the luminal domains (L) or membrane-spanning domain (M) leads to activation of the ERAD-L and ERAD-M pathways, respectively (Vembar 2008). The ERAD-L pathway requires ER-Golgi transport, and Der-1p and Hrd-1p E3 ubiquitin ligases. The ERAD-M pathway requires Hrd-1 and Hrd-3p (Carvalho 2006). In the 2004 study by Huyer *et al*, ERAD mediated degradation of Ste6p* (multispanning membrane protein with a cytosolic mutation) and CPY* (soluble luminal protein carboxypeptidase Y with mutant luminal domain) was examined. Ste6p*

degradation was dependent on Doa10p and independent of Hrd-1p/Der3p, while the opposite was true of CPY* (Huyer 2004). There is no clear distinction in the E3 proteins required for each pathway as more than one could participate in each pathway (Nakatsukasa 2008). The peptides must first pass the ERAD-C checkpoint followed by the ERAD-L checkpoint and then several other checkpoints after that in order to finally be functionally active (Vashist 2004). All three pathways, however, converge at the cdc48/p97 complex (Huyer 2004; Carvalho 2006).

1.04.4 Proteosomal Degradation

Degradation of the misfolded ERAD substrates occurs via proteases in the cytoplasm (McCracken 1996; Werner 1996). The 26S proteosome (made of 32 different proteins) resides in the cytoplasm and can degrade ER membrane and lumenal proteins. It contains a 20S core with three specific proteases that allow the catalytic degradation of the polypeptide, and an ATP-dependent 19S regulatory cap which recognizes, unfolds and translocates the polypeptide into the 20S core through a narrow-gated channel (Navon 2009; Goeckeler 2010). Cdc48/ p97 interacts with the 19S cap and also with other proteosome interacting factors to allow the translocation of the substrate to the proteosomes near the ER surface for degradation (Verma 2000). While still bound to the cdc48/p97 complex, the substrate polypeptide interacts with the proteosome or proteosome-associated factors, which assist in its degradation. Before or during substrate degradation, proteosome-associated enzymes allow for substrate deubiquitination and entry into the 20S core. This allows the ubiquitin molecules to be recycled (Finley 2009; Navon 2009). Several membrane and secretory proteins have been identified as being degraded by the proteosome including cystic fibrosis transmembrane conductance regulator (CFTR) (Jensen

1995) and Major histocompatibility class I (MHC I) in mammalian cells (Wiertz 1996), among others.

If ERAD efficiency is compromised, misfolded proteins may accumulate in the ER and form protein aggregates. In this case, the cell may resort to autophagy, where portions of the ER with the protein aggregates are engulfed by autophagosomes and delivered to lysosomes for degradation (Nair 2005).

1.05 ER Stress-induced Apoptosis

In the event that UPR and ERAD are insufficient to alleviate ER stress, apoptotic pathways are induced (Vembar 2008). Apoptosis is a form of cell death that involves specific action of several signaling pathways and members of caspase family of cystein proteases, which exist as procaspase zymogens in the cytoplasm. There are two main apoptotic pathways, the death receptor (extrinsic) pathway which activates caspase-8, and the mitochondrial (intrinsic) pathway which activates caspase-9. In the extrinsic pathway, death receptors such as Fas and TNF (tumor necrosis factor) bind specific multimeric ligands, aggregate and recruit intracellular adaptor proteins. The adaptor proteins then bind procaspase 8 molecules, which then cleave and activate other procaspase 8 molecules. This initiates a caspase cascade which eventually activates executioner caspase-3. The intrinsic pathway is activated when electron carrier protein cytochrome c is released from mitochondrial intermembrane space into the cytoplasm. Cytochrome c binds adaptor protein Apaf-1, which then aggregates and binds procaspase-9 (Alberts 2002). The cleaved caspase-9 then activates and initiates a caspase cascade leading to activation of cleaved caspase-3 (CC3). CC3 then cleaves cellular proteins such as nuclear

proteins, structural proteins and signaling proteins, and DNA, leading to disrupted cellular homeostasis and termination of survival signals.

In the intrinsic pathway, Bcl-2 family of proteins regulates intracellular procaspase activation. Bcl-2 and Bcl-xL (Bcl-2 like 1) inhibit apoptosis by blocking cytochrome c release from mitochondria, while Bak (Bcl-2 homologous antagonist/ killer) and Bax (Bcl-2 associated X-protein) stimulate cytochrome c release thereby promoting apoptosis. IAP (inhibitor of apoptosis) protein family inhibits apoptosis by binding and preventing activation of procaspases (Alberts 2002). Members of the Bcl-2 family have been shown to associate with the ER (Rao 2004). Overexpression of Bax and Bak leads to Ca^{2+} efflux from the ER and Ca^{2+} influx into the mitochondria, which leads to cytochrome c release (Nutt 2002).

Coupling ER stress to apoptosis may benefit the organism by destroying damaged and dysfunctional cells and also allowing recycling of molecules necessary for recovery of the organ function (Rao 2004). There are three known apoptotic pathways induced by ER-stress: 1) CHOP induction, 2) IRE-1α mediated induction of signal transducer c-Jun N-terminal kinases (JNK), and 3) activation of cleaved caspase 12 (CC12) (Ron 2007). The mechanistic details on how these pathways mediate ER stress-induced apoptosis have been reviewed recently and will not be discussed further here (Fonseca 2010; Shore 2011; Tabas 2011).

1.06 Type 2 Diabetes and the ER Stress Response in Pancreatic β-Cells

Pancreatic β-cells are the primary producers of insulin, a hormone required for maintenance of blood glucose homeostasis. As β-cells metabolize glucose, the cellular ATP/ ADP ratio increases, causing a closure of the ATP-regulated potassium channels, which leads to membrane depolarization and subsequent increase in calcium influx through the voltage-

dependent calcium channels. The increased levels of cytosolic calcium allow for the insulin release via exocytosis (Goodison 1992). Insulin stimulates the uptake of glucose in peripheral tissues such as muscle and adipose, while inhibiting hepatic gluconeogenesis (Taniguchi 2006; Volchuk 2010). Failure of pancreatic β-cells to secrete sufficient levels of insulin due to combined dysfunctional insulin secretion and premature cell death is the root cause of type 2 diabetes development.

Glucose also potently stimulates insulin biosynthesis such that insulin is approximately 40-50% of total protein produced by β-cells (Schuit 1998; Melloul 2002). In order to produce large amounts of insulin, the β-cell has a highly developed ER (Eizrik 2008). Since pancreatic β-cells are the only producers of circulating insulin, they are over-stimulated during states of insulin resistance such as in the obese condition. This makes them highly susceptible to ER stress. To accommodate for this sensitivity, β-cells express high levels of ER stress sensors IRE-1 and PERK (Araki 2003) in order to mount an efficient ER stress response.

The importance of the UPR to β-cell function is illustrated by various conditions where the UPR is perturbed. Mutations in UPR proteins have been shown to result in β-cell dysfunction and juvenile onset diabetes. For example, mutations in PERK leads to Wolcott-Rallison syndrome (WRS), a rare autosomal recessive disorder characterized by permanent neonatal or early infancy insulin-dependent diabetes (Delépine 2000). Mutation in the Wolfram Syndrome 1 (WFS1) gene, a UPR inducible ER calcium channel, can lead to Wolfram syndrome, an autosomal recessive neurodegenerative disorder defined by young-onset non-immune insulin-dependent diabetes mellitus and optic atrophy (Inoue 1998). Additionally, mouse models with eIF2α (S51A) knock-in that consequently lack PERK-mediated translational inhibition exhibit defective β-cell function and reduced β-cell mass (Scheuner 2008). Alternatively, enhanced

eIF2α phosphorylation by pharmaceutical agents such as salubrinal that inhibit eIF2α dephosphorylation leading to reduced translational rate, also results in β-cells dysfunction (Cnop 2007). In addition, whole body knockout of the co-chaperone Dnajc3/p58IPK results in the development of diabetes in rodents (Ladiges 2005). Thus, altered function of ER and ER stress response proteins results in β-cell dysfunction and loss, thereby contributing to the onset of type 2 diabetes.

Furthermore, mutations in the proinsulin molecule itself can lead to its accumulation in the ER and cause ER-stress. Such a condition is found in the Akita mouse model. The Akita mouse contains a C96Y missense mutation in the insulin 2 gene, and exhibit hyperglycemia and reduced β-cell mass without obesity (Wang 1999). The C96Y mutation precludes the formation of a disulphide bond between chain A and B in proinsulin leading to a conformational change in the molecule. The misfolded proinsulin accumulates in the ER and causes ER stress in β-cells. The Akita mice have progressive loss of β-cells due to prolonged ER stress and eventually develop a diabetic phenotype with dysfunctional insulin secretion (Oyadomari 2002). The Akita mice also exhibit an accompanying increase in the mRNA levels of GRP78/BiP and CHOP (Oyadomari 2002). Similarly, Munich mice possess a C95S mutation in the insulin 2 gene precluding the formation of A6-A11 interchain disulfide bond. Munich mice exhibit early onset hyperglycemia and insulin resistance, an enlarged ER, and significantly reduced total islet volume and β-cell density compared to wild type mice (Herbach 2007). This misfolded proinsulin molecule accumulates in the ER and complexes with GRP78/BiP. Furthermore, several studies have shown an increase in the expression of ER stress markers and pancreatic hypertrophy (indicative of protein accumulation in the ER) in β-cells from patients with type 2 diabetes (Cnop 2008).

ER-stress may also result from environmental causes associated with diabetes including high fat intake, which leads to lipotoxicity and excessive exposure to elevated glucose levels, which results in glucotoxicity (Cnop 2008; Jonas 2009). Chronic hyperglycemia and hyperlipidemia leads to β-cell functional deterioration and eventually results in type 2 diabetes (Poitout 2006; Eizrik 2008). Patients with type 2 diabetes have an elevated level of non-esterified free fatty acid [NEFA] level. Elevated NEFA levels can also lead to depletion of calcium stores in the ER, which leads to ER stress (Cnop 2008). Patients with type 2 diabetes demonstrate a marked reduction in β-cell mass and increased β-cell apoptosis, which may result from chronic glucotoxicity and lipotoxicity (Eizrik 2008).

In addition to being prone to ER stress as a result of the demands of insulin production, β-cells are also particularly susceptibility to oxidative stress, which can also cause ER stress. β-cells have a limited source of antioxidants, which may increase their susceptibility to normal ER stress-linked aging process (Welsh 1995; Lenzen 1996). Moreover, high glucose exposure leads to increased reactive oxygen species (ROS) levels, further reducing β-cell function and enhancing ER stress (Robertson 2004; Robertson 2004; Malhotra 2007). For example, rat islets treated with 30 mM glucose for 18h showed higher expression of GRP78/BiP, GRP94, EDEM and CHOP mRNA levels (Elouil 2007). It is possible that β-cells are more sensitive to the loss of translational control during ER stress in high glucose conditions since glucose regulates insulin translation. If β-cells are unable to strictly regulate insulin translation, they are likely more susceptible to ER stress and chronic ER stress mediated apoptosis (Scheuner 2008). The high glucose levels lead to high insulin demand, which along with other environmental stressors leads to ER stress. This limited capacity to deal with oxidative stress and excessive ER stress can lead to premature β-cell aging and dysfunction, thereby resulting in the onset of type 2 diabetes.

To study how pancreatic β-cells respond to ER stress in a pathophysiologically relevant manner, our lab generated an insulinoma clonal cell line, pTet-On Ins-1 INS-2(C96Y)-EGFP, modeled after the Akita mouse. This cell line expresses a green-fluorescence protein (GFP)-tagged mutant proinsulin with a cysteine to tyrosine (C96Y) mutation that precludes the formation of an interchain disulfide bond as described earlier for the Akita mouse model (Hartley 2010). A microarray analysis was conducted using this cell line, which revealed an upregulation of several ER-stress response genes including many protein folding and ERAD genes discussed earlier. One of the most highly upregulated genes in response to mutant proinsulin expression encodes for Stromal Cell-Derived Factor 2 Like-1 (SDF2L1) (discussed below). The function of this protein is largely unknown. However, its induction in the C96Y cell line implicates a role in the ER stress response.

1.07 Stromal Cell-Derived Factor 2 Like-1 (SDF2L1)

Stromal Cell-Derived Factor 2 Like-1 (SDF2L1) is a recently characterized protein localized to the ER (Fukuda 2001). While examining the differences in gene expression in radiation-induced B6C3F mice hepatocellular carcinoma cell lines, a cDNA fragment with 64% similarity to SDF2 was serendipitously identified by Fukuda *et al* in 2001. SDF2L1 contains a highly conserved motifs called **MIR** domains which are also found in Protein O-**M**annosyltransferases, **I**nositol 1,4,5-trisphosphate receptors and **R**yanodine receptors (Ryr), although the function of the domain is unknown (Schott 2010). This provides it with a limited homology to the central catalytic region of Pmt/rt family of Protein O-mannosyltransferases (POMTs). SDF2L1 has an ER-retention (HDEL) motif at the C-terminus and a single hydrophobic region at the N-terminus. It consists of 3 exons spanning about 2 kb in humans and

is localized on chromosome 22q.11.2. SDF2L1 is ubiquitously expressed and has high expression in testis, pancreas, spleen, and small intestine (Fukuda 2001). Its expression increases in ER stress conditions induced by tunicamycin and by calcium ionophore A23187 (Fukuda 2001). SDF2L1 does not have an ER-response element sequence in its promoter region, which is characteristic of other ER stress related proteins (Fukuda 2001). It is possible that SDF2L1 may be under a unique transcriptional control.

Although the function of SDF2L1 is unknown, as previously mentioned, it has been shown to associate as a complex with various chaperone proteins such as GRP78/BiP, GRP194, PDI, GRP94, CaBP1, UDP-glycosyltransferase, ERp72, cyclophilin B and GRP170 (Meunier 2002). It has also been reported that ERj3P (soluble glycoprotein of the pancreatic ER) associates with GRP78/BiP and SDF2L1 (Bies 2004). In addition, recent research indicates that SDF2L1 differentially interacts with α, β, and θ defensin propeptides (Tongaonkar 2009). Defensins are antimicrobial peptides involved in innate immunity. Much like insulin, defensins are packaged into secretory granules and contain three disulphide bonds. Thus, SDF2L1 may be interacting with nascent polypeptides in the ER as part of the ER chaperone complex (Tongaonkar 2009). In the 2009 study by Kang *et al*, SDF2L1 was suggested as a prognostic factor in breast cancer. Lower levels of SDF2L1 were associated with higher levels of metastasis, increased number of breast cancer related deaths, poor prognosis and increased number of grade-3 tumors (Kang 2009). It is possible that SDF2L1 has high expression in rapidly dividing cells.

Furthermore, SDF2 is suggested to be a downstream target of the UPR (Schott 2010). It is possible that SDF2L1 may also function to direct the localization of the folded substrates to the secretory pathways and the misfolded substrates to the ERAD machinery (Tongaonkar 2009).

SDF2 is also shown to contain a β-trefoil structure that may be involved in glycoprotein quality control (Schott 2010). It is also possible that SDF2L1 may interact with glycosylated proteins via its MIR domain. Clearly, there is limited knowledge about the function of SDF2L1 and more research is required to determine its role in the ER. This thesis focuses on examining the role of SDF2L1 in pancreatic β-cells.

1.08 Rationale and Hypothesis

Most *in vitro* ER stress models use pharmaceutical inducers of ER stress such as tunicamycin, thapsigargin or reducing agents. To provide a more physiologically relevant model of ER stress, a cell line pTET ON INS-1 (Insulin-2(C96Y)-GFP) was developed in our lab, which mimics chronic ER stress in a manner similar to that in the Akita mouse. It expresses GFP-tagged mutant proinsulin, with a C96Y mutation in the Ins-2 gene precluding the formation of a disulfide bond, in a doxycycline inducible manner (Hartley 2010). A microarray analysis of the genes expressed in this cell line showed high levels of SDF2L1 expression, implicating its role in ER stress and possible association with mutant proinsulin (Hartley 2010). Chronic ER stress has been implicated in β-cell dysfunction and the progression of diabetes (Tabas 2011). Understanding the function of ER-stress inducible genes is paramount in understanding the cellular response to this form of stress. Delineating the function of SDF2L1 in pancreatic β-cells will provide significant advances in our understanding of the ER-stress response in β-cells.

It is ***hypothesized*** that SDF2L1 is an ER-stress inducible protein required either as a molecular chaperone protein that promotes insulin folding in the ER or for degradation of misfolded proinsulin via the ERAD system. The objective of this thesis is to elucidate the function of SDF2L1 in pancreatic β-cells.

CHAPTER 2. METHODS

2.01 Cell Culture

Cell lines INS-1 832/13 (obtained from Dr. Chris Newgard, Duke University) and pTet-ON INS-1 (Insulin-2(C96Y)-EGFP) (Hartley 2010) were cultured in RPMI 1640 media (Gibco) supplemented with 11.1 mM Glucose, 1 mM sodium pyruvate, 10 mM Hepes, 10% Fetal Bovine Serum (FBS), 2 mM L-Glutamine, 55 μM β-mercaptoethanol, 100 units/ml penicillin and 100 μg/ml streptomycin. The mutant insulin producing cell line (C96Y) was maintained with selection drugs 200 μg/ml G418 and 50 μg/ml hygromycin, and treated with 2 μg/ml doxycyline to induce mutant insulin expression. HepG2 cells were obtained from the laboratory of Dr. Tianru Jin (University of Toronto) and cultured in DMEM (Gibco) media supplemented with 10% FBS, 25 mM glucose, 2 mM L-Glutamine, 100 units/ml penicillin and 100 μg/ml streptomycin. AD293, HELA and HEK293T cells were also maintained in supplemented DMEM media. Cells were passaged once they reached 70% confluence and incubated at 37°C in a 5% CO_2 enriched environment. Glial cell (C6 and U373) lysates and INS-1 lysate samples (treated with ATZ, oxidative stressors, arsenic or heat shock) were obtained from Dr. Ravi Vellanki in the Volchuk lab. Islet samples were prepared by Tracy Teodoro and Liling Zhang in the Volchuk lab.

2.02 Cell Treatment and Lysis

Cells were treated with pharmacological ER stress inducers: 1μM thapsigargin (Tg) for 6 h and 2 μg/mL tunicamycin (Tm) for 16 h. INS-1 832/13 samples treated with Tg or Tm were used as positive controls for ER stress. INS-1 832/13 cells treated with 0.3 μM staurosporin for 24 h were used as positive control for apoptosis, while lysates of cells treated with UV light for 15 mins were used as positive control for phospho-JNK activity. To obtain cell lysates, cells were

washed with ice cold PBS and incubated with 1% TX-100 (20 mM Hepes pH 7.4, 100 mM KCl, 2 mM EDTA, 1 mM PMSF, 10 µg/ml leupeptin, 10 µg/ml apoprotinin, 0.5 M NaF, 0.5 M Na_3VO_4, and 30 µM okadaic acid) on ice for 15 mins. Cells were then scraped and centrifuged at 13,200 rpm for 15 min at 4°C. The supernatant was stored in -80°C or protein concentration of samples was determined using bicinchoninic acid (BCA) reagent (Pierce).

Rat liver tissue was obtained from Tracy Teodoro. Liver homogenate was prepared by manual homogenization and overnight incubation of tissue with homogenization buffer (250 mM sucrose, 4 mM Hepes, 1 mM MgCl2, pH 7.4) supplemented with protease inhibitors (1 mM PMSF, 0.5 M NaF, 0.5 M Na_3VO_4, and 30 µM okadaic acid). Following incubation, the homogenate was centrifuged to remove debris and incubated with 500 µl 2X TX-100 lysis buffer supplemented with protease inhibitors (1 mM PMSF, 0.5 M NaF, 0.5 M Na_3VO_4, and 30 µM okadaic acid). The samples were centrifuged again and liver lysate was used in binding assays.

2.03 Transient Transfection

In order to test overexpression of SDF2L1 in pA-IRES plasmid (obtained from Dr. James Rini, University of Toronto), AD293 cells were transiently transfected using Lipofectamine 2000 reagent. 300, 000 cells were seeded per well in 12-well plates and incubated at 37°C in 5% CO_2 for 24 h. 100 µl of Opti-MEM media was combined with 4 µl Lipofectamine 2000 reagent. Another 100 µl of Opti-MEM media was combined with pA-SDF2L1 vector or pA-IRES (control) vector and incubated for 5 min. The mixtures were combined and incubated for an additional 25 min at room temperature and then combined with RPMI 1640 media without antibiotics. The media of the seeded cells was replaced with the fresh media with the DNA mixture. The plates were incubated for 24 h at 37°C in 5% CO_2. The cells were then lysed and

resolved on SDS-PAGE and analyzed via western blot. This protocol was also used to determine the over-expression of SDF2L1 in the pShuttle vector during SDF2L1 over-expressing adenovirus production. The pShuttle-SDF2L1 vector and pShuttle (control) vector were used to transiently transfect HEK293 cells.

2.04 Cloning of SDF2L1 in pShuttle- IRES-hr-GFP-2 vectors and Adenovirus production

Full length rat SDF2L1, which is 633 base pairs in length, was reverse transcribed from total RNA of C96Y cells exposed to 16 h of Tm using QIAGEN One-Step RT-PCR kit according to the manufacturer's instructions. In brief, 100 ng of RNA was combined with Qiagen RT-PCR buffer, One-Step Enzyme mix, dNTPs, and the following primers (ACTG Corporation; Toronto, Canada):

SDF2L1 forward: 5'-**ATG**TTGGGCGCGAGCCGC-3'

SDF2L1 Reverse: 5'-**TCA**GAGTTCATCGTGACCTGT-3'

The RT-PCR protocol consisted of reverse transcription for 30 min at 50°C, initial activation of PCR for 15 min at 95°C, 35 cycles of 1 min at 95°C, annealing for 1 min at 60°C and extension for 1 min at 72°C. The amplified RT-PCR products were subsequently resolved on 1.5% agarose gel and visualized using ethidium bromide. The 700 bp band was excised and purified from the agarose gel using Qiagen Gel Extraction Kit. Following extraction, the SDF2L1 cDNA was cloned into pcR II-TOPO vector (Invitrogen, Carlsbad, USA) to obtain SDF2L1 insert that is full length and SDF2L1 insert without HDEL retention sequence using the following primers:

SDF2L1 Forward: 5'-GCCACC**ATG**TTGGGCGCGAGCCGC-3'

SDF2L1 Reverse: 5'-**TCA**GAGTTCATCGTGACCTGT-3'

SDF2L1 (no HDEL) Reverse: 5'-TT**CTA**ACCTGTGGAGGGATCTGCTCC-3'

The vector was then transformed into OneShot®TOP10 chemically competent cells (Invitrogen, Carlsbad, USA) and purified using QIAamp® DNA Mini Kit (Qiagen, Maryland, USA). The presence of the SDF2L1 cDNA insert was verified by cutting the 633bp band using the EcoRI enzyme (New England BioLabs) and running out of the digested product on 1.5% agarose gel. Two plasmids were selected for sequencing (ACTG Corp., Toronto, ON).

For recombinant adenovirus production, the full length SDF2L1 cDNA and the no HDEL-SDF2L1 cDNA was cloned into pShuttle-IRES-hr-GFP-2 (Stratagene). The TOPO-SDF2L1 ($^{+}_{-}$ HDEL) construct and pShuttle-IRES-hr-GFP-2 vector were digested using NotI and SpeI (New England Biolabs) and ligated using Solution I (Takara). This construct was then transformed into DH5α cells and plated. The following day, kanamycin resistant clones were picked and amplified overnight. Plasmid DNA was then isolated using the QIampDNA Mini Kit. The pShuttle-IRES-hr-GFP-2-SDF2L1($^{+}_{-}$ HDEL) construct was amplified and isolated using Qiagen Plamid Mini Kit (Qiagen, Maryland, USA) and proper ligation of the SDF2L1 cDNA insert was verified with the above stated protocols.

The production of an SDF2L1-expressing adenovirus was attempted using the Adenoviral Vector System (Stratagene). Briefly, pAdEasy-1 vector (pShuttle vector containing the full length insert along with the supercoiled viral plasmid) was used to produce recombinant adenovirus plasmid via homologous recombination. The plasmid was subsequently purified and transfected into AD293 cells using the modified MBS Mammalian Transfection Kit (Stratagene). The primary viral stocks were then prepared by subjecting the infected cells to freeze-thaw cycles, followed by subjecting the resulting viral particles to one round of amplification. The primary virus was tested by infecting Ins-1 832/13 and AD293 cells and analyzing the lysates by western blot.

2.05 XBP-1 Splicing Assay

Rat XBP-1 cDNA was amplified by RT-PCR (Quiagen One STEP RT-PCR kit) using primers that flank the intron excised by IRE-1 endoribonucleas activity as described previously (Zhang 2009). Total RNA was first isolated using Trizol reagent (Invitrogen) followed by isolation using the RNeasy Mini Kit (Qiagen). RT-PCR was conducted using the forward XBP-1 Primer 5'-AAA CAG AGT AGC AGC ACA GAC TGC-3' and reverse XBP-1 primer 5'-TCC TTC TGG GTA GAC CTC TGG GAG-3' and the following PCR protocol: 50°C (30 mins), 95°C (15 mins), 30 cycles of [94°C (1min), 62°C (1 min), 72°C (1 min)], 72°C (10mins). The RT-PCR products were resolved on a 3% agarose gel and visualized using ethidium bromide.

2.06 Trichloroacetic Acid (TCA) Protein Precipitation

Cells were washed with phosphate-buffered saline (PBS) on ice, and 9% ice-cold trichloroacetic acid (200μL/well) was added. Following treatment, the cells were scraped into tubes and centrifuged at 13,000 rpm for 10 min at 4 °C. The pellet was washed with 1 ml of cold acetone and centrifuged at 13,000 rpm for 10 min at 4 °C. The pellet was resuspended in 2× LDS sample buffer (Invitrogen) without reducing agent.

2.07 Immunoprecipitation (IP) and Binding Assays (BA)

To determine if SDF2L1 interacts with mutant proinsulin C96Y-GFP cells (300, 000) were seeded in 12-well plates and incubated for 24 h. The cells were then treated with doxycycline for 48 h followed by incubation with 1 mM dithiobis(succinimidyl propionate) (DSP) for 30 min in the DSP cross-linking experiments. To immunoprecipitate mutant proinsulin, the cells were lysed and 250 µl of the lysates were incubated with 5 µg of mouse monoclonal α-GFP antibody (Clontech, 6323681) or control mouse IgG antibody. Samples were subjected to immunoprecipitation with Protein G dynabeads. Pellet (P) and supernatant (SN) fractions were analyzed by western blot.

To detect the proteins interacting with the protein A-tagged SDF2L1 produced by the pA-SDF2L1 #7 cell line, binding assays (BA) were performed. pASDF2L1#7 (300,000 cells/ well) were seeded in 10 cm dishes and incubated at 37°C in 5% CO_2 for 24 h. The cells were then treated or not with Tm for 16 h. Following treatment, the cells were lysed in ice cold 1% TX-100 buffer and the protein concentration was determined using BCA protein assay (Pierce). To immunoprecipitate (IP) the protein A-tagged SDF2L1, 25 µl rabbit IgG-agarose beads or control protein A-agarose beads were added to 100 µl of the cell lysate. The samples were incubated overnight with rotation at 4°C. The next day, the samples were centrifuged for 15 min at 13,200 rpm at 4°C, the supernatants were transferred to a new tube and the pellets were washed with lysis buffer three times for 5 min at 4°C. The pellets were then incubated overnight with lysates from proinsulin C96Y-GFP cells (treated or not with dox), or lysates from INS-1 832/13 cells (treated with 2 µg/ml Tm for 16 h or with 20 mM glucose) or liver tissue lysates. Following 24 h incubation with liver lysate, samples were centrifuged again for 15 min at 13,200 rpm at 4°C, the

supernatants were transferred to new tubes and the pellets were washed with lysis buffer three times for 5 min at 4°C. The pellet samples were then boiled in 25 µl LSB, resolved on SDS-PAGE or NuPAGE gels and analyzed by western blot.

2.08 Short Interfering RNA (siRNA) Transfection

To knock down cellular SDF2L1 or GRP78/BiP mRNA, cells were transfected using Lipofectamine RNAiMax reagent. 12 pmol of SDF2L1, GRP78 or control siRNA (Luciferase, GFP, or Lac Z) was mixed with 200 µl Opti-MEM media (Invitrogen) supplemented with 2 µl of Lipofectamine RNAiMax reagent (Invitrogen) in 12-well plates. The plates were incubated at room temperature for 25 min. During the incubation, cultured cells were trypsinized, counted, and resuspended in complete RPMI 1640 media (without antibiotics) to a final concentration of 150,000 cells/ml for AD293 cells or 300,000 cells for INS-1 832/13 and proinsulin C96Y-GFP cells. Following the incubation, 1 ml of diluted cells were gently applied to each well to a final concentration of 10 nM siRNA/Lipofectamine RNAiMax complexes. The cells were then incubated for 24 h at 37C in 5% CO2 before further treatment. The knockdown was confirmed using western blot or real-time PCR.

2.09 Degradation Assay

Proinsulin C96Y-GFP cells were transfected with SDF2L1 siRNA or luciferase control siRNA for 48 h (or GRP78 siRNA for 72 h) as described above. After 48 h (or 72 h), cells were treated with 100 µM cycloheximide (chx) for 0h, 3 h or 6 h or no treatment then lysed and analyzed by western blot. α-GFP antibody was used to detect the degradation of GFP-tagged mutant proinsulin over time.

2.10 Western Blot Analysis

Treated or untreated cells were washed with PBS, lysed in ice-cold TX-100 lysis buffer for 15 min on ice, and lysates were centrifuged at 13,200 rpm for 10 min at 4°C. The protein concentration of the samples was determined using BCA protein assay (Pierce) and equal amounts of protein were boiled in 2X Laemmli sample buffer supplemented with 10% β-mercaptoethanol. The samples were resolved on SDS-PAGE followed by transfer to Hybond-ECL nitrocellulose membranes (GE Healthcare). To detect smaller size proteins such as CC3 and insulin, samples were resolved on 4-12% NuPAGE gels (Invitrogen). The membranes were then incubated in blocking buffer composed of 3% milk in Western Wash Buffer (PBS supplemented with 0.05% Tween-20 and 0.05% Nonidet P-40) for 1hr. After blocking the blots were incubated at 4°C overnight with primary antibody. The following primary antibodies were used: CHOP (Santa Cruz, sc-575; 1:500), KDEL (StressGen, SPA-827; 1:1000), Insulin (Santa Cruz; 1:250), γ-tubulin (Sigma, T6557; 1:1000), Polyclonal GFP (obtained from Dr. James E. Rothman, Yale University, 1:1000), Monoclonal GFP (Clontech, 632381; 1:2000), Cleaved-caspase-3 (Cell Signaling, 9661S; 1:1000), SDF2L1 (Sigma, HPA005638; 1:500), GM130 (Transduction Laboratories, G65120; 1:500), and Protein-A (Sigma, P2921; 1:5000). The blots were then washed with WWB 3 times for 15 min and incubated in secondary antibody conjugated with Horseradish Peroxidase (HRP) for 1 h. The blots were washed again 3 times for 15 min and the bands were detected using the enhanced chemiluminescence system (GE healthcare). For some of the blots, densitometry was performed for quantitative analysis of the band intensity. For this, the photographic film was scanned and relative band darkness was measured using Scion Image

software. The relative intensity of the loading control band was used to normalize the signals of the proteins of interest.

2.11 Insulin Secretion Assay and Rat Insulin Radioimmunoassay (RIA)

To determine the effect of siRNA mediated KD of SDF2L1 on insulin secretion, 400,000 INS-1 832/13 cells/ well were transfected in 12-well plates with SDF2L1 siRNA or Lac Z control siRNA for 48 h. The cells were then washed twice with 2 ml Krebs-Ringer Bicarbonate HEPES (KRBH) buffer containing 128.8 mM NaCl, 4.8 mM KCl, 1.2 mM KH_2PO_4, 1.2 mM $MgSO_4$, 2.5 mM CaCl2, 5 mM $NaHCO_3$, 10 mM HEPES, pH 7.4 and supplemented with 0.1% BSA. They were then incubated with 2 ml KRBH buffer with no glucose for 1 h at 37°C in 5% CO_2. The cells were then incubated in 1 ml KRBH buffer with 2.8 mM glucose (for low glucose condition) or 16.7 mM glucose (for high glucose condition) for 1 h. Following treatment, the cells were placed on ice and 700 µl of the supernatant was collected and centrifuged at 5,400 rpm for 5 min at 4°C. The supernatants from the spin were subsequently collected and stored at -80°C. The insulin secreted into the KRBH buffer was measured using Rat insulin radioimmunoassay (RIA) (Linco Research Inc.) according to manufacturer's instructions. The cells remaining in the plate were lysed with ice-cold 1% TX-100 lysis buffer and the protein concentration was measured using BCA assay (Pierce). The insulin secretion was expressed as the amount of insulin released into the KRBH buffer (in nanograms) per milligram of protein content in each condition. The assay was performed in duplicate for each condition from six independent experiments.

2.12 Apoptosis Assay

Apoptosis was measured using the Cell Death Detection ELISA^{PLUS} Assay kit (Roche Diagnostics) according to manufacturer's instructions. Briefly, INS-1 832/13 cells (300 000) were transfected with SDF2L1 siRNA or Lac Z control siRNA in 12-well plates for 24 h and treated or not with Tm for another 24 h. Following treatment, the cells were lysed and oligonucleosomes in the cytoplasm (indicative of apoptosis-associated DNA degradation) were quantified according to the manufacturer's instructions. Parallel experiments were conducted to determine total protein concentration of the samples. The relative apoptotic signal was normalized for total protein. Control samples (with control siRNA and no Tm treatment) had background levels of cytoplasmic oligonucleosomes, thus this condition was used to normalize all the other treatment conditions.

2.13 ^{3}H-Mannose Labelling

ProinsulinC96Y-GFP cells were seeded (500,000 cells/well) in 12-well plates. The cells were then incubated in Krebs Ringer Buffer with HEPES (KRBH) and dox for 24 h. Following incubation, the cells were labeled with 1 mCi/ml ^{3}H-mannose for 90 min. Following treatment, the cells were lysed and the GFP-tagged mutant proinsulin was immunoprecipitated using α-GFP antibodies. The pellet (P) samples were filtered using Whatman glass fibre filters and supernatant (SN) samples were first TCA precipitated then filtered. The filters were air dried before addition of liquid scintillation cocktail and radioactivity measurement with liquid scintillation counting (LSC) or autoradiography.

2.14 Immunofluorescence and Fluorescence Microscopy

pA-SDF2L1#7 cells were seeded on glass coverslips in a 24-well dish (250,000 cells/ well) and incubated overnight at 37°C in 5% CO_2. Following incubation, the cells were washed twice with PBS and fixed for 30 min in 3% paraformaldehyde (PFA) in PBS at room temperature. The cells were washed again twice with PBS and incubated for 15 min in 100 mM glycine in PBS at room temperature. The cells were then washed once with PBS and permeabilized using 0.1% TX-100/0.5% BSA in PBS for 15 min at room temperature. The cells were then washed three times with PBS and blocked for 1 h in 2% BSA/ 2% non-fat dry milk in PBS. The primary antibodies: rabbit polyclonal SDF2L1 (1:500) (Sigma, HPA005638) or Protein-A (Sigma, P2921; 1:5000) was added to the blocking solution for 1 h. The cells were then washed three times for 5 min with PBS and secondary antibody: Oregon green goat anti-rabbit IgG (1:1000) in blocking solution was added to the cells for 1 h in the dark. The cells were washed again three times with PBS in the dark and mounted on glass slides using Fluoromount G Mounting Medium (Electron Microscopy Sciences, Inc.). Fluorescence from the samples was visualized subsequently using fluorescence microscope (Olympus, IX71).

Similarly, the protocol described above was used with HEK293 cells to detect the presence of SDF2L1 in control and Tm treated cells. Briefly, HEK293 (150,000 cells/well) were seeded on glass coverslips in a 24-well dish and incubated overnight at 37°C in 5% CO_2. Following incubation, the cells were treated or not with Tm for 16 h. After treatment, the cells were analyzed by fluorescence microscopy to test vector transfection efficiency.

To determine the efficiency of the pShuttle-SDF2L1 (full length) vector for adenovirus production, HEK293 cells were transiently transfected with pShuttle-SDF2L1 vector or Lipofectamine 2000 control for 24 h. The cells were subsequently washed twice with PBS and

fixed for 30 min in 3% paraformaldehyde (PFA) in PBS at room temperature. The cells were washed again two times with PBS and mounted on glass slides using Fluoromount G Mounting Medium (Electron Microscopy Sciences, Inc.). Fluorescence from the samples was visualized subsequently using fluorescence microscope (Olympus, IX71).

2.15 Extraction and Real-Time Quantitative Polymerase Reaction (qPCR)

Total RNA was isolated from INS-1 832/ 13 cells treated or not with Tm of proinsulin C96Y-GFP cells treated or not with dox using Trizol Reagent (Invitrogen) and the RNeasy Mini Kit (Qiagen). Total RNA (1.95 μg) was reverse transcribed to single-stranded cDNA using High-Capacity cDNA Reverse Transcription Kit (Applied Biosystems). The resulting cDNA was used for qPCR analysis by the TaqMan Gene Expression system (Applied Biosystems). The following primers were obtained from Applied Biosystems: CHOP (Rn00492098_g1), ATF-4 (Rn00824644), GRP78 (Rn00565250_m1), SDF2L1 (Rn01404681_g1), and β-Actin (4352931E). Serial dilutions of the no treatment control cDNA were used to generate a standard curve. The reactions were run on an ABI Prism 7900 HT Sequence Detection System (Applied Biosystems) using the following protocol: 10 min at 95°C, 40 cycles of 15 s at 95°C and 1 min at 60°C. The standard curve and the corresponding values for each sample were determined by the SDS 2.1 software of the ABI Prism 7900HT instrument. Samples were run in triplicates or duplicates. The values were normalized to the expression of β-Actin mRNA and presented as a mean +/-SE of 3 independent experiments.

2.16 Statistical Analysis

Results are presented as the mean $\pm$SE. Statistical significance between two experimental conditions was analyzed using two-sample *t*-test assuming equal variance. Data from several or more groups was analyzed by ANOVA, followed by Tukey post hoc test. $p<0.05$ was considered statistically significant.

CHAPTER 3: SDF2L1 EXPRESSION IN PANCREATIC β -CELLS AND ISLETS, AND THE EFFECT OF SDF2L1 KNOCK-DOWN ON THE ER STRESS RESPONSE IN β-CELLS

3.01 Introduction

Several studies have implicated chronic ER-stress as a potential contributor to β-cell dysfunction and death leading to the onset of type 2 diabetes (Eizirik 1996; Jonas 2009). Thus, understanding how pancreatic β-cells respond to ER stress may offer novel strategies for improving β-cell survival and function in order to prevent or treat the disease. We recently discovered that SDF2L1 is highly inducible at the mRNA and protein level in the proinsulin C96Y-GFP cell line that mimics the Akita mouse model of ER-stress induced β-cell dysfunction (Hartley 2010). In this chapter I examine the expression of SDF2L1 in other cells lines and models of diabetes, and also determine the effect of various cellular stressors on SDF2L1 expression.

SDF2L1 is found in complex with ER chaperones, co-chaperones and foldases such as GRP78/BiP, GRP194, PDI, GRP94, CaBP1, UDP-glycosyltransferase, ERp72, cyclophilin B and GRP170 (Meunier 2002), and at least one study has shown SDF2L1 to be induced by ER stressors such as Tm and calcium ionophores (Fukuda 2001). However, the role of SDF2L1 in the ER stress response has not been examined and requires further elucidation. This chapter will also examine if the absence of SDF2L1 sensitizes β-cells to ER-stress and ER-stress induced apoptosis. Specifically, the effect of siRNA mediated knock down of SDF2L1 on UPR markers in response to ER-stress will be examined. In addition, the effect of SDF2L1 knock down on ER-stress-induced apoptosis will be examined. I ***hypothesize*** that the absence of SDF2L1 up-regulation in response to ER stress will increase markers of ER stress (i.e. result in greater ER stress in the cell) and enhance ER stress-induced apoptosis.

3.02 Results

3.02.1 Examine SDF2L1 expression under ER and other stress conditions

Microarray analysis of the proinsulin C96Y-GFP cell line revealed that SDF2L1 expression is significantly induced with 24 h, 48 h and 5 day doxycycline (dox) treatment (Hartley 2010). I therefore confirmed the expression of SDF2L1 at the mRNA level in the proinsulin C96Y-GFP cell line using real time PCR analysis (**Figure 3.1 A**). A significant increase in SDF2L1 mRNA expression was observed following 24 h of dox treatment, confirming the microarray data. In addition, expression of SDF2L1 protein in proinsulin C96Y-GFP cells was examined (**Figure 3.1 B**). SDF2L1 protein expression increased in response to dox treatment, suggesting that SDF2L1 protein levels increase as mutant proinsulin accumulates in the ER of proinsulin C96Y-GFP cells. Although expression of SDF2L1 is detected in control proinsulin C96Y-GFP cells at higher exposures (not shown), the expression is induced markedly in response to mutant insulin expression.

SDF2L1 mRNA appears to be ubiquitously expressed (Fukuda 2001), although protein expression has not been tested. Therefore, SDF2L1 protein expression was examined in several cell lines (**Figure 3.2**). SDF2L1 expression was not detectable in the human U373 and rat C6 glial cells even in response to Tg or Tm-induced ER stress (which was evident based on upregulation of GRP78). However, HELA and HEK293 cells had high expression of SDF2L1 protein even under non-stress conditions, and the expression was further increased in response to Tm-induced ER stress. INS-1 832/13 cells also showed an increase in SDF2L1 expression with Tm treatment. Thus, SDF2L1 protein is expressed in some, but not all cell lines and where detected, expression is increased in response to pharmacological ER stress.

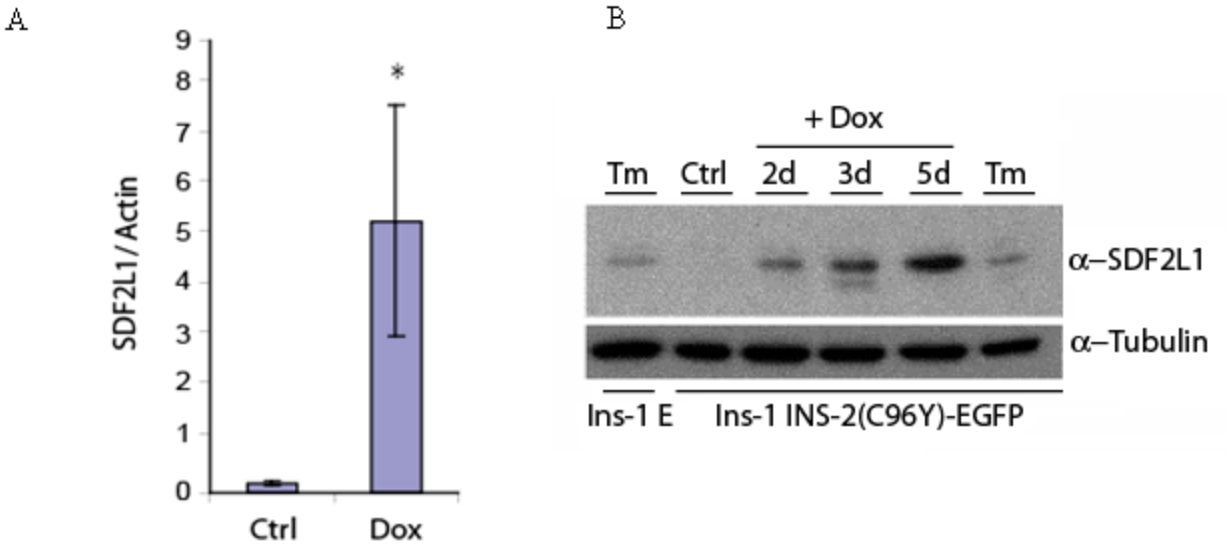

Figure 3.1: **SDF2L1 expression increases in proinsulin C96Y-GFP cells at the mRNA and protein level with Dox induction.** Proinsulin C96Y-GFP cells were untreated (Ctrl) or treated with 2 μg/ml doxycyline (Dox) for 24 h, total RNA was isolated and the samples were analyzed by qPCR. The SDF2L1 mRNA levels are normalized to cellular β-actin. (N=3, *$p<0.05$ relative to control) (**A**). Proinsulin C96Y-GFP cells were untreated (Ctrl) or treated with 2 μg/ml doxycyline (+ Dox) for the times indicated. Following treatment the cells were washed with PBS, lysed and equal amounts of protein was resolved by SDS-PAGE and immunoblotted with α-SDF2L1 and α-tubulin antibodies. INS-1 cells treated with 2 μg/ml Tm for 16 h were used as positive controls for SDF2L1 expression (**B**).

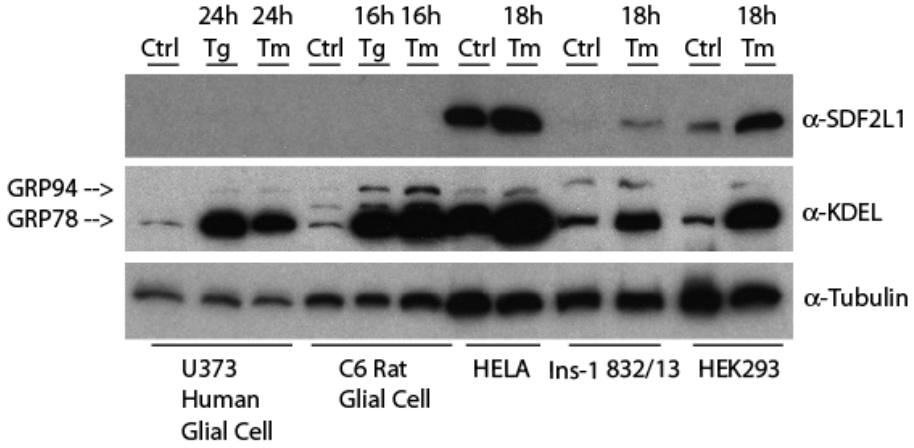

Figure 3.2: **SDF2L1 protein expression in various cell lines in control and ER stress conditions.** Lysates from glial cell lines (human U373 and rat C6 cells) untreated (Ctrl), treated with thapsigargin (Tg) or tunicamycin (Tm) were prepared (Methods 2.1). HELA, Ins-1 832/13 and HEK293 cells were untreated (Ctrl) or treated with 2 μg/ml Tm for 18h. Following treatment the cells were washed with PBS, lysed and equal amounts of protein was resolved by SDS-PAGE and immunoblotted with α-SDF2L1, α-KDEL and α-tubulin antibodies.

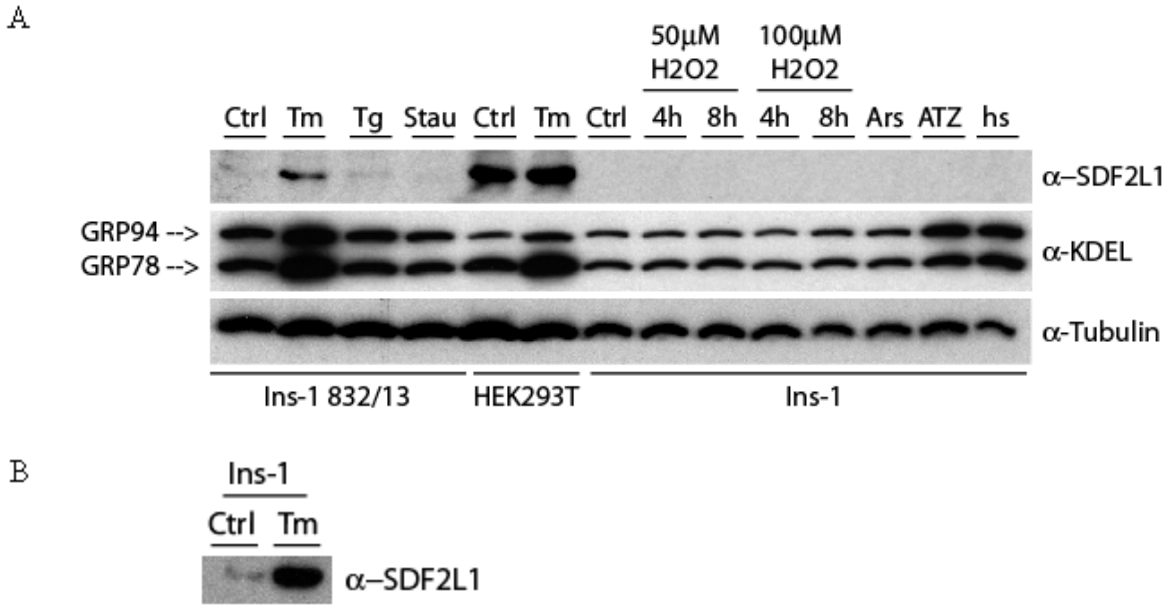

Figure 3.3: **SDF2L1 protein expression is specific to ER stress.** INS-1 832/13 cells were untreated (Ctrl) or treated with 2 μg/ml Tunicamycin (Tm) for 16 h, 1 μM Thapsigargin (Tg) for 4 h or 0.3 μM staurosporine (Stau) for 16 h. HEK293T cells were untreated (Ctrl) or treated with 2 μg/ml Tm for 16h. INS-1 cells were untreated (Ctrl) or treated with oxidative stressor (H_2O_2) with the concentrations and times indicated, as well as with other stressors such as arsenic, ATZ and heat shock (42°C). The INS-1 samples were obtained from Dr. Vellanki. Following treatment the cells were washed with PBS, lysed, and equal amounts of protein was resolved by SDS-PAGE and immunoblotted with α-SDF2L1, α-KDEL and α-tubulin antibodies (**A**). INS-1 cells were untreated (Ctrl) or treated with 2 μg/ml tunicamycin (Tm) for 16 h. Following treatment the cells were washed with PBS, lysed, and equal amounts of protein was resolved by SDS-PAGE and immunoblotted with α-SDF2L1 antibody (**B**).

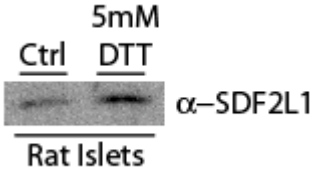

Figure 3.4: **SDF2L1 protein expression is detected in isolated rat islets and increases in islets exposed to the reducing dithiothreitol.** Rat islets were untreated (Ctrl) or treated with 5 mM dithiothreitol (DTT) for 30 min. Following treatment the samples were lysed, equal amounts of protein was resolved by SDS-PAGE and immunoblotted with α-SDF2L1 antibody.

I next examined if SDF2L1 protein expression is specific to ER-stress or is induced with other cellular stressors (**Figure 3.3**). SDF2L1 expression increases in Tm treated INS-1 832/13 cells compared to control samples. However, Tg and Staurosporine (stau) treatment did not lead to significant induction of SDF2L1. SDF2L1 expression was, however, specific to ER stress conditions and did not increase with oxidative stress (H2O2), Arsenic, 3-Amino-1,2,4-triazole (ATZ) or even heat shock treatment in INS-1 cells (**Figure 3.3A**) in contrast to Tm, which markedly induces SDF2L1 in this pancreatic β-cell line (**Figure 3.3B**). ER stress and heat shock stress were confirmed by monitoring GRP78/ BiP and GRP94 levels, which were both increased by Tm and heat shock. Thus, although both ER stress and heat shock can induce ER chaperone levels, only ER stress induces SDF2L1 in pancreatic β-cell lines.

In preliminary experiments I also examined SDF2L1 protein expression in isolated primary islets and the effect of ER stress caused by the reducing agent dithiothreitol (DTT). SDF2L1 protein expression was detected in control rat islets and the levels were increased slightly by DTT (**Figure 3.4**). Future experiments are required to determine if this effect is significant and examine if other ER stressors also induce SDF2L1 in primary rodent islets. However, in several rodent models of type 2 diabetes ER stress markers have been shown to be elevated in islets from diabetic animals compared to non-diabetic controls, including the db/db and MKR mouse models (Laybutt 2007; Lu 2008). MKR mice express a dominant negative insulin-like growth factor 1 (IGF1) receptor in skeletal muscles. This leads to a diabetic phenotype with peripheral insulin resistance and hyperglycemia at 8 weeks (Fernandez 2001; Lu 2008). In collaboration with Dr. Michael Wheeler (University of Toronto), islets from MKR and control mice for SDF2L1 expression were examined. Islet samples were obtained from the Wheeler lab and analyzed for SDF2L1 mRNA and protein expression (**Figure 3.5**). Interestingly,

the MKR mice exhibit significant induction of SDF2L1 at both the mRNA and protein level. Thus, SDF2L1 expression is detected in rat and mouse islets, is induced by ER stress and is increased in models of type 2 diabetes.

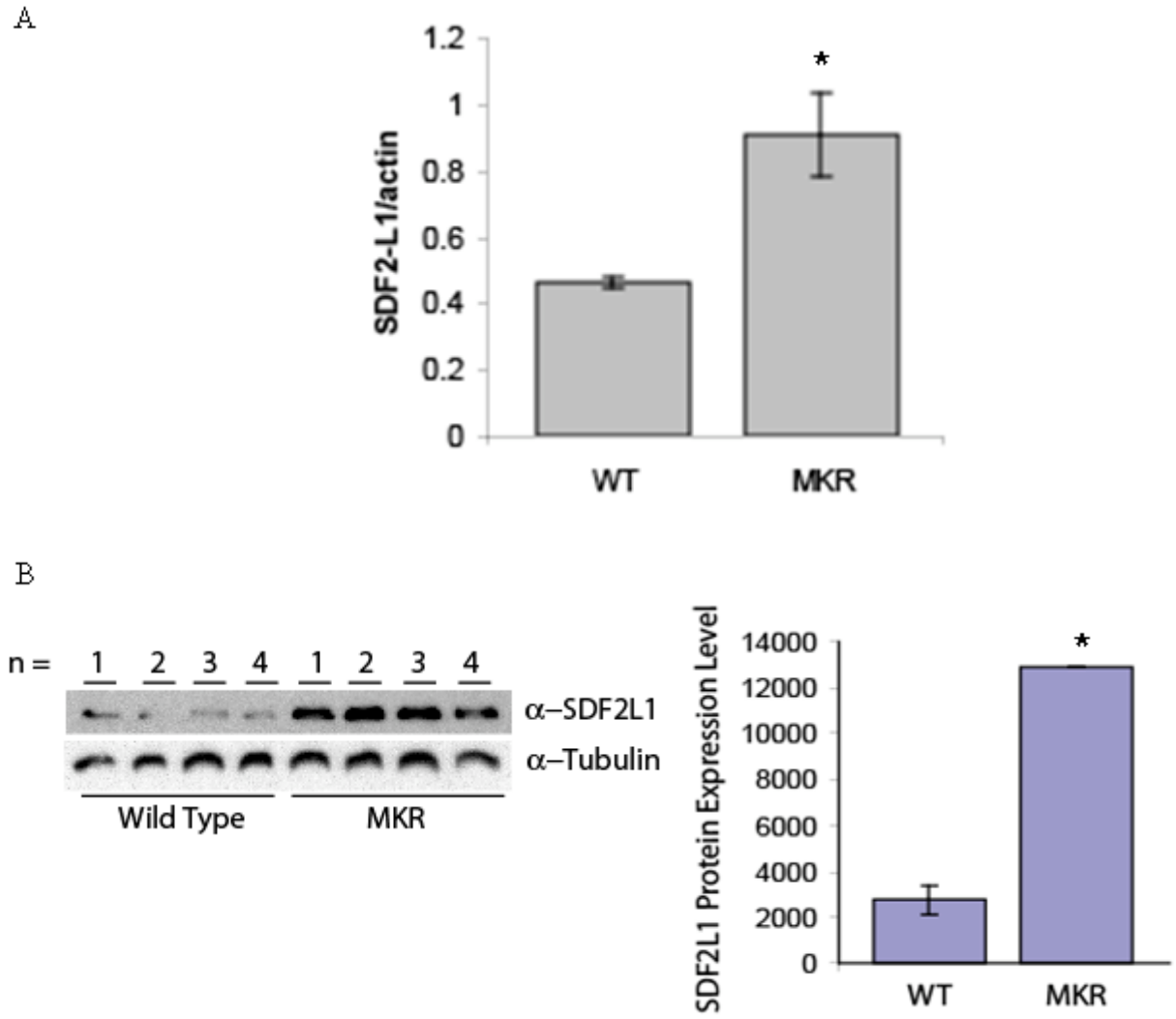

Figure 3.5: **SDF2L1 expression is increased in islets from MKR mice at the mRNA and protein level.** Total RNA isolated from 8 week old MKR and WT islets was analyzed by real-time PCR. The SDF2L1 mRNA levels are normalized to cellular β-actin. (N=3, *p<0.05 relative to control) (**A**). Total protein was isolated from 8 week old MKR and WT islets and analyzed by western blot. Tubulin is used as loading control. SDF2L1 protein level is significantly induced in MKR mice islets compared to WT mice islets. Band intensities were quantified and expressed as arbitrary units (right panel) (N=4, *p<0.05) (**B**).

3.02.2 Examine if SDF2L1 depletion sensitizes β-cells to ER-Stress

SDF2L1 is highly induced in response to ER stress, suggesting that it is an important and possibly essential component of the ER-stress response. To test this, the effect of the absence of SDF2L1 on the unfolded protein response (UPR) markers was examined. It is **hypothesized** that removal of SDF2L1 in β-cells will sensitize them to ER-stress, thus upregulating ER-stress response markers to a greater extent for a given amount of stress than in cells expressing SDF2L1.

SDF2L1 knock down was performed using an siRNA approach. INS-1 832/13 cells were transfected for 48 h with an SDF2L1 specific siRNA (S), control GFP siRNA (G) or cells were untreated (C). Total mRNA or total protein was isolated and analyzed by qPCR and western blot, respectively (**Figure 3.6**). SDF2L1 was efficiently knocked-down at both the mRNA and protein level, which is better observed under ER stress conditions. siRNA-mediated knock down of SDF2L1 in proinsulin C96Y-GFP cells could also be observed (data not shown).

Since SDF2L1 is markedly induced by ER stress I tested whether knock-down of SDF2L1 results in increased ER stress as reflected in the levels of ER stress response genes. Thus, the level of ER stress response gene induction is reflective of the level of ER stress sensed by the cell. The effect of SDF2L1 KD on the mRNA levels of markers such as GRP78/BiP, ATF-4 and CHOP was determined by transfecting INS-1 832/13 cells with SDF2L1 or control siRNA and analyzing the samples by real time PCR. The mRNA level of GRP78/BiP increased with both the low dose (0.2μg/ml) and high dose (2μg/ml) Tm treatment in Ins-1 832/13 cells, as expected. There was no difference, however, in the expression of GRP78/BiP with SDF2L1 siRNA as compared to untreated or control siRNA conditions (**Figure 3.7 A**).

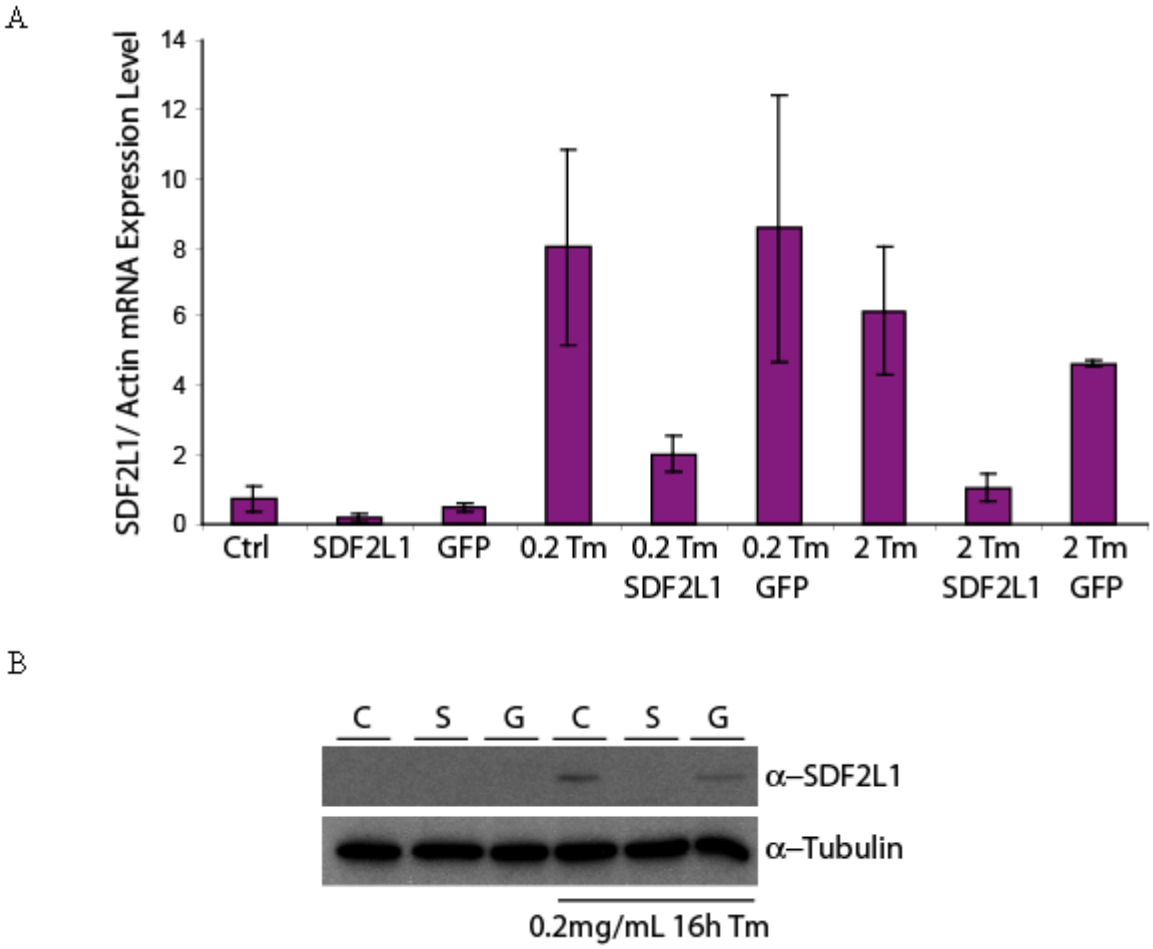

Figure 3.6: **SDF2L1 is effectively knocked-down using an siRNA approach at both mRNA and protein levels.** INS-1 832/13 cells were transfected with SDF2L1 siRNA (SDF2L1), GFP siRNA (GFP) or untreated (Ctrl), for 48 h. At 24 h following transfection, the cells were untreated or treated with either low dose (0.2 μg/ml) or high dose (2 μg/ml) Tm for 16 h. Following treatment, the total mRNA was isolated and the samples were analyzed by real time PCR. The SDF2L1 mRNA levels are normalized to cellular β-actin (N=3) (**A**). INS-1 832/13 cells were transfected with SDF2L1 siRNA (S), GFP siRNA (G) or untreated (C), for 48 h. At 24 h following transfection, the cells were untreated or treated with low dose (0.2 μg/ml) Tm for 16 h. Following treatment the cells were washed with PBS, lysed, and equal amounts of protein was resolved by SDS-PAGE and immunoblotted with α-SDF2L1 and α-tubulin antibodies. Result is representative of N=3 experiments.

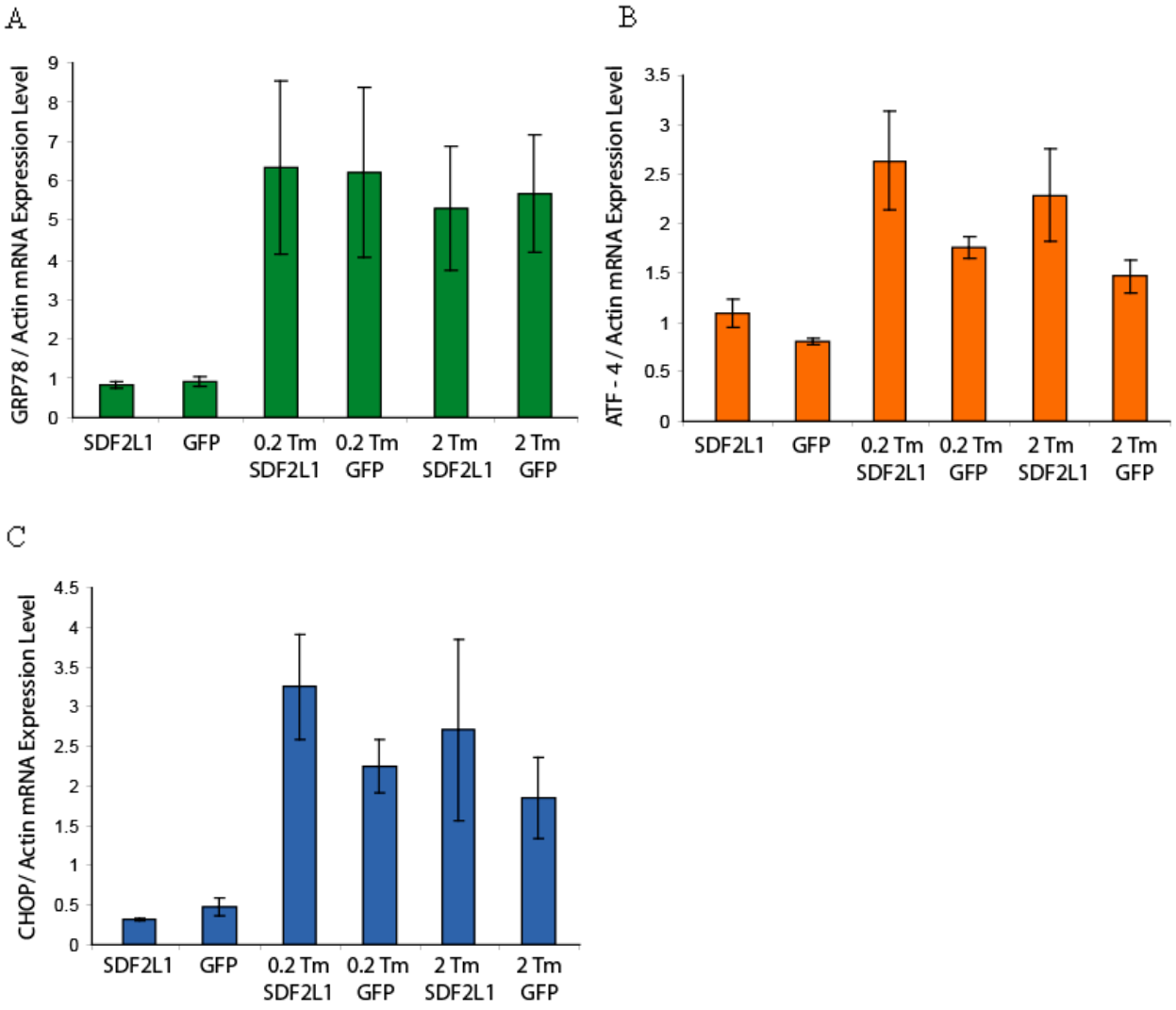

Figure 3.7: **SDF2L1 KD does not significantly affect the mRNA levels of GRP78/BiP, ATF-4 or CHOP.** INS-1 832/13 cells were transfected with SDF2L1 siRNA (SDF2L1) or GFP siRNA (GFP) for 48 h. At 24 h following transfection, the cells were untreated or treated with either low dose (0.2 µg/ml) or high dose (2 µg/ml) Tm for 16 h. Following treatment, the total mRNA was isolated and the samples were analyzed by real time PCR for GRP78/BiP (**A**), ATF-4 (**B**) and CHOP (**C**) expression. The mRNA levels are normalized to cellular β-actin (results is from N=3 independent experiments).

Similarly, ATF-4 mRNA levels increased in INS-1 832/13 cells with low dose and high dose Tm treatment, however, there was no significant difference in ATF-4 mRNA levels in the SDF2L1 KD compared with control siRNA conditions (**Figure 3.7 B**). However, in both the low dose and high dose Tm treatment conditions there is a slight increase in the mRNA levels of ATF-4, suggesting that there may be a trend towards increased induction in SDF2L1 KD conditions. In fact, the same effect is observed with CHOP mRNA levels. CHOP mRNA is induced in both low dose and high dose Tm treatment conditions (**Figure 3.7 C**). Although there is no significant difference in CHOP mRNA in SDF2L1 KD conditions compared with control siRNA conditions, there is a trend towards higher CHOP mRNA levels in cells depleted of SDF2L1. Thus, although under these ER stress conditions SDF2L1 KD does not significantly affect GRP78/BiP, ATF-4 or CHOP mRNAs levels, there is a clear trend towards an increased level of ATF-4 and CHOP in the absence of SDF2L1.

Although SDF2L1 did not have a significant effect on the mRNA levels of the UPR markers, it is possible that there may be a more prominent effect at the protein level. The effect of SDF2L1 KD on the protein levels of ER chaperones GRP78/ BiP and GRP94 was determined by transfecting INS-1 832/13 cells with SDF2L1 siRNA or control siRNA and analyzing the samples by western blot (**Figure 3.8 A**). In addition, the effect of SDF2L1 on the protein levels of the ERAD component HERP was also assessed. The resulting immunoblots were quantified using Scion Image. GRP78/BiP protein levels increase with high dose (2μg/ml) Tm treatment. Compared to untreated and control siRNA conditions there was no greater induction of GRP78/BiP with SDF2L1 KD (**Figure 3.8 B**). However, although not significant, a slight increase in GRP78/BiP protein levels was observed in the SDF2L1 KD condition compared to

control with Tm treatment. A similar result was observed for GRP94 (**Figure 3.8 C**) and HERP (**Figure 3.8 D**).

In preliminary experiments I also examined activation of the IRE-1α pathway to determine if this branch of the UPR is upregulated in the absence of SDF2L1. An XBP-1 splicing assay was performed as described in the Methods **2.04**. Higher spliced XBP-1 levels were observed in the low dose and high dose Tm treatment as compared to control conditions, although transfection with siRNAs in general increased spliced XBP-1 levels compared to untransfected cells. However, compared to the control GFP siRNA conditions, no significant change in the XBP-1 splicing was observed with the SDF2L1 KD conditions at either low or high dose Tm treatment conditions (**Figure 3.9**), although additional experiments are required to confirm this. In addition, the activation of the IRE-1-JNK pathway was examined by examining the levels of JNK phosphorylation in the absence of SDF2L1. At the high dose Tm treatment the level of JNK phosphorylation is only slightly induced by Tm treatment and it does appear that there may be increased phospho-JNK levels in SDF2L1 KD conditions (**Figure 3.10**). However, this preliminary result requires additional experimentation to verify this finding.

In summary, although not definitive, the results in this section suggest that pancreatic β-cells which are unable to induce SDF2L1 may be at a disadvantage in responding to ER stress, i.e. they may have an inadequate ER stress response and experience greater ER stress levels. As a consequence these cells may potentially be more susceptible to ER stress-induced cell death.

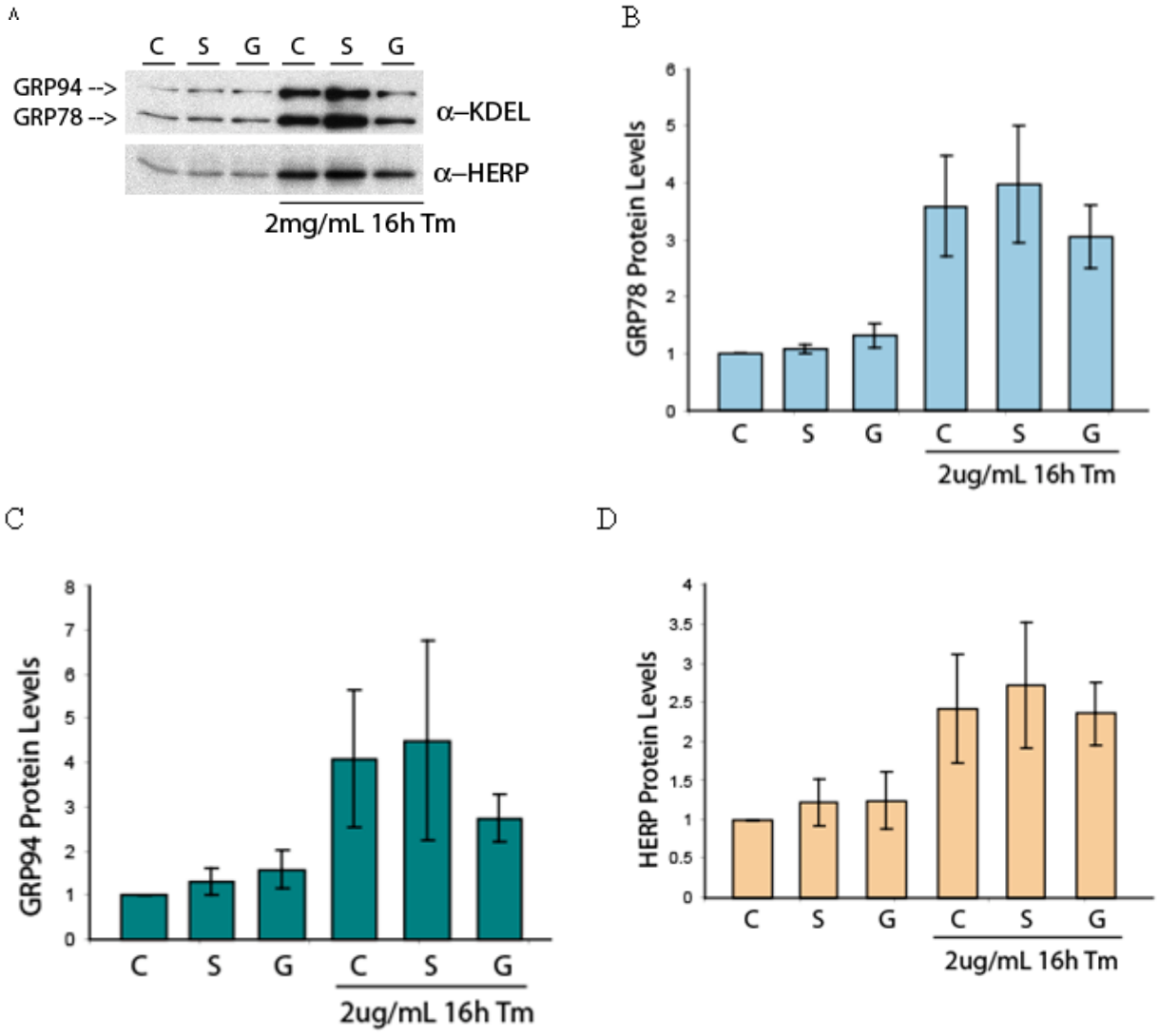

Figure 3.8: **SDF2L1 KD does not significantly affect the protein levels of GRP78/BiP, GRP94 or HERP.** INS-1 832/13 cells were transfected with SDF2L1 siRNA (S), GFP siRNA (G) or untreated (C), for 48 h. At 24 h following transfection, the cells were untreated or treated with high dose (2 μg/ml) Tm for 16 h. Following treatment the cells were washed with PBS, lysed, and equal amounts of protein was resolved by SDS-PAGE and immunoblotted with α-KDEL and α-HERP antibodies (**A**). The resulting blots were quantified using Scion Image. Quantification of GRP78 (N=6) (**B**). Quantification of GRP94 (N=6) (**C**). Quantification of HERP (N=3) (**D**).

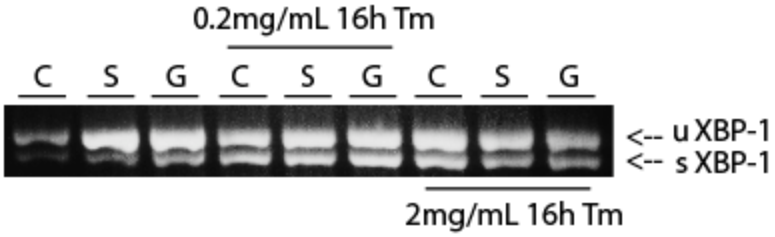

Figure 3.9: XBP-1 splicing is not affected by SDF2L1 KD. INS-1 832/13 cells were transfected with SDF2L1 siRNA (S), GFP siRNA (G) or untreated (C), for 48 h. At 24 h following transfection, the cells were untreated or treated with either low dose (0.2 μg/ml) or high dose (2 μg/ml) Tm for 16 h. Following treatment, the total mRNA was isolated and the samples were analyzed for unspliced and spliced XBP-1 as described in Methods section (2.04) (N=2).

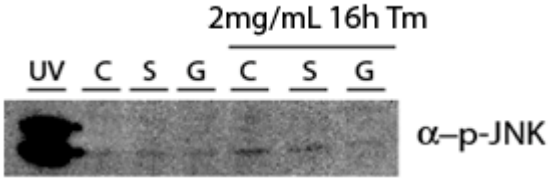

Figure 3.10: **Effect of SDF2L1 KD on phospho-JNK levels.** INS-1 832/13 cells were transfected with SDF2L1 siRNA (S), GFP siRNA (G) or untreated (C), for 48 h. At 24 h following transfection, the cells were untreated or treated with 2μg/ml Tm for 16 h. Following treatment the cells were washed with PBS, lysed, and equal amounts of protein was resolved by SDS-PAGE and immunoblotted with α-phospho-JNK antibody. Cells exposed for 15 min to UV light serve as a positive control for phosphor-JNK. (N=1)

3.02.3 Examine if SDF2L1 depletion sensitizes β-cells to ER-stress-induced apoptosis

As previously mentioned, the UPR leads to global translational attenuation, however, some proteins such as ATF-4 are selectively translated and activate the UPR target genes, including CHOP, which leads to apoptosis. The absence of SDF2L1 led to a non-significant but slight trend towards increased ATF-4 and CHOP mRNA levels in response to ER stress as shown in **Figure 3.7**. Thus, it is possible that the absence of SDF2L1 may be sensitizing β-cell to ER stress and potentially apoptosis. Since the UPR markers were not significantly induced, under control conditions it is unlikely that the SDF2L1 KD cells will show detectable apoptosis. However, it is **hypothesized** that under ER stress conditions apoptosis may be greater in SDF2L1 KD cells compared to control.

To test this hypothesis, INS-1 832/13 cells were transfected with control or SDF2L1 siRNA, then treated with Tm and analyzed for their expression of the apoptotic marker cleaved caspase 3 (CC3). When the cells were treated with high dose Tm (2μg/ml), SDF2L1 expression increased and this increase was blunted at both basal and Tm treatment conditions in SDF2L1 siRNA transfected cells (**Figure 3.11**). CC3 expression was only detected with Tm treatment. However, no significant difference could be observed in the expression level in SDF2L1 KD cells compared to the Lac Z control siRNA transfected cells.

As shown in **Figure 3.6A**, the expression of SDF2L1 tends to be higher with low dose Tm treatment compared to high dose Tm treatment. In fact, a similar result is observed with the chaperone GRP78/BiP (**Figure 3.7A)**. Since induction of chaperone proteins is one of the principle actions of the UPR, it is likely that chaperones are highly upregulated with lower levels of ER-stress, to effectively alleviate it without resorting to apoptosis, i.e. the level of ER stress

may be surmountable by the activated UPR. Thus, it is possible that at lower doses of Tm the effect of SDF2L1 on Tm-induced apoptosis may be more apparent, if indeed SDF2L1 upregulation is an essential aspect of the UPR.

To test this hypothesis, INS-1 832/13 cells were treated or not with low dose (0.2μg/ml) Tm in the presence or absence of SDF2L1 knock-down (**Figure 3.12**). In the Tm treatment conditions there is slight increase in the CC3 levels in the SDF2L1 KD condition compared to the untreated and the GFP KD control conditions. The difference, however, is not significant. None-the-less there appears to be a trend towards greater apoptosis in SDF2L1 knock-down cells. This result is consistent with **Figure 3.7C**, where the mRNA levels of the apoptotic marker CHOP tended to be higher in SDF2L1 KD cells treated with low dose Tm (0.2μg/ml) compared to control siRNA-treated cells.

Although there was a slightly higher CC3 expression in SDF2L1 KD cells compared to controls in INS-1 832/13 cells with low dose Tm treatment, the increase was not significant. It is possible that western blotting is not sensitive enough to detect small changes in the amount of apoptotic cells. Thus, an apoptosis ELISA assay was used to detect cell apoptosis (see Methods). This ELISA assay detects oligonuclosomes in the cytosol, which is indicative of the endonuclease activity during apoptosis. INS-1 832/13 cells were transfected with control Lac Z siRNA or SDF2L1 siRNA for 48 h then treated with Tm for 16 h. The cells were then washed in PBS and lysed in 1% TX-100 lysis buffer to determine total cellular protein levels or cell cytosol was prepared for analysis by the ELISA kit. As shown in **Figure 3.13A**, total cellular protein levels were lower in the Tm treated samples and protein levels were slightly lower in SDF2L1 KD vs. control siRNA-treated samples. Relative apoptosis levels as measured by the apoptosis

ELISA and normalized to relative protein levels in the wells were significantly higher in Tm treated conditions compared to control conditions as expected. Importantly, apoptosis in the presence of Tm was significantly higher in SDF2L1 siRNA-treated cells relative to the control (Lac Z siRNA)-treated cells (**Figure 3.13 B**). This indicates that in the absence of SDF2L1 a greater percentage of INS-1 832/13 cells undergo ER stress-induced apoptosis, suggesting that SDF2L1 is an important and cell protective component of the UPR response.

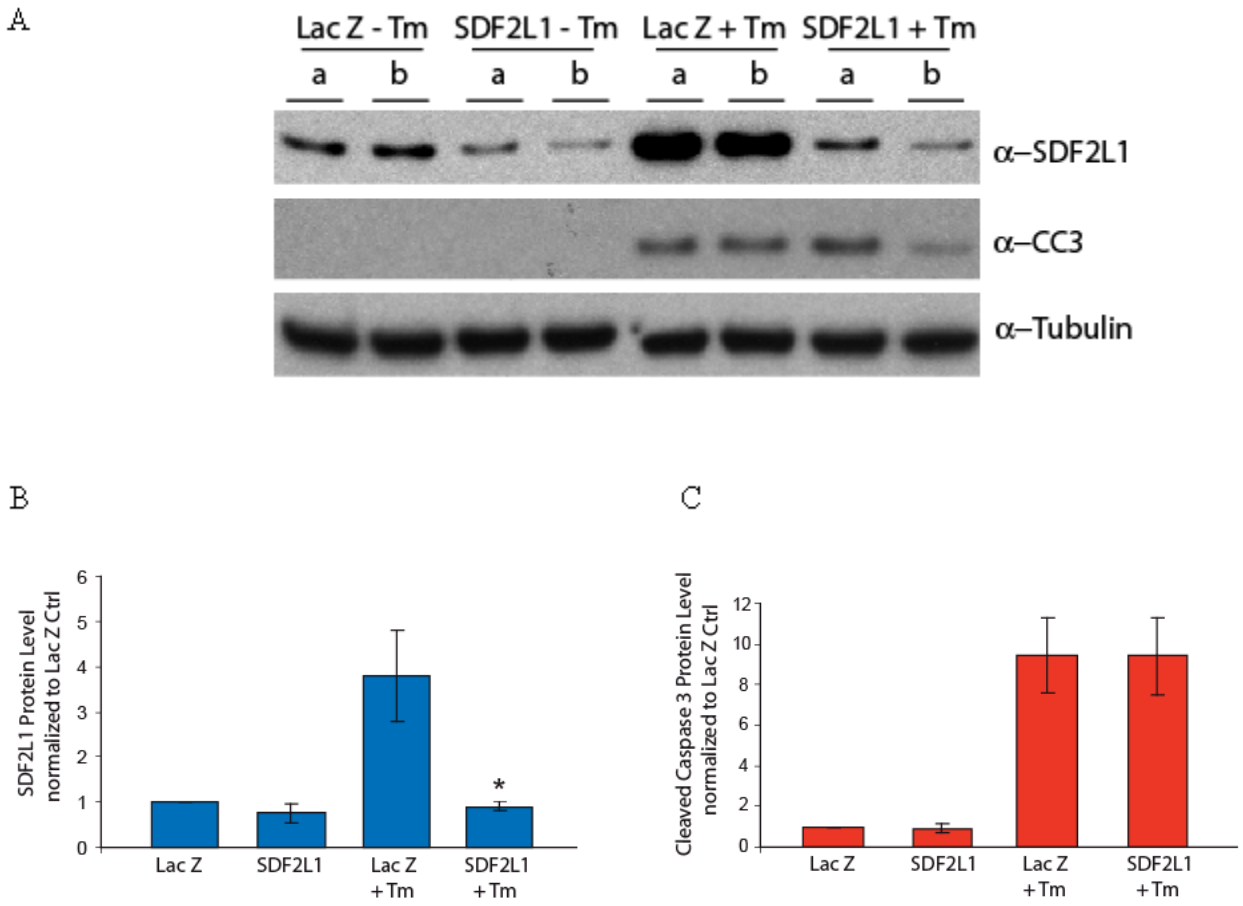

Figure 3.11: **Effect of SDF2L1 KD on cleaved caspase 3 (CC3) protein levels in cells treated with high dose Tm.** INS-1 832/13 cells were transfected with SDF2L1 siRNA (SDF2L1) or Lac Z siRNA (Lac Z) for 48 h. At 24 h following transfection, the cells were untreated or treated with high dose Tm (2µg/ml) for 16 h. Following treatment the cells were washed with PBS, lysed, and equal amounts of protein were resolved by SDS-PAGE and immunoblotted with α-SDF2L1, α-CC3 and α-Tubulin antibodies (**A**). The resulting blots were quantified using Scion Image. Quantification of SDF2L1 reveals an 85% reduction in protein levels with siRNA in Tm treatment condition (*$p<0.05$; N=6) (**B**). Quantification of CC3 (N=6) (**C**).

A

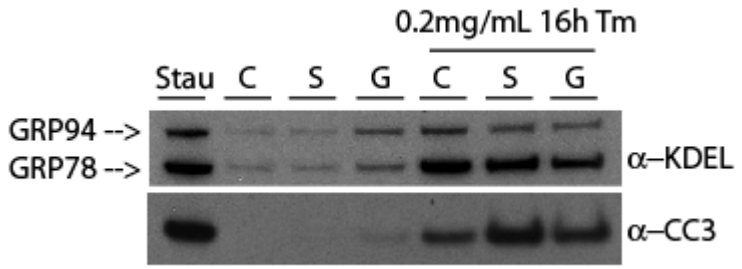

B

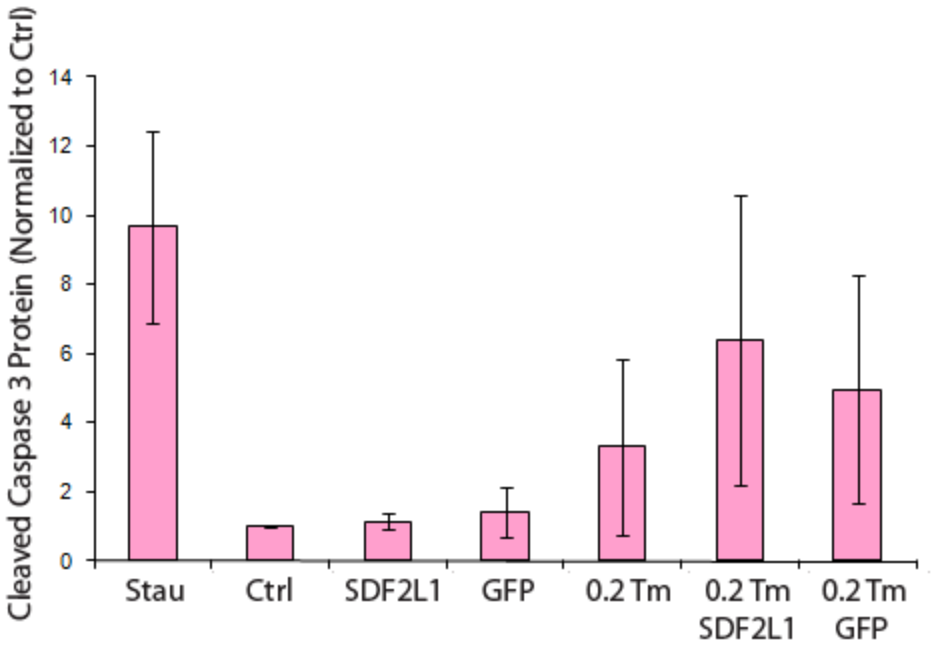

Figure 3.12: **The effect of SDF2L1 KD on cleaved caspase 3 (CC3) levels with low dose Tm.** INS-1 832/13 cells were transfected with SDF2L1 siRNA (S), GFP siRNA (G) for 48 h or were untreated (C). At 24 h following transfection, the cells were untreated or treated with low dose (0.2μg/ml) Tm for 16 h. Staurosporine (Stau) treated cells were used as positive controls for CC3 expression. Following treatment the cells were washed with PBS, lysed, and equal amounts of protein was resolved by SDS-PAGE and immunoblotted with α-KDEL and α-CC3 antibodies (**A**). The resulting blots were quantified using Scion Image. Quantification of CC3 (N=3) (**B**).

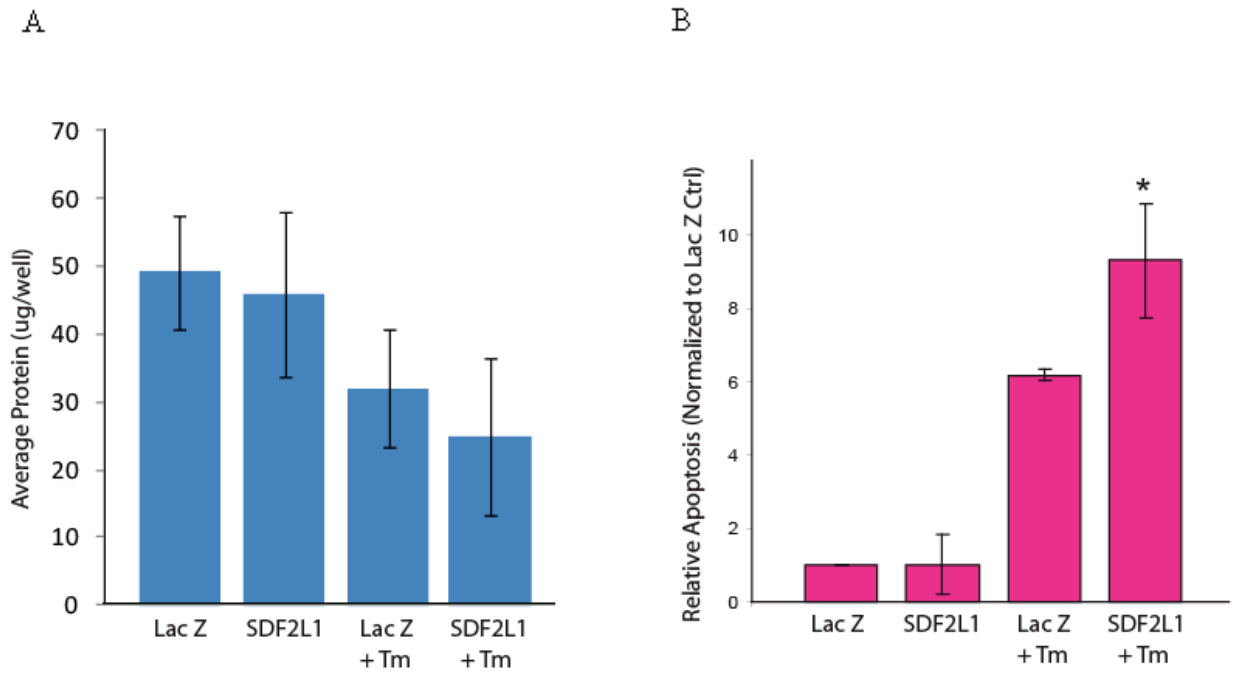

Figure 3.13: **Effect of SDF2L1 KD on ER-stress induced apoptosis as detected by Roche apoptosis ELISA Assay.** INS-1 832/13 cells were transfected with SDF2L1 siRNA (SDF2L1) or Lac Z siRNA (Lac Z) for 48 h. At 24 h following transfection, the cells were untreated or treated with high dose (2µg/ml) Tm for 16 h. Following treatment the cells were washed with PBS, lysed, and the protein levels in the various conditions were determined using a BSA protein assay (**A**). The apoptotic signal was analyzed by the Roche Apoptosis Eliza Assay that detects cytoplasmic DNA-oligosomes, as described in the Methods section 2.11 (*$p<0.05$; N=4) (**B**).

3.03 Discussion

By microarray studies on the ER stress response in pancreatic β-cells, it was discovered that SDF2L1 was markedly induced by expression of a folding-deficient proinsulin (Hartley 2010). SDF2L1 is a relatively novel protein that was discovered to be induced by ER-stress and initial northern blotting indicated that SDF2L1 is a wide tissue distribution (Fukuda 2001). However, there are only a limited number of publications on this protein and many questions remain regarding its induction by cell stress, protein distribution and its role in the ER stress response. In this chapter the goal was to establish whether SDF2L1 mRNA and protein are induced by ER stress and potentially other cell stressors in pancreatic β-cells and other cell types and to identify if SDF2L1 is an essential or important component of the ER stress response in pancreatic β-cells.

The general ER stress response is well-established and includes an initial translational attenuation, followed by upregulation of the UPR genes including chaperones, ERAD components, and apoptotic genes. However, it is becoming apparent that different cell types respond differently to ER stress by upregulating a unique set of genes depending on the cell's function and secretory proteins produced (Hutt 2009). Indeed, I found a differential expression pattern of SDF2L1 protein with some cell types having robust expression (Hela, HEK293), moderate expression (pancreatic β-cell lines) and no apparent expression (glial cell lines) (**Figure 3.2**). The 2001 study by Fukuda *et al*, using northern blot analysis found that SDF2L1 mRNA expression is low in murine brain tissue and absent in human brain tissue, which is consistent with our findings. Interestingly, it has been previously shown that SDF2L1 has higher mRNA expression in certain cancers (Kang 2009). SDF2l1 is also shown to be associated with

the Metastasis Efficiency Modifier Ribosomal RNA Processing 1 Homolog B (RRP1B), which is a chromatin-associated factor (Crawford 2009). Therefore, SDF2L1 may be required for cells that replicate rapidly and therefore produce large amounts of protein. It is interesting to note that HEK293 and HELA cells, express high levels of SDF2L1 even under basal conditions. It is possible that these cancer cells lines are undergoing some ER stress even under basal conditions. Several cancers have been linked to ER stress including pancreatic cancer, prostate cancer and breast cancer (Kang 2009; Mahadevan 2010; Hess 2011).

Importantly, SDF2L1 expression was also detected in primary rat islets and appears to be induced by ER stress in vitro, although the results are preliminary (**Figure 3.4**). However, well established murine models of diabetes are associated with elevated ER stress markers in pancreatic islets. Indeed, I observed elevated levels of SDF2L1 mRNA and protein in islets isolated from diabetic MKR mice **Figure 3.5**. MKR mice have dominant negative insulin-like growth factor receptor mutations in skeletal muscles and severe insulin resistance in that tissue, which leads to excessive secretion burden on the β-cell and diabetes at 8 weeks (Fernandez 2001; Lu 2008). ER stress markers have been found to be elevated in these islets, which are dysfunctional (i.e. have insulin secretion defects), but are not apoptotic. Thus, elevated levels of SDF2L1 and other UPR genes/ proteins may be protective in these mice. It will be interesting and important to examine SDF2L1 expression in other rodent models of type 2 diabetes.

It has been previously shown that SDF2L1 mRNA expression increases with Tm, calcium ionophore A23187 and heat shock treatments (Fukuda 2001). To determine if SDF2L1 expression is specific to ER-stress, other cellular stressors such as staurosporine (an inhibitor of protein kinases and an activator of CC3), thapsigargin (inhibitor of SERCA pump), H_2O_2

(oxidative stressor), 3-Amino-1,2,4-triazole (a competitive inhibitor of the HIS3 gene product imidazoleglycerol-phosphate dehydratase which catalyzes histidine production), and Arsenic (a potent inhibitor of the Kreb's cycle) were used (**Figure 3.3**). Tm was the only treatment that significantly increased SDF2L1 protein levels in the cell types that express this protein, thus induction is specific to ER stress. Induction of ER stress was confirmed by monitoring expression of GRP78/BiP and GRP94, which were also significantly with Tm treatment in all cell lines. ATZ and heat shock treatments also led to mild induction of the GRP78/BiP and GRP94 proteins in INS-1 cells, yet SDF2L1 expression was not changed. The ER stress specificity of SDF2L1 induction remains to be established.

Given that SDF2L1 is expressed in pancreatic β-cell lines and rodent islets and is markedly induced under ER stress conditions, I wanted to determine whether SDF2L1 up-regulation is a cell survival aspect of the UPR and whether this is important or essential. I attempted to answer this question by preventing the up-regulation of SDF2L1 in response to ER stress to determine if this affected the "level" of ER stress in the cell and whether this affected ER stress-induced apoptosis. An siRNA mediated knock down approach was used to determine if SDF2L1 is an essential component of the UPR and if its absence leads to β-cell sensitization to ER-stress and ER-stress induced apoptosis.

SDF2L1 was effectively knocked down by siRNA in INS-1 832/13 cells (**Figure 3.6**). To determine the effect of SDF2L1 knock-down on cellular ER stress I monitored the induction of several ER stress response genes (GRP78, ATF4, CHOP) and the level of IRE1a pathway activation (XBP-1 splicing and phosphor-JNK levels) in response to both low and high dose tunicamycin (Tm) treatment. Although, the results were not conclusive, there was a trend

towards higher levels of ATF4, CHOP and phospho-JNK upregulation in SDF2L1 knock-down cells, potentially suggesting that these cells may be experiencing greater levels of ER stress and as such try and mount a more robust ER stress response. It should be noted that the levels of these UPR response genes tended to be higher at the low dose of Tm compared to high dose even in control cells. This is likely explained by the fact that at higher doses of Tm (greater ER stress) the IRE-1 endoribinuclease activity is greater leading to increased degradation of mRNAs encoding secretory proteins (Han 2009).

The trend towards increased ER stress experienced by cells unable to up-regulate SDF2L1 suggested that they may be more sensitive to ER stress-induced apoptosis. Indeed, although the effect was small, a quantitative and sensitive assay of apoptosis did detect that Tm-induced apoptosis was higher in INS-1 832/13 cells depleted of SDF2L1 expression (**Figure 3.13**) and there was a trend towards higher levels of the pro-apoptotic marker CHOP. Thus, upregulation of SDF2L1 in response to ER stress is likely to be a cell beneficial response, that when absent predisposes the cells to increased ER stress and consequently ER stress-induced apoptosis. This result is consistent with the particularly high levels of SDF2L1 found in fast dividing cancer cells such as HELA and HEK293 cells (**Figure. 3.2, 3.3**), which likely experience some basal ER stress and require high levels of ER chaperones and other ER proteins to maintain rapid cell growth and survival.

Future studies need to examine the actual role that this pro-survival ER stress-inducible protein plays in cells and in particular the pancreatic β-cell.

3.04 Summary and Future Directions

SDF2L1 is expressed in insulinoma cell lines (INS-1, INS-1 832/13, INS-1 proinsulinC96Y-GFP) and in various other cell types including HEK293 and HeLa cells, but not glial cell lines. Thus, SDF2L1 has a restricted protein distribution. Indeed, it would be interesting to extend this analysis to other transformed cell lines and more importantly to healthy tissues. The restricted cell distribution suggests that SDF2L1 is unlikely to have a general role in the cell, such as ubiquitous ER chaperones like GRP78 or calnexin. More likely it may have specialized roles in the ER, which would be more like DNAJ type co-chaperone proteins that likely also have more restricted cell distribution.

Importantly, SDF2L1 was detected in primary rodent islets and was found to be upregulated in islets from one rodent model of diabetes, the MKR mouse. This is an interesting finding since, although ER stress markers are up-regulated in islets from MKR mice, which are diabetic, islet mass in these animals is normal (Fernandez 2001; Lu 2008). Thus, apoptosis of β-cells is not the primary reason for the reduced insulin secretion in these animals. It appears that the ER stress response (including SDF2L1 induction) is sufficient to deal with the ER stress otherwise cell death should be detected. Indeed, it would be interesting to examine the effect of β-cell specific knock-out of SDF2L1 in the MKR background. Indeed, if SDF2L1 contributes to promoting cell survival as our results suggest, then removal may predispose the β-cells to ER stress-induced apoptosis, which would exacerbate diabetes development in these animals. Additionally, it would be interesting to examine SDF2L1 expression in other rodent models of diabetes, particularly those in which β-cell death (apoptosis) contributes to diabetes development, such as in high fat fed C57Bl6 mice, db/db mouse and Zucker Diabetic Fatty rats.

Our results suggest that the induction of SDF2L1 protein is ER stress specific. Similar experiments should also test the effect of various stressors on the mRNA level. However, I have shown that ER stress induced by Tm (and mutant proinsulin expression) induces SDF2L1 mRNA expression. Thus, it would be interesting to identify the regulatory elements in the promoter region of SDF2L1 that are responsible for its upregulation in response to ER stress. In addition, it would be interesting to identify which of the ER stress-induced transcription factors bind these regions to induce SDF2L1 transcription. These studies can be done using luciferase-based promoter activation studies and by gel-shift assays to identify potential transcription factors that bind the SDF2L1 promoter.

Finally, preliminary results are presented that favor the hypothesis that SDF2L1 is likely to have a protective role as part of the UPR. However, for the most part the results show clear trends, but are not significant and thus not conclusive. Some of the experiments such as monitoring ER stress-induced expression of UPR genes (ATF4, CHOP mRNA) in SDF2L1 knock-down and control cells can be repeated to generate a greater N number, which may reveal significant results. Additionally, even lower doses of Tm can be tried to perhaps tease out a significant result. It appears that even with the low dose Tm used here, the UPR is almost maximally induced making it difficult to reveal a higher level of ER stress in SDF2L1 knock-down cells.

However, it is encouraging that SDF2L1 KD did significantly sensitize the cells to ER-stress (Tm-induced) apoptosis as measured by the Cell Death ELISA. However, since the cleaved caspase 3 result was not significant the result remains tenuous. Thus, additional

quantitative apoptosis assays can be performed such as TUNEL staining followed by FACS analysis.

Overall, our results are suggestive of a cell protective role of SDF2L1 when the cell is faced with ER stress and the next challenge is to identify what function this small protein has in the ER lumen. The next chapter attempts to identify its interacting proteins and cellular function.

CHAPTER 4. IDENTIFICATION OF SDF2L1 INTERACTING PROTEINS AND ANALYSIS OF POTENTIAL ROLE IN ERAD

4.01 Introduction

SDF2L1 is upregulated in an ER-stress specific manner and the knock down of SDF2L1 in pancreatic β-cells leads to what appears to be a compromised ER-stress response and enhanced ER stress-induced apoptosis (Chapter 3). The function of SDF2L1 in the ER lumen is unknown. In proinsulin C96Y-GFP cells, which mimic the Akita mouse model of ER-stress induced β-cell dysfunction, SDF2L1 expression is increased (**Figure 3.1B**). It is possible that SDF2L1 may be interacting with the mutant proinsulin assisting with protein folding or possibly assisting in targeting of the terminally misfolded proinsulin to the ERAD machinery for degradation. It has been speculated that SDF2L1 may have a potential role in protein folding due to its association with the GRP78/BiP chaperone complex (Meunier 2002) and defensin proteins which are secreted by immune cells (Tongaonkar 2009).

If the proteins that interact with SDF2L1 were identified, it may provide insight into the function of SDF2L1. Thus, it is ***hypothesized*** that SDF2L1 may interact with ER molecular chaperones such as GRP78/BiP and possibly other ER-resident proteins, as well as misfolded proteins such as GFP-tagged mutant proinsulin. In this chapter, the interaction of SDF2L1 with mutant proinsulin and GRP78/BiP will be examined. In addition, binding assays will be conducted using a protein A-tagged SDF2L1 to identify proteins that interact with SDF2L1. Finally, the potential role of SDF2L1 in mutant proinsulin degradation will be evaluated.

4.02 Results

4.02.1 Examine potential SDF2L1 interacting proteins

A microarray analysis conducted with the proinsulin C96Y-GFP cell line identified that the one of the most highly upregulated genes in response to the expression of the mutant proinsulin was SDF2L1 (Hartley 2010). I have confirmed this result showing that SDF2L1 is upregulated at both the mRNA and protein level in response to misfolded proinsulin expression induced by doxycycline (**Chapter 3**). Given the fact that SDF2L1 is localized to the ER and is upregulated by accumulation of misfolded proinsulin it is possible that SDF2L1 interacts with the mutant proinsulin in the ER to either assist with folding of molecule or in its degradation by the ERAD system. I first examined if SDF2L1 interacts with proinsulin C96Y-GFP.

The proinsulin C96Y-GFP cells were treated with dox for 48 h to induce mutant insulin expression then the cells were lysed. The GFP-tagged mutant proinsulin was subsequently immunoprecipitated using α-GFP or α-IgG (control) antibodies and the samples were analyzed by western blot. As shown in **Figure 4.1**, SDF2L1 was detected in the supernatant fraction (SN), but not in the pellet (P) fraction for both the control IgG and the GFP immunoprecipitations. Thus, SDF2L1 does not appear to interact strongly with mutant proinsulin since it could not be co-immunoprecipitated, although it is still possible that SDF2L1 interacts weakly or transiently with the mutant proinsulin.

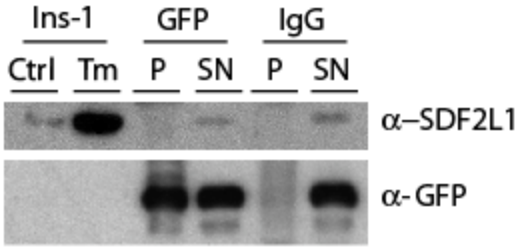

Figure 4.1: SDF2L1 is not associated with mutant proinsulin as detected by immunoprecipitation (IP). Proinsulin C96Y-GFP cells were incubated with doxycyline for 48 h. Following treatment the cells were washed with PBS and lysed. 100 µl of the lysate was incubated with either 5 µg mouse α-GFP or 5µg mouse IgG antibodies. Samples were subjected to immunoprecipitation with Protein G dynabeads; pellet (P) and 10 µg of supernatant (SN) fractions were resolved by SDS-PAGE and immunoblotted with α-SDF2L1 and rabbit α-GFP antibodies. INS-1 cells were treated with 2 µg/ml Tm for 16 h was used as a positive control for SDF2L1 expression.

If the interaction between SDF2L1 and mutant proinsulin is weak or transient, prior treatment with dithiobis(succinimidyl propionate) (DSP) cross-linker (which covalently cross-links closely associated proteins), should reveal any such weak interactions. To test this, dox treated proinsulin C96Y-GFP cells were incubated with 1 mM DSP prior to lysis and immunoprecipitation of the GFP-tagged mutant proinsulin (**Figure 4.2A**). The samples were analyzed by western blotting and revealed an interaction between SDF2L1 and proinsulin C96Y-GFP under the crosslinking conditions. This was not observed in the IgG control samples or in the non-crosslinked samples. This suggests that the interaction between SDF2L1 and mutant proinsulin may in fact be weak or transient and possibly indirect.

Given that SDF2L1 has been shown to be in a large complex containing GRP78/BiP (Meunier 2002) and other ER chaperones, it is possible that SDF2L1 interacts with mutant proinsulin through an association with GRP78/BiP. This was examined by repeating the

crosslinking study and analyzing the interaction between mutant proinsulin with GRP78/BiP and GRP94 (as detected with the α-KDEL antibody) (**Figure 4.2B**). A small amount of GRP78/BiP was found associated with mutant proinsulin even under non-crosslinked conditions. This suggests that GRP78/BiP likely interacts directly with mutant proinsulin, which is not surprising as GRP78/BiP has been found to associate with various misfolded proteins in the ER. In the DSP cross-linking samples the interaction between GRP78/BiP and mutant proinsulin was significantly increased as compared to the IgG control samples and the non-crosslinked samples. GRP94 did not show any interaction with mutant proinsulin in the non-crosslinked condition, but DSP treatment revealed some interaction with mutant proinsulin compared to the IgG control samples. This suggests that similar to SDF2L1, GRP94 only interacts weakly or transiently with mutant proinsulin.

In summary, it appears that SDF2L1 may interact weakly or transiently with the mutant proinsulin C96Y-GFP in the ER and that this interaction may possibly be via the chaperone GRP78/BiP, which interacts with mutant proinsulin with higher affinity given that cross-linking conditions are not required to detect an interaction. I next wanted to determine if SDF2L1 can interact with GRP78/BiP directly, as well as identify additional proteins that interact with SDF2L1. I thus generated a fusion protein construct containing protein A at the N-terminus linked to SDF2L1. Mammalian cell lines stably expressing and secreting this protein were generated so that it could be purified from either the cell lysate or from the cell media using affinity chromatography (**Appendix Section 6.02**). A mammalian cell line was used to generate the SDF2L1 fusion protein as opposed to bacterial expression in case potential post-translational modifications of SDF2L1 are required for protein interaction.

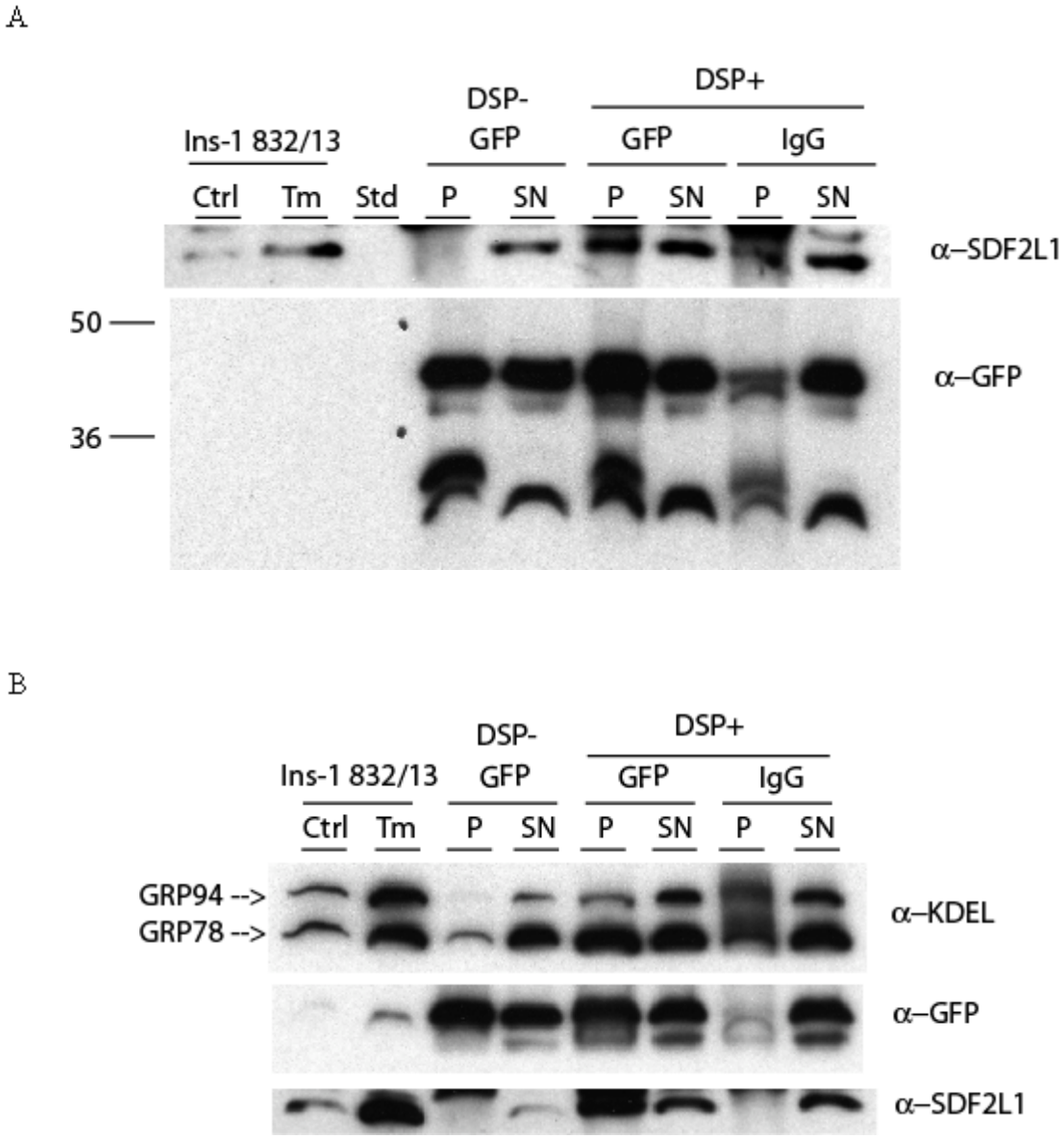

Figure 4.2: Interaction of mutant proinsulin with SDF2L1 and chaperone proteins GRP78/BiP and GRP94, as determined by DSP cross-linking. Proinsulin C96Y-GFP cells were treated with dox for 48 h followed by 30 min incubation with 1 mM dithiobis(succinimidyl propionate) (DSP), a thio-cleavable cross-linker. Following treatment the cells were washed with PBS and lysed. 100 µl of the lysate was incubated with either 5 µg mouse α-GFP or 5 µg mouse IgG antibodies. Samples were subjected to immunoprecipitation with Protein G dynabeads; pellet (P) and 10 µg supernatant (SN) fractions were resolved by SDS-PAGE and immunoblotted with α-SDF2L1 and rabbit α-GFP antibodies. INS-1 832/13 cells treated with 2 µg/ml Tm for 16 h were used as positive control for SDF2L1 (**A**). The experiment was repeated and analyzed by Western blot using α-SDF2L1, α-KDEL and α-GFP antibodies (**B**).

Protein A-tagged SDF2L1 was immunoprecipitated from the pA-SDF2L1#7 cell line using rabbit IgG agarose beads and utilized in binding assays to discover proteins interacting with SDF2L1. Since the DSP crosslinking studies revealed a weak or transient interaction of SDF2L1 with the mutant proinsulin, it was important to confirm this data using pA-SDF2L1 as a bait protein. pA-SDF2L1 bound to rabbit IgG agarose beads or control protein-A agarose beads were incubated with lysate from proinsulin C96Y-GFP cells. After an overnight incubation, the supernatant was removed and the pellet samples were washed. The pellet (P) and supernatant (SN) samples were then analyzed via western blot (**Figure 4.3**). The protein A-tagged SDF2L1 is detected as a large band at approximately 55 kDa. This band was not apparent in the supernatant samples or the protein A-agarose bead control sample. The GFP-tagged mutant proinsulin was only present in the supernatant samples and not the pA-SDF2L1 pellet, suggesting that mutant proinsulin does not directly interact with SDF2L1 under these conditions. The same result was observed for GRP94, as it was absent from the pellet lanes, suggesting that SDF2L1 does not directly interact with GRP94. Similarly, protein disulfide isomerase (PDI) did not show any direct interaction with pA-SDF2L1. However, GRP78/BiP was detected in the pA-SDF2L1 pellet, but not the control protein A pellet, indicating that GRP78/BiP is able to directly interact with SDF2L1. This interaction was increased in the Tm treated proinsulin C96Y-GFP samples likely due to higher GRP78/BiP expression in response to greater ER stress. As a control for specificity, the cytosolic chaperone HSP90 was not associated with pA-SDF2L1.

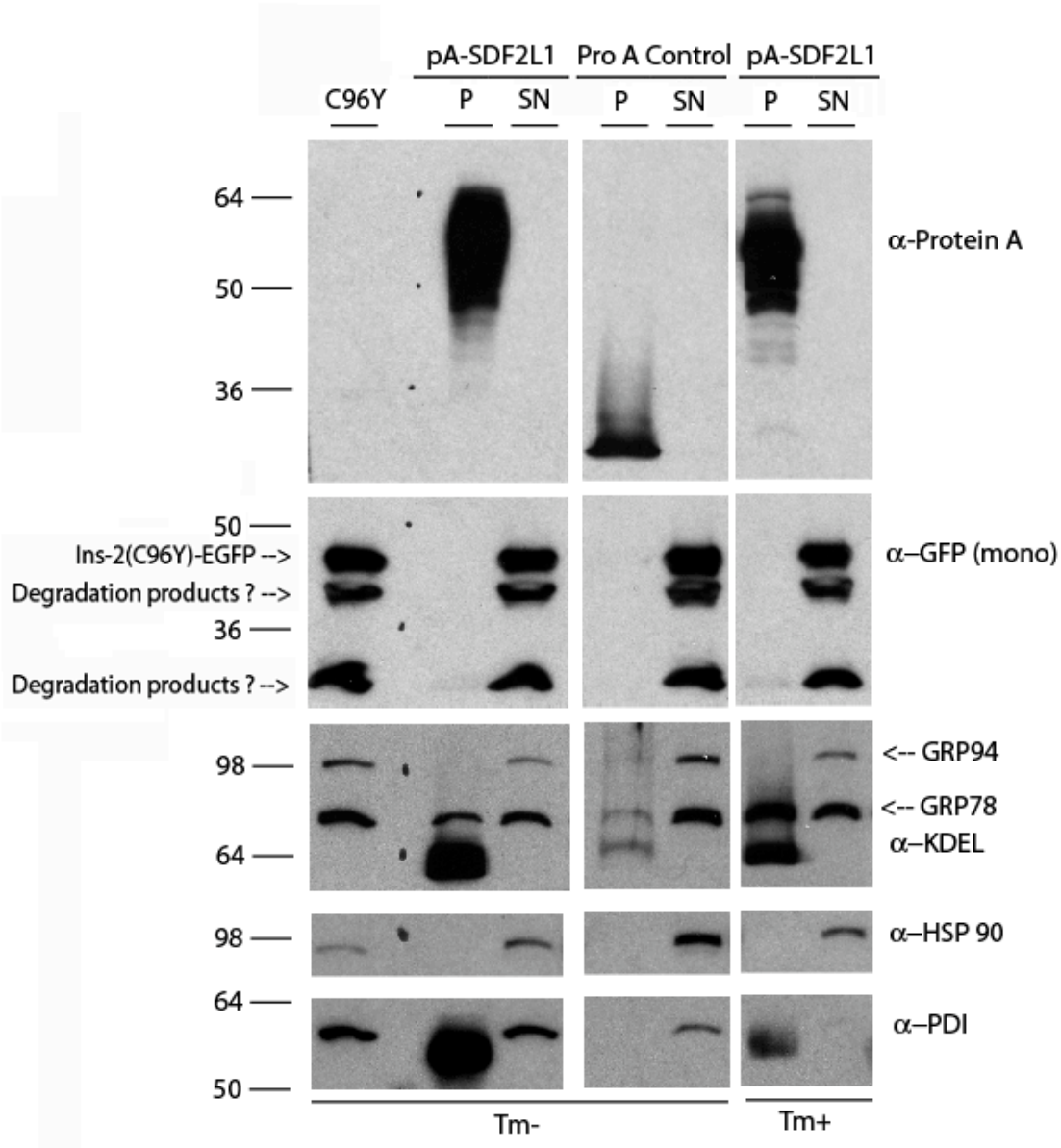

Figure 4.3: Protein A-tagged SDF2L1 interacts directly with GRP78/BiP. pA-SDF2L1 was isolated from lysates of pA-SDF2L1#7 cells using rabbit IgG-agarose beads as described in the Appendix section 6.02. The pA-SDF2L1 agarose beads (pA-SDF2L1) or Protein-A agarose control beads (ProA control) were incubated with 200 μg protein lysate from proinsulin C96Y-GFP cells untreated or treated with 2 μg/ml Tm overnight. After 24 h the supernatant fractions (SN) were removed, the pellets (P) were washed and 100% of the pellet fractions and 10 μg of the supernatant fractions were resolved by SDS-PAGE and immunoblotted with α-protein A, α-GFP, α-KDEL, α-HSP90 and α-PDI antibodies. 10 μg of lysate from proinsulin C96Y-GFP cells treated with 2μg/ml Tm for 16 h was run in Lane 1.

SDF2L1 directly interacts with molecular chaperone GRP78/BiP, which also interacts with mutant proinsulin. Thus, SDF2L1 may interact with mutant proinsulin indirectly, which may be the reason why cross-linking conditions are required to detect an interaction of mutant insulin with SDF2L1. Furthermore, although SDF2L1 can interact with GRP78/BiP it does not appear to directly interact with other chaperones including GRP94 or PDI.

To identify additional SDF2L1 interacting proteins binding assays were performed using concentrated lysates from mouse liver, a tissue with high secretory capacity and readily available compared to primary islets. The samples were resolved on SDS-PAGE, Coomassie blue stained and a prominent band specific to the protein A-SDF2L1 pellet (as compared to control protein A-agarose bead pellets) was analyzed via mass spectrometry (**Appendix section 6.03**). The peptides identified by mass spectrometry corresponded to several proteins. However, the protein with the highest percent coverage and highest number of peptides identified was the mammalian AAA+ protein p97/Valosin containing protein (VCP), also known as cdc48 in yeast.

As mentioned in the Introduction, p97/VCP is a ring-shaped hexameric type II ATPase, which is part of the AAA (**A**TPase **A**ssociated with diverse cellular **A**ctivities) protein family. It binds polyubiquinated ER-associated degradation substrates at the cytoplasmic face of the ER membrane, extracts the substrate using its ATPase activity and transfers the substrate to the 26S proteosome for degradation (Wójcik 2006). p97/VCP increases ERAD function and decreases ER stress as part of the UPR (Zhong 2004). Since p97/VCP is a cytosolic component of the ERAD machinery, it was necessary to confirm its interaction with pA-SDF2L1 by binding assays followed by western blot analysis.

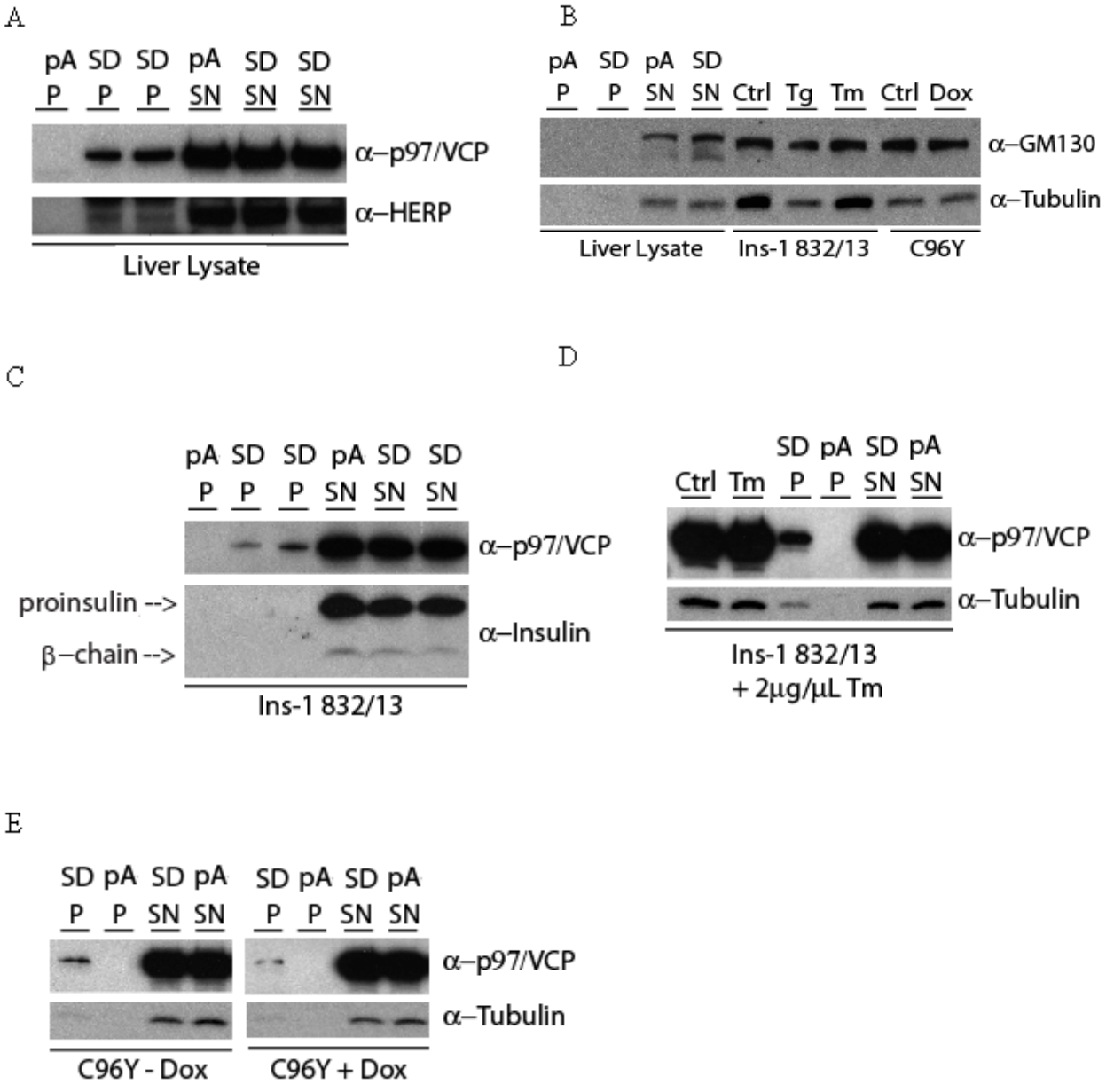

Figure 4.4: **Protein A-tagged SDF2L1 interacts with p97/VCP.** pA-SDF2L1 was isolated from pA-SDF2L1#7 cells using rabbit IgG agarose beads as described in Figure 4.3. pA-SDF2L1 agarose beads (SD) or protein A agarose control beads (pA) were incubated with 200 μg protein lysate from rat liver tissue. The pellet (P) and 10 μg of supernatant (SN) fractions were resolved by SDS-PAGE and immunoblotted with α-p97/VCP and α-HERP antibodies (**A**). The binding assay was repeated using liver lysate and immunoblotted for the control proteins GM130 and tubulin (**B**). To examine interactions in β-cells, the binding assay was repeated using lysates from INS-1 832/13 cells (**C**) and INS-1 832/13 cells treated with 2 μg/mL Tm for 16 h (**D**), and proinsulin C96Y-GFP cells treated or not with dox (**E**). Pellet and supernatant fractions were immunoblotted for the proteins indicated.

The protein A-tagged SDF2L1 was immunoprecipitated from pA-SDF2L1#7 cells and the pellet samples were incubated with liver lysate. The samples were washed and the pellet (P) and supernatant (SN) samples were analyzed by western blot to determine any potential interaction between SDF2L1 and p97/VCP (**Figure 4.4A**). Indeed, p97/VCP was detected in the pA-SDF2L1 pellet, which was not present in the protein A-agarose bead control pellet. This confirms the mass spectrometry data, suggesting an interaction between SDF2L1 and the ERAD component p97/VCP in liver lysates. To ensure that the binding observed was specific the binding assay was repeated and immunoblotted for two proteins not expected to interact with SDF2L1: GM130 (Golgi membrane protein) and tubulin (microtubule monomer protein) (Nakamura 1995; Howard 2003). No binding of either protein with pA-SDF2L1 was observed (**Figure 4.4B**).

I also tested whether pA-SDF2L1 interaction with p97/VCP could be detected using pancreatic β-cell lysates. The binding assay was repeated using lysates from untreated INS-1 832/13 cells and INS-1 832/13 cells treated with 2 μg/ml Tm for 16 h (**Figure 4.4C,D**). The presence of p97/VCP was detected in the pA-SDF2L1 pellet lane, which was not apparent in the protein A control samples. INS-1 832/13 cells produce proinsulin in the ER, which did not co-immunoprecipitate with pA-SDF2L1 (**Figure 4.4C**), although some tubulin could be detected in the pA-SDF2L1 pellet fraction, suggesting some non-specific binding in this experiment. Similarly, p97/VCP interaction with pA-SDF2L1 was detected using lysates from proinsulin C96Y-GFP cells (**Figure 4.4E**). Overall these results reveal an interaction between SDF2L1 and the ERAD component p97/VCP.

SDF2L1 is able to pull-down the ERAD component p97/VCP from both liver and β-cell TX-100 lysates. However, in the intact cell the interaction must be indirect since p97/VCP is localized to the cytosol, while SDF2L1 contains an N-terminal signal sequence and a C-terminal ER retention sequence and is an ER resident protein (Fukuda 2001. It is possible that SDF2L1 interacts with p97/VCP via other ERAD components. To test this hypothesis, binding assays were analyzed by western blotting for members of the ERAD machinery that have regions exposed to the ER lumen including Derlin-1, Derlin 2, Hrd-1 and EDEM. Compared to the protein A control pellet, the presence of Derlin-1 was apparent in the pA-SDF2L1 pellet fraction (**Figure 4.5A**). This suggests that there is an interaction between SDF2L1 and Derlin-1, which could potentially be direct. It is possible that SDF2L1 may have a role in the ERAD of non-glycosylated proteins. Derlin-1 expression did not increase in Ins-1 832/13 cells treated with Tm or Tg compared to untreated cells, or in proinsulin C96Y-GFP cells treated with Dox compared to untreated samples. This suggests that Derlin-1 is not an ER-stress inducible protein.

Similarly, Derlin-2 expression was visible in the pA-SDF2L1 pellet lane and not in the protein A control pellet (**Figure 4.5B**). This indicates that SDF2L1 may interact with Derlin-2 and have a role in the ERAD of glycosylated proteins. In addition, Derlin-2 expression also did not change in an ER-stress dependent manner in INS-1 832/13 cells or proinsulin C96Y-GFP cells. The same experiment was repeated for Hrd-1 and EDEM, however, the bands in the pA-SDF2L1 pellet were not clearly visible, likely because these antibodies are polyclonal and recognized by the protein A tag on SDF2L1. Thus, it is unclear whether these ERAD components are precipitated by pA-SDF2L1. Regardless, it does appear that ERAD components other than p97/VCP also associate with SDF2L1, suggesting that SDF2L1 could interact with the ERAD complex in vivo and may potentially have a functional role in the ERAD process.

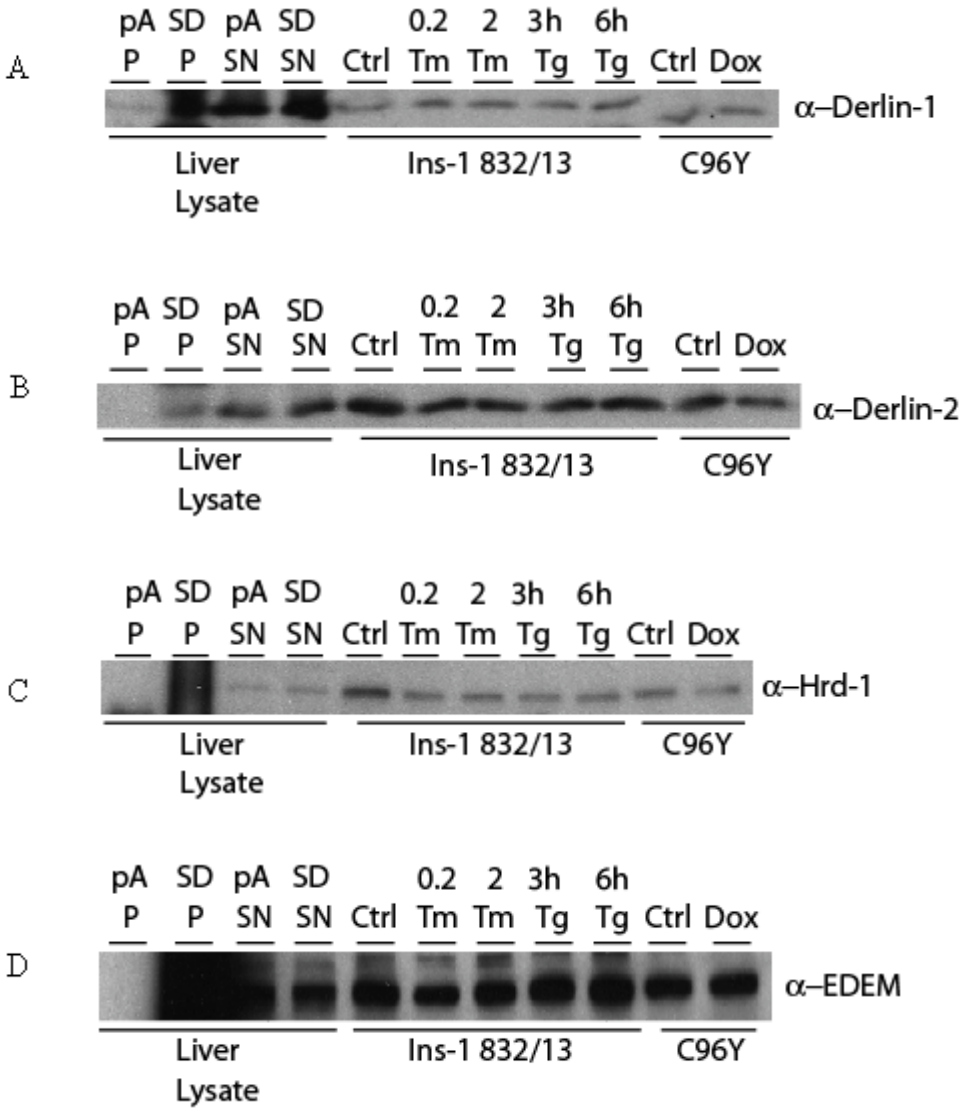

Figure 4.5: **Protein A-tagged SDF2L1 interacts with other ERAD components.** Binding assays were performed using liver lysates as described in Fig. 4.4. pA-SDF2L1 pellets (SD) and control protein A pellets (pA) and 10 μg of supernatant fractions were probed with antibodies to the indicated ERAD components. To test if the ERAD proteins are ER stress inducible, INS-1 832/13 cells untreated (Ctrl) or treated with 0.2 μg/ml Tm for 16 h, 2 μg/ml Tm for 16 h, 1μM Tg for 3 h or 6 h, and proinsulin C96Y-GFP cell untreated (Ctrl) or treated with dox were loaded in parallel to the binding assay samples.

4.02.2 SDF2L1 plays a role in the degradation of mutant proinsulin

Since SDF2L1 interacts with ERAD components p97/VCP, Derlin-1, Derlin-2 and potentially others, I hypothesize that SDF2L1 may be involved in the ERAD process. Previous studies from our lab established that mutant proinsulin (proinsulin C96Y-GFP) degradation requires the ERAD component protein HERP (Hartley 2010), and thus proinsulin C96Y-GFP is an ERAD substrate. Thus, to test this hypothesis, the effect of SDF2L1 knock-down on mutant proinsulin C96Y-GFP degradation was examined. I first looked at the effect of SDF2L1 KD on steady-state mutant proinsulin levels in proinsulin C96Y-GFP cells (**Figure 4.6**). Cells were transfected with either a control siRNA (directed to β-galactosidase; LacZ) or SDF2L1 siRNA for 48 h in the presence or absence of dox. In the dox treatment conditions, there was no difference observed in the steady state levels of mutant proinsulin between the SDF2L1 KD conditions compared to the control. In the basal condition without dox induction the cells produce a small amount of the mutant proinsulin fusion protein (**Figure 4.6**). In this condition compared to the control siRNA SDF2L1 KD led to a reduction in the steady state levels of mutant proinsulin (proinsulin C96Y-GFP).

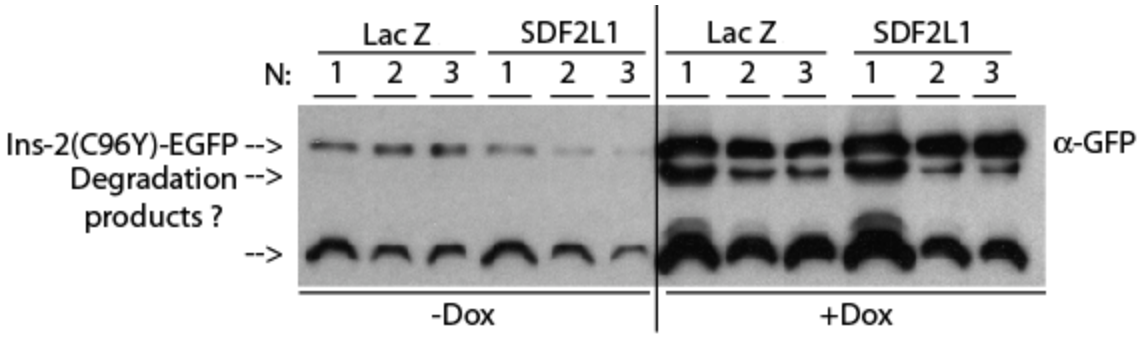

Figure 4.6: Effect of SDF2L1 KD on steady-state mutant proinsulin levels. Proinsulin C96Y-GFP cells were transfected with SDF2L1 or Lac Z siRNA for 48 h in the presence or absence of dox. Cells were lysed and samples were analyzed by western blot. Mutant proinsulin was detected using α-GFP antibody (samples from N=3 independent experiments is shown).

This suggests that when the ERAD machinery is not overwhelmed (i.e. low levels of mutant insulin production), the removal of SDF2L1 appears to result in lower levels of the mutant insulin, suggesting that the SDF2L1 may somehow slow the degradation. This is opposite to the effect of inhibiting ERAD components such as HERP or with proteasome inhibitors that results in increased cellular levels of mutant proinsulin (Hartley 2010).

To determine if the absence of SDF2L1 leads to a faster degradation rate of mutant proinsulin C96Y-GFP cells were transfected with either a control siRNA or SDF2L1 siRNA for 48 h, then treated with 100 μM of protein biosynthesis inhibitor cycloheximide (chx) for various times. Following treatment, the cells were washed, lysed and analyzed by western blot (**Figure 4.7**). Mutant proinsulin expression was similar at the time 0 start between control and SDF2L1 siRNA (**Fig. 4.7B**) and decreased as the treatment time with chx increased in both the control and SDF2L1 KD conditions. Interestingly, the rate of mutant proinsulin degradation was significantly faster in the SDF2L1 KD condition as compared to the control siRNA at the 6 h time point ($N=3$, $p<0.05$) (**Figure 4.7C**). No difference in the rate of degradation of the Golgi protein GM130 was observed between the two conditions. Thus, depletion of SDF2L1 results in enhanced degradation of the mutant proinsulin.

As shown earlier SDF2L1 forms a complex with GRP78/BiP and can interact (although weakly) with mutant proinsulin. As mentioned in the Introduction, the multifunctional protein GRP78/BiP has been implicated in the ERAD process. Thus, it is possible that SDF2L1 reduces mutant proinsulin availability for ERAD destruction in conjunction with GRP78/BiP. To test this hypothesis, the degradation experiments were repeated using GRP78/BiP siRNA to determine if the absence of GRP78/BiP leads to an increase in the rate of degradation of mutant proinsulin.

Proinsulin C96Y-GFP cells were transfected with either control siRNA (directed to luciferase) or GRP78/BiP siRNA for 48 h, then treated with chx for various times. Following treatment, the cells were washed, lysed and analyzed by western blot (**Figure 4.8A**). In these experiments there was already a dramatic reduction (~50%) in the levels of mutant proinsulin following siRNA treatment prior to chx addition in GRP78/BiP KD cells (**Figure 4.8B**). Furthermore, similar to the results with SDF2L1 KD, the rate of mutant proinsulin degradation was faster in the absence of GRP78/BiP compared to the control condition as is evident at the 3 h time point, although additional experiments are required to make this trend statistically significant (**Figure 4.8C**). The loading control GM130 levels were somewhat variable in these experiments, although this may be due to stripping and re-probing the nitrocellulose membranes in these experiments, which was necessary so that the level of GRP78/BiP knock-down could be assessed (**Figure 4.8A**).

The absence of GRP78/BiP leads to a significant increase in the rate of mutant proinsulin degradation, which is even greater than that observed with SDF2L1 KD. Thus SDF2L1-GRP78/BiP may work together to reduce flux of misfolded proteins to the ERAD system.

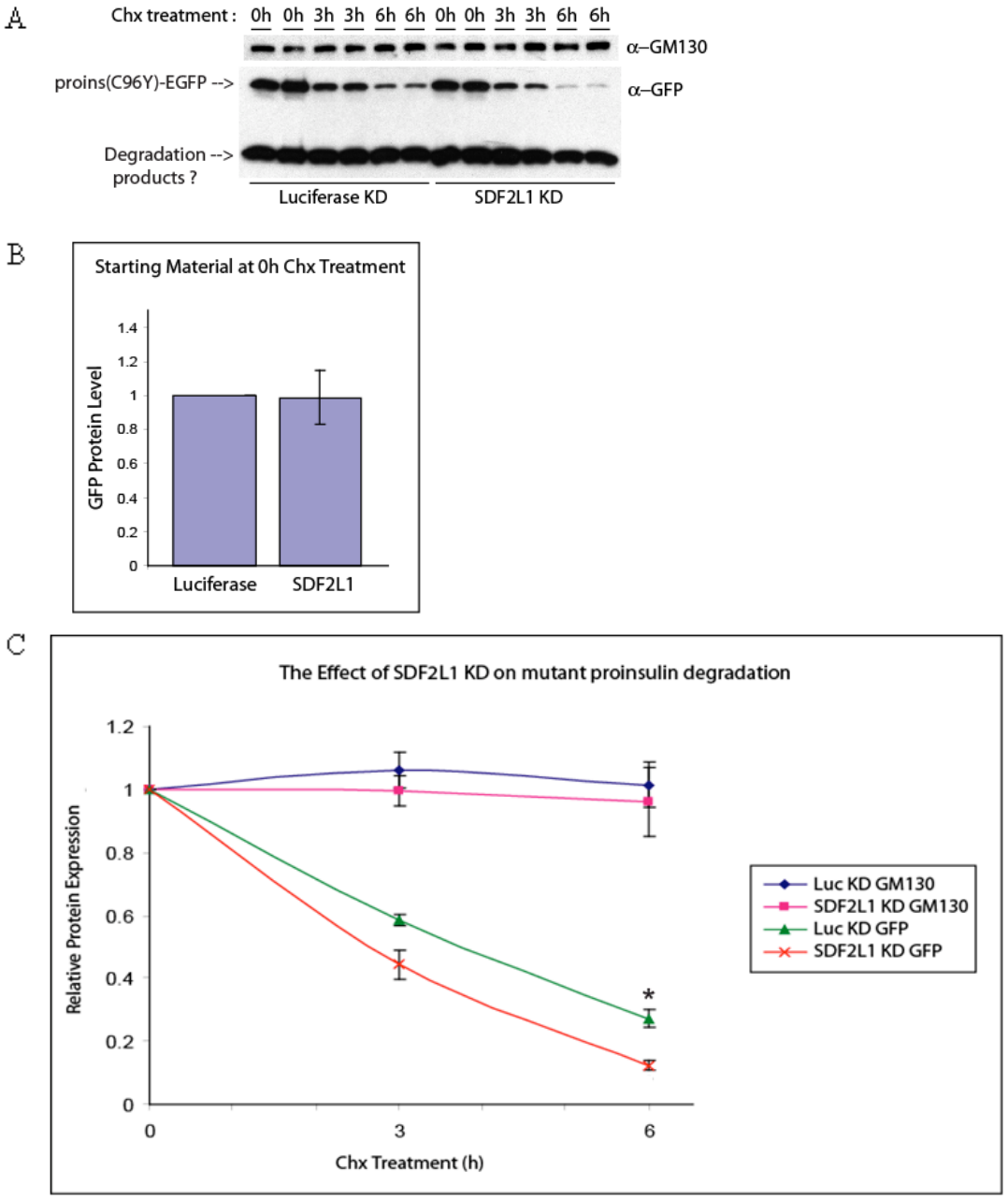

Figure 4.7: **The effect of SDF2L1 KD on mutant proinsulin degradation.** Proinsulin C96Y-GFP cells were transfected with SDF2L1 siRNA (SDF2L1) or luciferase siRNA (Luc) for 48 h. The cells were then untreated (0 h) or treated with 100 μM cycloheximide (chx) for 3 h or 6 h. Following treatment the cells were washed with PBS, lysed, and equal amounts of protein was resolved by SDS-PAGE and immunoblotted with α-GFP and α-GM130 antibodies (**A**). The amount of mutant proinsulin detectable at time 0 in the SDF2L1 KD as compared to control siRNA was quantified using Scion Image (**B**). The GM130 and mutant proinsulin-GFP levels in the SDF2L1 siRNA and control siRNA conditions were quantified and the relative levels were normalized to starting level at time 0 (*, $p<0.05$, mutant proinsulin levels in SDF2L1 siRNA vs. control siRNA conditions; N=3) (**C**).

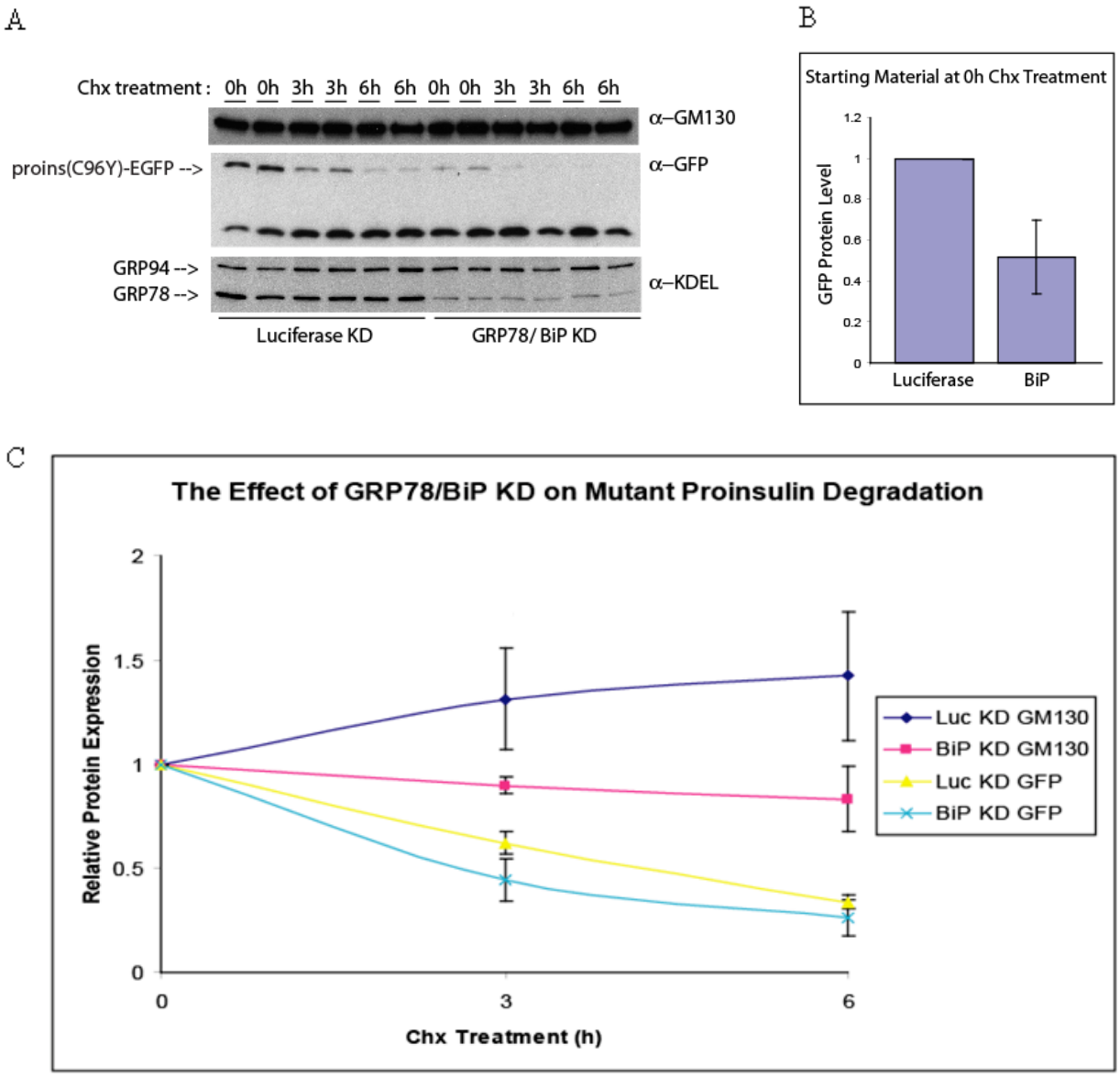

Figure 4.8: **The effect of GRP78/BiP KD on mutant proinsulin degradation.** Proinsulin C96Y-GFP cells were transfected with GRP78/BiP siRNA (BiP) or luciferase siRNA (Luc) for 48 h. At 48 h, the samples were untreated (0 h) or treated with 100 μM cycloheximide (chx) for 3 h or 6 h. Following treatment the cells were washed with PBS, lysed, and equal amounts of protein was resolved by SDS-PAGE and immunoblotted with α-GFP and α-KDEL antibodies. The blots were stripped and reblotted for α-GM130 (**A**). The starting level of mutant proinsulin (0 h) in the GRP78/BiP siRNA compared to control siRNA conditions was quantified using Scion Image (**B**). The GM130 and mutant proinsulin-GFP levels in the GRP78/BiP siRNA and control siRNA conditions were quantified and the relative levels were normalized to starting level at time 0, which was normalized to 1 (N=3) (**C**).

4.03 Discussion

To gain insight into the molecular function of SDF2L1 I used the inducible proinsulin C96Y-GFP cell line as the main model system to identify potential interacting proteins and assess if SDF2L1 has a role in the degradation of mutant proinsulin via the ERAD system. This cell line was used because the lab has already established that expression of this folding-deficient proinsulin induces an ER stress response (which includes up-regulation of SDF2L1 mRNA and protein as shown in the previous chapter) and the mutant proinsulin is degraded by the ERAD pathway (Hartley 2010).

Initial experiments attempted to determine if SDF2L1 can actually interact with the misfolded proinsulin, which was a reasonable assumption given the large induction of this ER-localized protein in response to increased levels of a single mutant protein in the ER and the fact that SDF2L1 has been found to be in a large ER chaperone complex that includes a number of proteins including GRP78/BiP (Meunier 2002). By mass spectrometry Meunier *et al* found that SDF2L1 is part of the heavy chain-GRP78/BiP chaperone complex (Meunier 2002). Furthermore, it has also been reported that SDF2L1 interacts with ERdj3, an ER Hsp40 co-chaperone, which also associates with GRP78/BiP (Bies 2004). Indeed, by immunoprecipitation using cross-linking conditions I was able to detect SDF2L1 in mutant proinsulin-GFP precipitates. This interation under TX-100 lysis conditions is weak since no interaction was seen without the cross-linker and purified protein A-tagged SDF2L1 did not bind misfolded proinsulin. The interaction between mutant proinsulin and SDF2L1 is likely mediated by the ER chaperone GRP78/BiP, since I found GRP78/BiP to interact with SDF2L1 and mutant

proinsulin. Indeed, it was been previously shown that GRP78/BiP can interact with misfolded proinsulin in the Akita mice (Wang 1999), which is consistent with our results.

A clue into a potential function for SDF2L1 came with the use of the protein A-tagged SDF2L1 protein that was used to pull out potential interacting proteins from a mouse liver TX-100 lysate. Liver was chosen since hepatocytes secrete a large number of serum proteins and the tissue was readily available. Coomassie staining identified a few bands that seemed to be enriched in the pA-SDF2L1 pull-down compared to pA alone and I sequenced the band that was highly enriched in the pA-SDF2L1 pellet. Mass spectrometry identified this band as the cytosolic ERAD component p97/VCP, a AAA+ which allows the extraction of ERAD substrates from the ER lumen (or membrane) to the cytosol (Schuberth 2005). Additional binding studies and western blot analysis confirmed that this protein could indeed be specifically pulled out of a liver (and pancreatic β-cell) lysate using pA-SDF2L1 as bait. Although in intact cells SDF2L1 and p97 are on opposite sides of the ER membrane, ERAD components exist as a complex and indeed chaperones such as BiP and ERDj5 have been found to be part of these complexes (**Figure 1.2**). Furthermore, I found that additional ERAD components (Derlin-1, Derlin-2) could be pulled out of liver lysates using pA-SDF2L1 as bait. Thus, by association SDF2L1 may have a role in ERAD. It is formally possible that the reason pA-SDF2L1 seems to interact with the ERAD components is that it may be recognized as a misfolded protein, since the HDEL retention sequence was removed when generating the pA fusion construct. However, this is unlikely to be the case since the pA-SDF2L1 protein is readily secreted in the pA-SDF2L1#7 cell line, thus it passes ER quality control and consequently should be correctly folded (**Appendix 6.02**).

To determine if SDF2L1 is involved in the ERAD process I resorted to the mutant proinsulin C96Y-GFP cell line, in which it has been previously established that the mutant proinsulin is degraded in an ERAD-dependent manner (Hartley 2010). Reducing ERAD by knocking down ERAD components or inhibiting the proteasome leads to increased cellular levels of mutant proinsulin (Hartley 2010). Proinsulin C96Y-GFP is a non-glycosylated substrate, since both proinsulin and GFP lack glycosylation signals and is likely degraded via the non-glycolysated substrate ERAD pathway (**Figure 1.2**). Thus, I hypothesized that SDF2L1 (and GRP78/BiP) might be required for transferring the mutant proinsulin to the ERAD machinery and if these components are absent this process would be inefficient, resulting in increased mutant proinsulin (i.e. reduced degradation). However, in preliminary experiments in SDF2l1 knock-down cells I noticed that steady-state mutant proinsulin levels tended to be reduced in these cells compared to controls (**Figure 4.6**), suggesting that SDF2L1 has a counterintuitive effect i.e. prevents the degradation of misfolded mutant proinsulin. Indeed, degradation assays revealed that knock-down of SDF2L1 results in a more rapid rate of mutant proinsulin degradation (**Figure 4.7**) an effect that is also produced by knocking down GRP78/BiP, which I identified can interact with SDF2L1.

Thus, SDF2L1 and GRP78/BiP function to prevent mutant proinsulin from accessing the ERAD pathway. Such a process may be employed in an attempt to increase the time the mutant proinsulin resides in the ER and allow it a greater chance to fold correctly. If it does not then some will find its way to the ERAD pathway since the interaction of GRP78/BiP-SDF2L1 with the mutant proinsulin is likely weak as demonstrated by our binding studies. Although clearly this process is not helpful in the case of mutant proinsulin, such a process would be beneficial for proteins that have a difficult time folding and require more time. Thus, I propose that *in vivo* this

system may give partially misfolded or unfolded proteins a better chance is obtaining a proper fold instead of a quick death via the ERAD pathway.

GRP78/BiP is likely the component that interacts with the misfolded proteins, so what is the role of SDF2L1 in this process? Clearly both proteins are induced when large amounts of misfolded proteins accumulate in the ER i.e. when the cell experiences ER stress, but GRP78/BiP levels are already high even in control cells, while SDF2L1 appears to be much less abundant (certainly in pancreatic β-cells) in the basal state. Thus, it could be that SDF2L1 is markedly induced to assist GRP78/BiP or provide a parallel pathway to achieve the same effect i.e. to provide added time for misfolded proteins to fold correctly, or potentially to buy some time so that chaperone capacity fully increases to better handle protein load as part of the ER stress response. Indeed, it would be interesting to establish the kinetics of SDF2L1 induction compared to other UPR response proteins upon ER stress.

SDF2L1 has been found to interact with defensin proteins (Tongaonkar 2009). These small proteins are non-glycosylated and contain multiple disulfide bonds, similar to proinsulin. Indeed, they are likely produced in large amounts by immune cells (similar to proinsulin in β-cells) especially when stimulated. Thus, SDF2L1 may provide some level of protection for these abundant proteins in the ER from ERAD destruction particularly under stimulatory conditions. The generality of this effect however, requires future study.

4.04 Summary and Future Directions

This chapter aimed to elucidate the role of SDF2L1 by examining its interacting proteins. Our data reveals that SDF2L1 interacts with GFP-tagged mutant proinsulin weakly as it was only detected under DSP cross-linking conditions and that this interaction may be via GRP78/BiP,

which I found also binds SDF2L1. Future studies using purified SDF2L1 and GRP78/BiP should be performed to determine if these proteins indeed interact directly. Additionally, various truncation mutants of both proteins can be made, epitope-tagged and pull-down experiments performed to identify which parts of each molecule is responsible for the binding. Indeed, SDF2L1 contains MIR motifs also found in protein O mannosyltransferases (PMT), inositol 1,4,5-triphosphate receptors (IP3R) and ryanodine receptors (RyR) (Schott 2010). Although the function of this domain is unknown, they are mainly arranged in several 50-residue structures (Ponting 2000). In future studies, the interaction of specific MIR domains of SDF2L1 can be used to further define the interaction between SDF2L1 and GRP78/BiP. Binding experiments may be done through yeast 2 hybrid studies. This method may also reveal other interacting partners of SDF2L1. This project is currently underway in the lab. Finally, the interaction of SDF2L1 with lectin chaperones cnx/crt should be examined. The SDF2L1 homologous protein SDF-2 has been shown through crystallization studies to contain binding motifs for glycosylated proteins (Schott 2010). Thus, SDF2L1 may function with the cnx/crt chaperone system, and may thereby also bind glycosylated proteins.

I also discovered that SDF2L1 is able to interact with the ERAD complex as several ERAD components were bound to pA-SDF2L1 from both liver and pancreatic β-cell lysates, including p97/VCP, Derlin-1 and Derlin-2. In addition, the interaction of SDF2L1 with other components of the ERAD machinery should be examined. The Np14/Ufd1 proteins interact with the D1 and D2 domains of p97/VCP. In fact, p97/VCP binding of polyubiquitinated substrate is mediated by Udf1 and VIMP (Ye 2003). Thus, the interaction of SDF2L1 with these proteins should also be examined. Also, the interaction of SDF2L1 with Hrd-1 E3 ubiquitin ligase should

be reexamined by repeating the binding assays and immunoblotting for Hrd-1 with a monoclonal antibody.

Importantly, I also identified that SDF2L1 modulates substrate delivery for ERAD since knock-down of SDF2L1 increased the degradation rate of mutant proinsulin. A similar effect was observed with GRP78/BiP knock-down, which I hypothesize are working together (or perhaps in parallel) to retain misfolded proteins in the ER to give extra time to try and achieve normal folding. Although the degradation assay using cycloheximide to inhibit protein synthesis is effective and we did observe significant differences between control and SDF2L1 knock-down cells on mutant proinsulin degradation, these experiments should be confirmed using the gold standard assay for protein degradation. This involves radiolabelling the cells post- siRNA transfection with 35-S-methionine for a short time (~5 min) followed by chase with cold methionine and immunoprecipitation of the mutant insulin. Degradation kinetics are measured by monitoring the level of the radiolabelled mutant insulin over time. However, based on the cycloheximide experiments I expect that this assay would merely confirm the results.

The discovery that SDF2L1 prevents to some degree efficient destruction of misfolded proteins is an exciting finding and clearly similar experiments should be performed with other misfolded protein substrates such as CFTRΔ508, α1-antitrypsin genetic variant-null Hong Kong, β-glucocerebroisidase, among others. These misfolding prone proteins have human disease connections and modulation of SDF2L1 may be exploited to enhance the time these types of proteins have to attain a correct fold in the ER to increase functional protein levels as a potential therapeutic strategy for these diseases (Cohen 2003).

CHAPTER 5. REFERENCES

Alberts, B. (2002). Molecular Biology of the Cell 4th Ed. New York, Garland Science.

Araki, E. (2003). "Impact of endoplasmic reticulum stress pathway on pancreatic beta-cells and diabetes mellitus." Exp Biol Med **228**(10): 1213-1217.

Berridge, M. (2002). "The endoplasmic reticulum: a multifunctional signaling organelle." Cell Calcium **32**(5-6): 235-249.

Bertolotti, A. (2000). "Dynamic interaction of BiP and ER stress transducers in the unfolded-protein response." Nat Cell Biol **2**(6): 326-332.

Bies, C. (2004). "Characterization of pancreatic ERj3p, a homolog of yeast DnaJ-like protein Scj1p." Biol Chem **385**(5): 389-395.

Blond-Elguindi, S. (1993). "Affinity panning of a library of peptides displayed on bacteriophages reveals the binding specificity of BiP." Cell **75**(4): 717-728.

Brodsky, J. (2007). "The protective and destructive roles played by molecular chaperones during ERAD (endoplasmic-reticulum-associated degradation)." Biochem J **404**(3): 353-363.

Caramelo, J. (2003). "UDP-Glc:glycoprotein glucosyltransferase recognizes structured and solvent accessible hydrophobic patches in molten globule-like folding intermediates." Proc Natl Acad Sci U S A **100**(1): 86-91.

Carvalho, P. (2006). "Distinct ubiquitin-ligase complexes define convergent pathways for the degradation of ER proteins." Cell **126**(2): 361-373.

Cnop, M. (2007). "Selective inhibition of eukaryotic translation initiation factor 2 alpha dephosphorylation potentiates fatty acid-induced endoplasmic reticulum stress and causes pancreatic beta-cell dysfunction and apoptosis." J Biol Chem **282**: 3989–3997.

Cnop, M. (2008). "An update on lipotoxic endoplasmic reticulum stress in pancreatic beta-cells." Biochem Soc Trans **36**(Pt 5): 909-915.

Cohen, F. (2003). "Therapeutic approaches to protein-misfolding diseases." Nature **426**(6968): 905-909.

Coughlan, C. (2004). "Degradation of mutated bovine pancreatic trypsin inhibitor in the yeast vacuole suggests post-endoplasmic reticulum protein quality control." J Biol Chem **279**(15): 15289-15297.

Crawford, N. (2009). "The metastasis efficiency modifier ribosomal RNA processing 1 homolog B (RRP1B) is a chromatin-associated factor." J Biol Chem **284**(42): 28660-28673.

Delépine, M. (2000). "EIF2AK3, encoding translation initiation factor 2-alpha kinase 3, is mutated in patients with Wolcott-Rallison syndrome." Nat Genet **25**(4): 406-409.

Eizirik, D. (1996). "Beta-cell defence and repair mechanisms in human pancreatic islets." Horm Metab Res **28**(6): 302-305.

Eizrik, D. (2008). "The role for endoplasmic reticulum stress in diabetes mellitus." Endocrine Reviews **29**: 42-61.

Ellgaard, L. (2003). "Quality control in the endoplasmic reticulum." Nat Rev Mol Cell Biol **4**(3): 181-191.

Elouil, H. (2007). "Acute nutrient regulation of the unfolded protein response and integrated stress response in cultured rat pancreatic islets." Diabetologia **50**: 1442-1452.

Fagioli, C. (2001). "Glycoprotein quality control in the endoplasmic reticulum. Mannose trimming by endoplasmic reticulum mannosidase I times the proteasomal degradation of unassembled immunoglobulin subunits." J Biol Chem **276**(16): 12885-12892.

Feige, M. (2009). "An unfolded CH1 domain controls the assembly and secretion of IgG antibodies." Mol Cell **34**(5): 569-579.

Fernandez, A. (2001). "Functional inactivation of the IGF-1 and insulin receptors in skeletal muscle causes type 2 diabetes." Genes Dev **15**: 1926-1934.

Finley, D. (2009). "Recognition and processing of ubiquitin-protein conjugates by the proteasome." Annu Rev Biochem **78**: 477-513.

Finne, J. (1979). "Novel mannitol-containing oligosaccharides obtained by mild alkaline borohydride treatment of a chondroitin sulfate proteoglycan from brain." J Biol Chem **254**(20): 10295-10300.

Flierman, D. (2003). "Polyubiquitin serves as a recognition signal, rather than a ratcheting molecule, during retrotranslocation of proteins across the endoplasmic reticulum membrane." J Biol Chem **278**(37): 34774-34782.

Fonseca, S. (2010). "Stress hypERactivation in the β-cell." Islets **2**(1): 1-9.

Fukuda, S. (2001). "Murine and human SDF2L1 is an endoplasmic reticulum stress-inducible gene and encodes a new member of the Pmt/rt protein family." Biochem Biophys Res Commun **280**(1): 407-414.

Gauss, R. (2006). "The Hrd1p ligase complex forms a linchpin between ER-lumenal substrate selection and Cdc48p recruitment." EMBO J **25**(9): 1827-1835.

Gething, M. (1992). "Protein folding in the cell." Nature **355**: 33–45.

Gething, M. (1999). "Role and regulation of the ER chaperone BiP." Semin Cell Dev Biol **10**(5): 465-472.

Goeckeler, J. (2010). "Molecular chaperones and substrate ubiquitination control the efficiency of endoplasmic reticulum-assocaited degradation." Diabetes, Obesity and Metabolism **12**(Suppl. 2): 32-38.

Goodison, S. (1992). "Control of insulin gene expression by glucose." Biochem J **285**: 563-568.

Haas, I. (1983). "Immunoglobulin heavy chain binding protein." Nature **306**(5941): 387-389.

Hammond, C. (1994). "Folding of VSV G protein: sequential interaction with BiP and calnexin." Science **266**(5184): 456-458.

Han, D. (2009). "IRE1alpha kinase activation modes control alternate endoribonuclease outputs to determine divergent cell fates." Cell **138**: 562-575.

Harding, H. (2003). "An integrated stress response regulates amino acid metabolism and resistance to oxidative stress." Mol Cell **11**(3): 619-633.

Hartley, T. (2010). "Endoplasmic reticulum stress response in an INS-1 pancreatic beta-cell line with inducible expression of a folding-deficient proinsulin." BMC Cell Biol **26**: 59-77.

Harty, C. (2001). "O-Mannosylation protects mutant alpha-factor precursor from endoplasmic reticulum-associated degradation." Mol Biol Cell **12**(4): 1093-1101.

Haze, K. (1999). "Mammalian transcription factor ATF6 is synthesized as a transmembrane protein and activated by proteolysis in response to endoplasmic reticulum stress." Mol Biol Cell **10**(11): 3787-3799.

Herbach, N. (2007). "Dominant-negative effects of a novel mutated Ins2 allele causes early-onset diabetes and severe beta-cell loss in Munich Ins2C95S mutant mice." Diabetes **56**(5): 1268-1276.

Hess, D. (2011). "Extensive Pancreas Regeneration Following Acinar-Specific Disruption of Xbp1 in Mice." Gastroenterology [Epub ahead of print].

Hirao, K. (2006). "EDEM3, a soluble EDEM homolog, enhances glycoprotein endoplasmic reticulum-associated degradation and mannose trimming." J Biol Chem **281**(14): 9650-9658.

Hollien, J. (2006). "Decay of endoplasmic reticulum-localized mRNAs during the unfolded protein response." Science **313**(5783): 104-107.

Hoseki, J. (2010). "Mechanism and components of endoplasmic reticulum-associated degradation." J Biochem **147**(1): 19-25.

Hosokawa, N. (2001). "A novel ER alpha-mannosidase-like protein accelerates ER-associated degradation." EMBO Rep **2**(5): 415-422.

Hosokawa, N. (2010). "EDEM1 accelerates the trimming of alpha1,2-linked mannose on the C branch of N-glycans." Glycobiology **20**(5): 567-575.

Hosokawa, N. (2010). "The role of MRH domain-containing lectins in ERAD." Glycobiology **20**(6): 651-660.

Howard, J. (2003). "Dynamics and mechanics of the microtubule plus end." Nature **422**(6933): 753-758.

Hu, H. (2011). "Conditional knockout of protein O-mannosyltransferase 2 reveals tissue-specific roles of O-mannosyl glycosylation in brain development." J Comp Neurol **519**(7): 1320-1337.

Hu, Y. (2011). "Large induces functional glycans in an O-mannosylation dependent manner and targets GlcNAc terminals on alpha-dystroglycan." PLoS One **6**(2): e16866.

Hutt, D. (2009). "The proteostasis boundary in misfolding diseases of membrane traffic." FEBS Lett **583**(16): 2639-2646.

Huyer, G. (2004). "Distinct machinery is required in Saccharomyces cerevisiae for the endoplasmic reticulum-associated degradation of a multispanning membrane protein and a soluble luminal protein." J Biol Chem **279**(37): 38369-38378.

Inoue, H. (1998). "A gene encoding a transmembrane protein is mutated in patients with diabetes mellitus and optic atrophy (Wolfram syndrome)." Nat Genet **20**(2): 143-148.

Jensen, T. (1995). "Multiple proteolytic systems, including the proteasome, contribute to CFTR processing." Cell **83**(1): 129-135.

Jessop, C. (2009). "Protein disulphide isomerase family members show distinct substrate specificity: P5 is targeted to BiP client proteins." J Cell Sci **122**(Pt 23): 4287-4295.

Jonas, J. (2009). "Glucose regulation of islet stress responses and beta-cell failure in type 2 diabetes." Diabetes Obes Metab **11**(Suppl. 4): 65-81.

Kanehara, K. (2007). "The EDEM and Yos9p families of lectin-like ERAD factors." Semin Cell Dev Biol **18**(6): 743-750.

Kang, H. (2009). "Transcript analyses of stromal cell derived factors (SDFs): SDF-2, SDF-4 and SDF-5 reveal a different pattern of expression and prognostic association in human breast cancer." Int J Oncol **35**(1): 205-211.

Kaufman, R. (1999). "Stress signaling from the lumen of the endoplasmic reticulum: coordination of gene transcriptional and translational controls." Genes Dev **13**(10): 1211-1233.

Kaufman, R. (2010). "The unfolded protein response is required to maintain the integrity of the endoplasmic reticulum, prevent oxidative stress and preserve differentiation in β-cells." Diabetes, Obesity and Metabolism **12**(Suppl. 2): 99-107.

Kimata, Y. (2007). "Two regulatory steps of ER-stress sensor Ire1 involving its cluster formation and interaction with unfolded proteins." J Cell Biol **179**(1): 75-86.

Knittler, M. (1995). "Molecular chaperones involved in protein degradation in the endoplasmic reticulum: quantitative interaction of the heat shock cognate protein BiP with partially folded immunoglobulin light chains that are degraded in the endoplasmic reticulum." Proc Natl Acad Sci U S A **92**(5): 1764-1768.

Ladiges, W. (2005). "Pancreatic beta-cell failure and diabetes in mice with a deletion mutation of the endoplasmic reticulum molecular chaperone gene P58IPK." Diabetes **54**: 1074–1081.

Laybutt, D. (2007). "Endoplasmic reticulum stress contributes to beta cell apoptosis in type 2 diabetes." Diabetelogia **50**: 752-763.

Lee, A. (1987). "Coordinated regulation of a set of genes by glucose and calcium ionophore in mammalian cells." Trends Biochem Sci **12**: 20–24.

Lenzen, S. (1996). "Low antioxidant enzyme gene expression in pancreatic islets compared with various other mouse tissues." Free Radic Biol Med **20**: 463-466.

Lilley, B. (2004). "A membrane protein required for dislocation of misfolded proteins from the ER." Nature **429**(6994): 834-840.

Lu, H. (2008). "The identification of potential factors associated with the development of type 2 diabetes: a quantitative proteomics approach." Mol Cell Proteomics **7**(8): 1434-1451.

Määttänen, P. (2010). "Protein quality control in the ER: the recognition of misfolded proteins." Semin Cell Dev Biol **21**(5): 500-511.

Mahadevan, N. (2010). "Prostate cancer cells undergoing ER stress in vitro and in vivo activate transcription of pro-inflammatory cytokines " Journal of Inflammation Research **3**: 99 - 103.

Malhotra, J. (2007). "Endoplasmic reticulum stress and oxidative stress: a vicious cycle or a double-edged sword?" Antioxid Redox Signal **9** 2277-2293.

Mayer, M. (2000). "BiP and PDI cooperate in the oxidative folding of antibodies in vitro." J Biol Chem **275**(38): 29421-29425.

McCracken, A. (1996). "Assembly of ER-associated protein degradation in vitro: dependence on cytosol, calnexin, and ATP." J Cell Biol **132**(3): 291-298.

Melloul, D. (2002). "Regulation of insulin gene transcription." Diabetelogia **45**: 309-326.

Meunier, L. (2002). "A subset of chaperones and folding enzymes form multiprotein complexes in endoplasmic reticulum to bind nascent proteins." Mol Biol Cell **13**(12): 4456-4469.

Molinari, M. (2002). "Sequential assistance of molecular chaperones and transient formation of covalent complexes during protein degradation from the ER." J Cell Biol **158**(2): 247-257.

Molinari, M. (2003). "Role of EDEM in the release of misfolded glycoproteins from the calnexin cycle." Science **299**(5611): 1397-1400.

Morishima, N. (2004). "Translocation of Bim to the endoplasmic reticulum (ER) mediates ER stress signaling for activation of caspase-12 during ER stress-induced apoptosis." J Biol Chem **279**(48): 50375-50381.

Nair, U. (2005). "Molecular mechanisms and regulation of specific and nonspecific autophagy pathways in yeast." J Biol Chem **280**(51): 41785-41788.

Nakagawa, T. (2000). "Caspase-12 mediates endoplasmic-reticulum-specific apoptosis and cytotoxicity by amyloid-beta." Nature **403**(6765): 98-103.

Nakamura, N. (1995). "Characterization of a cis-Golgi matrix protein, GM130." J Cell Biol **131**(6 Pt 2): 1715-1726.

Nakatsukasa, K. (2004). "Roles of O-mannosylation of aberrant proteins in reduction of the load for endoplasmic reticulum chaperones in yeast." J Biol Chem **279**(48): 49762-49772.

Nakatsukasa, K. (2008). "Dissecting the ER-associated degradation of a misfolded polytopic membrane protein." Cell **132**(1): 101-112.

Navon, A. (2009). "The 26 S proteasome: from basic mechanisms to drug targeting." J Biol Chem **284**(49): 33713-33718.

Nishikawa, S. (2001). "Molecular chaperones in the yeast endoplasmic reticulum maintain the solubility of proteins for retrotranslocation and degradation." J Cell Biol **153**(5): 1061-1070.

Nishikawa, S. (2005). "Roles of molecular chaperones in endoplasmic reticulum (ER) quality control and ER-associated degradation (ERAD)." J Biochem **137**(5): 551-555.

Nishitoh, H. (1998). "ASK1 is essential for JNK/SAPK activation by TRAF2." Mol Cell **2**(3): 389-395.

Nutt, L. (2002). "Bax and Bak promote apoptosis by modulating endoplasmic reticular and mitochondrial Ca2+ stores." J Biol Chem **277**(11): 9219-9225.

Okuda-Shimizu, Y. (2007). "Characterization of an ERAD pathway for nonglycosylated BiP substrates, which require Herp." Mol Cell **28**(4): 544-554.

Otero, J. (2010). "Life and death of a BiP substrate." Semin Cell Dev Biol **21**(5): 472-478.

Oyadomari, S. (2002). "Targeted disruption of the Chop gene delays endoplasmic reticulum stress-mediated diabetes." J Clin Invest **109**(4): 525-532.

Pilon, M. (1998). "Sec61p serves multiple roles in secretory precursor binding and translocation into the endoplasmic reticulum membrane." Mol Biol Cell **9**(12): 3455-3473.

Poitout, V. (2006). "Regulation of the unsulin gene by glucose and fatty acids." The Journal of Nutrition **136**: 873-876.

Ponting, C. (2000). "Novel repeats in ryanodine and IP3 receptors and protein O-mannosyltransferases." Trends Biochem Sci **25**: 48-50.

Proszynski, T. (2004). "O-glycosylation as a sorting determinant for cell surface delivery in yeast." Mol Biol Cell **15**(4): 1533-1543.

Rao, R. (2002). "Coupling endoplasmic reticulum stress to the cell death program. An Apaf-1-independent intrinsic pathway." J Biol Chem **277**(24): 21836-21842.

Rao, R. (2004). "Coupling endoplasmic reticulum stress to the cell death program." Cell Death Differ **11**(4): 372-380.

Richly, H. (2005). "A series of ubiquitin binding factors connects CDC48/p97 to substrate multiubiquitylation and proteasomal targeting." Cell **120**(1): 73-84.

Robertson, R. (2004). "Beta-cell glucose toxicity, lipotoxicity, and chronic oxidative stress in type 2 diabetes." Diabetes **53**: S119-S124.

Robertson, R. (2004). "Chronic oxidative stress as a central mechanism for glucose toxicity in pancreatic islet beta cells in diabetes." J Biol Chem **279**: 42351-42354.

Ron, D. (2006). "Stressed cells cope with protein overload." Science **313**(52-53).

Ron, D. (2007). "Signal integration in the endoplasmic reticulum unfolded protein response." Nat Rev Mol Cell Biol **8**(7): 519-529.

Sanders, S. (1999). "O-Glycosylation of Axl2/Bud10p by Pmt4p is required for its stability, localization, and function in daughter cells." J Cell Biol **145**(6): 1177-1188.

Scheuner, D. (2001). "Translational control is required for the unfolded protein response and in vivo glucose homeostasis." Mol Cell **7**(6): 1165-1176.

Scheuner, D. (2008). "The unfolded protein response: a pathway that links insulin demand with beta-cell failure and diabetes." Endocrine Reviews **29**: 317–333.

Schmitz, A. (1995). "In vivo iodination of a misfolded proinsulin reveals co-localized signals for Bip binding and for degradation in the ER." EMBO J **14**(6): 1091-1098.

Schott, A. (2010). "Arabidopsis stromal-derived Factor2 (SDF2) is a crucial target of the unfolded protein response in the endoplasmic reticulum." J Biol Chem **285**(23): 18113-18121.

Schröder, M. (2005). "The mammalian unfolded protein response." Annu Rev Biochem **74**: 739-789.

Schuberth, C. (2005). "Membrane-bound Ubx2 recruits Cdc48 to ubiquitin ligases and their substrates to ensure efficient ER-associated protein degradation." Nat Cell Biol **7**(10): 999-1006.

Schuit, F. (1998). "Glucose stimulates proinsulin biosynthesis by a dose-dependent recruitment of pancreatic beta cells." Proc Natl Acad Sci U S A **85**(11): 3865-3869.

Schulze, A. (2005). "The ubiquitin-domain protein HERP forms a complex with components of the endoplasmic reticulum associated degradation pathway." J Mol Biol **354**(5): 1021-1027.

Scott, D. (2008). "Role of Sec61p in the ER-associated degradation of short-lived transmembrane proteins." J Cell Biol **181**(7): 1095-1105.

Shore, G. (2011). "Signaling cell death from the endoplasmic reticulum stress response." Curr Opin Cell Biol **23**(3): 143-149.

Strahl-Bolsinger, S. (1999). "Protein O-Mannosylation." Biochimica et Biophysica Acta **1462**(2): 297-307.

Stronge, V. (2001). "Relationship between calnexin and BiP in suppressing aggregation and promoting refolding of protein and glycoprotein substrates." J Biol Chem **276**(43): 39779-39787.

Tabas, I. (2011). "Integrating the mechanisms of apoptosis induced by endoplasmic reticulum stress." Nat Cell Biol **13**(3): 184-190.

Taniguchi, C. (2006). "Critical nodes in signalling pathways: insights into insulin action." Nat Rev Mol Cell Biol. **7**: 85-96.

Taylor, S. (2003). "Glycopeptide specificity of the secretory protein folding sensor UDP-glucose glycoprotein:glucosyltransferase." EMBO Rep **4**(4): 405-411.

Tongaonkar, P. (2009). "SDF2L1, a component of the endoplasmic reticulum chaperone complex, differentially interacts with {alpha}-, {beta}-, and {theta}-defensin propeptides." J Biol Chem **284**(9): 5602-5609.

Trombetta, S. (1992). "Purification to apparent homogeneity and partial characterization of rat liver UDP-glucose:glycoprotein glucosyltransferase." J Biol Chem **267**(13): 9236-9240.

Urano, F. (2000). "Coupling of stress in the ER to activation of JNK protein kinases by transmembrane protein kinase IRE1." Science **287**(5453): 664-666.

Ushioda, R. (2008). "ERdj5 is required as a disulfide reductase for degradation of misfolded proteins in the ER." Science **321**(5888): 569-572.

Vashist, S. (2004). "Misfolded proteins are sorted by a sequential checkpoint mechanism of ER quality control." J Cell Biol **165**(1): 41-52.

Vembar, S. (2008). "One step at a time: endoplasmic reticulum-associated degradation." Nat Rev Mol Cell Biol **9**(12): 944-957.

Verma, R. (2000). "Proteasomal proteomics: identification of nucleotide-sensitive proteasome-interacting proteins by mass spectrometric analysis of affinity-purified proteasomes." Mol Biol Cell **11**(10): 3425-3439.

Volchuk, A. (2010). "The endoplasmic reticulum stress response in pancreatic β-cells." Diabetes, Obesity and Metabolism **12**(Suppl. 2): 48-57

Walsh, P. (2004). "The J-protein family: modulating protein assembly, disassembly and translocation." EMBO Rep **5**(6): 567-571.

Wang, J. (1999). "A mutation in the insulin 2 gene induces diabetes with severe pancreatic beta-cell dysfunction in the Mody mouse." J Clin Invest **103**(1): 27-37.

Wearsch, P. (1997). "Interaction of endoplasmic reticulum chaperone GRP94 with peptide substrates is adenine nucleotide-independent." J Biol Chem **272**(8): 5152-5156.

Welsh, N. (1995). "Differences in the expression of heatshock proteins and antioxidant enzymes between human and rodent pancreatic islets: implications for the pathogenesis of insulin-dependent diabetes mellitus." Mol Med **1**: 806-820.

Werner, E. (1996). "Proteasome-dependent endoplasmic reticulum-associated protein degradation: an unconventional route to a familiar fate." Proc Natl Acad Sci U S A **93**(24): 13797-13801.

Wiertz, E. (1996). "The human cytomegalovirus US11 gene product dislocates MHC class I heavy chains from the endoplasmic reticulum to the cytosol." Cell **84**(5): 769-779.

Willer, T. (2003). "O-mannosyl glycans: from yeast to novel associations with human disease." Curr Opin Struct Biol **13**(5): 621-630.

Wójcik, C. (2006). "Valosin-containing protein (p97) is a regulator of endoplasmic reticulum stress and of the degradation of N-end rule and ubiquitin-fusion degradation pathway substrates in mammalian cells." Mol Biol Cell **17**(11): 4606-4618.

Ye, Y. (2003). "Function of the p97-Ufd1-Npl4 complex in retrotranslocation from the ER to the cytosol: dual recognition of nonubiquitinated polypeptide segments and polyubiquitin chains." J Cell Biol **162**(1): 71-84.

Ye, Y. (2004). "A membrane protein complex mediates retro-translocation from the ER lumen into the cytosol." Nature **429**(6994): 841-847.

Yoneda, T. (2001). "Activation of caspase-12, an endoplastic reticulum (ER) resident caspase, through tumor necrosis factor receptor-associated factor 2-dependent mechanism in response to the ER stress." J Biol Chem **276**(17): 13935-13940.

Zhang, L. (2009). "GRP78, but Not Protein-disulfide Isomerase, Partially Reverses Hyperglycemia-induced Inhibition of Insulin Synthesis and Secretion in Pancreatic β-Cells." J Biol. Chem. **284**: 5289-5298.

Zhong, X. (2004). "AAA ATPase p97/valosin-containing protein interacts with gp78, a ubiquitin ligase for endoplasmic reticulum-associated degradation." J Biol Chem **279**(44): 45676-45684.

CHAPTER 6. APPENDIX

6.01 Analysis of potential O-mannosylation of mutant proinsulin C96Y-GFP

6.01.1 Introduction

As mentioned in the Introduction, SDF2L1 contains **MIR** domains, also found in Protein O-**M**annosyltransferases, **I**nositol 1,4,5-trisphosphate receptors and **R**yanodine receptors (Ryr) (Schott 2010). This domain provides SDF2L1 with a limited homology to the central catalytic region of Protein O-mannosyltransferases (POMTs) (Fukuda 2001). SDF2L1 is shown to have an approximately 31% homology to protein O-mannosyltransferase (POMTs), specifically in the amino acid region 20-176, which overlaps part of the signal sequence and the core protein (**Figure 6.1A**). Alternatively, when examining the protein O-mannosyltransferase in *Sacromyces cerevisiae*, the amino acids overlapping between SDF2L1 and POMTs are in the catalytic region of *Sc*Pmt1p (**Figure 6.1B**). This domain is also found in plant SDF-2, an ER protein predicted to have a role in glycoprotein quality control (Schott 2010). The homology of SDF2L1 to POMTs may allow it to interact with glycosylated mutant proteins and modify them with mannosyl residues via the MIR domains.

Protein O-mannosylation initiates in the ER with the transfer of mannose from dolichyl activated mannose to the ser/thr residues of secretory proteins by protein O-mannosyltransferases (POMTs). An extensive POMT gene family has been identified in yeast (Pmt1-7) and similar proteins are found in mammals. Around four to five short chains of O-linked mannosyl residues are attached to the ser/thr sites in some secretory proteins (Strahl-Bolsinger 1999). Dol-P-Man serves as the initial mannosyl donor and the mannosylation continues in the Golgi where GDP-Man serves as the mannosyl donor. POMTs are integral membrane proteins with a central hydrophilic domain and several transmembrane spanning domains. Most O-glycosylated

proteins are rich in ser/thr residues which are often arranged in clusters. The general function of O-mannosylation is unknown, however, potential roles could include protection of glycosylated proteins from protease mediated degradation, anchoring of proteins to cell wall, cell growth and proliferation, protein secretion, maintenance of the cell wall integrity, and budding. In mammals, proteins such as bovine nerve α-dystroglycan, brain proteoglycans, and rabbit brain protein HNK-1 have been reported to be O-mannosylated (Hu 2011; Hu 2011).

The role if any of protein O-mannosylation in the ER is unclear. However, in a 2000 study by Harty *et al*, it was found that prolonged ER residence by mutant proteins such as mutant yeast pheromone precursor prepro-α-factor can lead to O-mannosyl modifications that may protect the mutant protein by blocking its retrotanslocation into the cytosol via Sec61 and thus preventing its degradation (Harty 2001). A similar study looked at the effects of O-mannosylation of pre-pro α factor and found that O-mannosylation solubalizes mutant proteins making them less dependent on ER chaperone proteins and allows their exocytosis thereby reducing ER load (Nakatsukasa 2004).

Given that SDF2L1 has some homology to the POMTs and O-mannosylation can potentially affect the fate of some proteins in the ER (at least in yeast) I examined if mutant proinsulin is O-mannosylated and if so is does this involve SDF2L1. GFP-tagged mutant proinsulin produced by proinsulin C96Y-GFP cells contains Ser and Thr residues, although not in clusters, which can be potential targets for O-mannosylation.

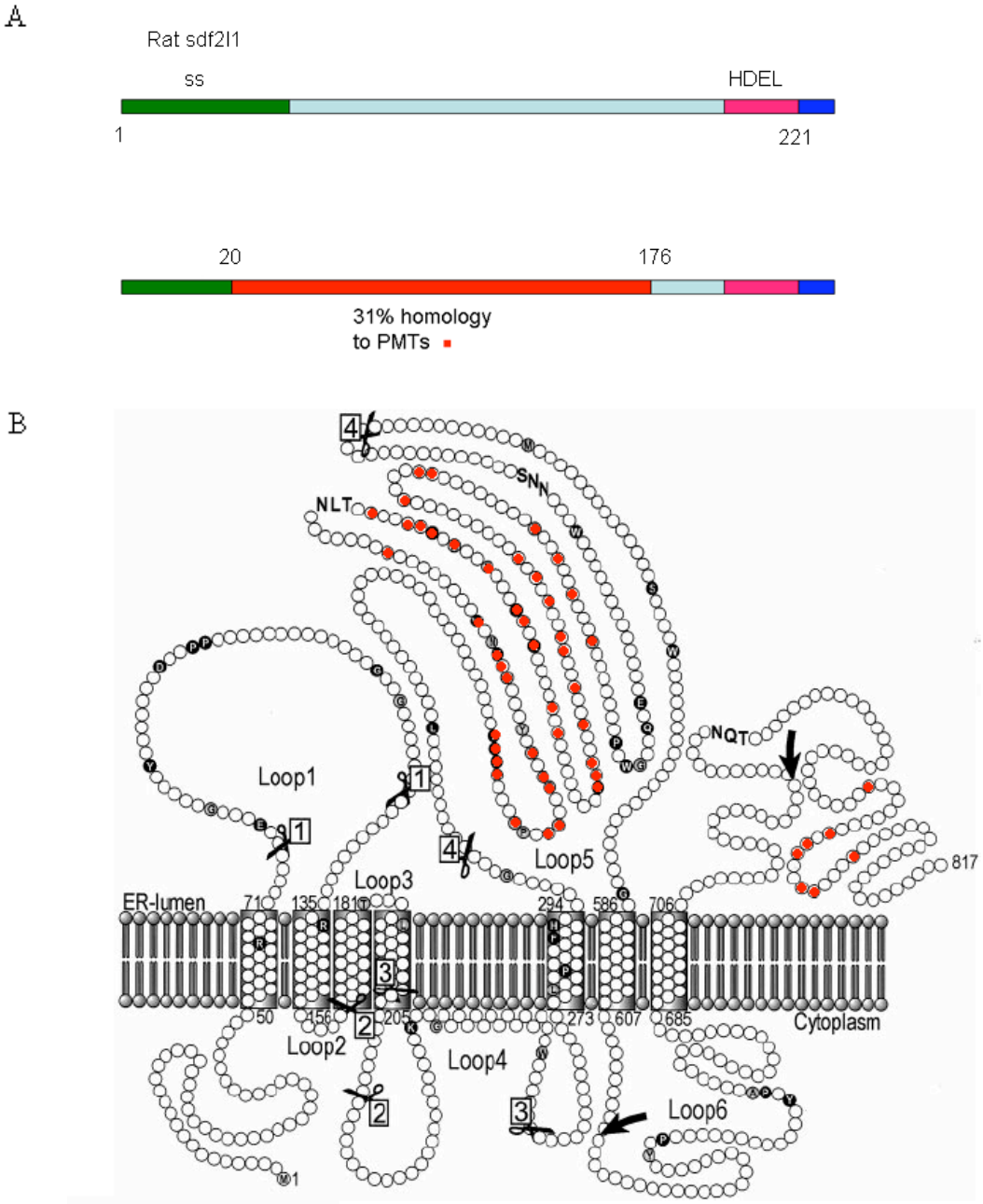

Figure 6.1: The homology of SDF2L1 with Protein O-mannosyltransferase in *Sachromyces Cerevisiae*. SDF2L1 protein contains 31% homology to *Sc*Pmt1p as determined by Pubmed Homologene (**A**). *Sc*Pmt1p is an intergral ER membrane glycoprotein with seven transmembrane-spanning domains. Its N-terminal faces the cytoplasm while the C-terminal faces the ER lumen. Two major hydrophilic domains Loop 1 and Loop 5 are oriented towards the lumen and are essential for the protein O-mannosyltransferase activity. The red dots correspond to *Sc*Pmt1p amino acids homologous to SDF2L1 (Willer 2003). There is an overall 31% identity between *Sc*Pmt1p and SDF2L1 in the hydrophilic region (Loop 5) (**B**).

5.01.2 Results & Discussion

I first examined if GFP-tagged mutant proinsulin is O-mannosylated. Proinsulin C96Y-GFP cells were treated with dox for 24 h to induce abundant levels of mutant proinsulin. Following incubation, the cells were labeled with 1 mCi/mL ^{3}H-mannose for 90 min. The cells were then lysed and the mutant proinsulin was immunoprecipitated using α-GFP antibody. The pellet (P) samples were filtered and supernatant (SN) samples were TCA precipitated then filtered to insure that only proteins present in the supernatant are being examined. Following filtration, the filters were allowed to air dry before addition of the liquid scintillation cocktail and radioactivity measurement by liquid scinitillation (N=2). The SN samples of both the GFP and the IgG control conditions show ^{3}H-mannose incorporation in the cellular proteins. However, when examining the pellets, both the GFP pellet and the IgG pellet had no incorporation of the ^{3}H-mannose in the immunoprecipitate pellet (**Figure 6.2 A, B**). As shown previously (**Figure 4.1**) the GFP antibody is able to efficiently precipitate mutant proinsulin, thus if the mutant insulin was mannosylated this should theoretically be detected. Thus, these results suggest that the mutant proinsulin did not incorporate any ^{3}H-mannose and thus is likely not O-mannosylated, although examining a positive control protein that should be O-mannosylated would strengthen this conclusion.

Since O-mannosylation of mutant proinsulin was not detected I did not test the effect of SDF2L1 knock-down. Indeed, it is unlikely that SDF2L1 will have O-mannosyltransferase activity since the MIR domain is also found in other proteins (inositol 1,4,5-trisphosphate (IP3) receptors, ryanodine receptors (Ryr), SDF-2 (Berridge 2002; Schott 2010). However, this domain may provide SDF2L1 with a potential binding site for glycosylated proteins.

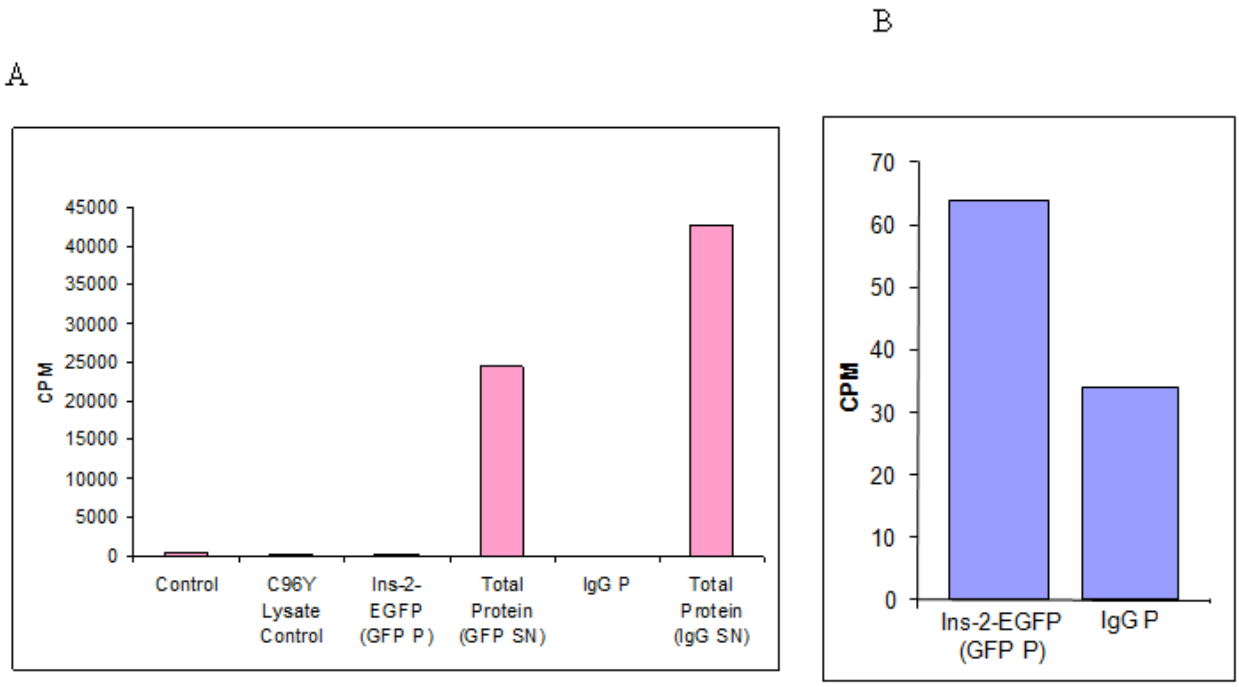

Figure 6.2: The incorporation of ^{3}H-Mannose in mutant proinsulin compared to other cellular proteins. Proinsulin C96Y-GFP cells were treated with dox for 24 h. Following treatment, the cells were incubated with 1 mCi/mL ^{3}H-mannose for 90 min at 37°C then lysed. The lysates were incubated with either 5µg α-GFP or 5µg mouse IgG antibodies. Samples were subjected to immunoprecipitation with Protein G dynabeads; pellet (P) and supernatant (SN) fractions were obtained. The P samples were filtered and SN samples were first TCA precipitated then filtered. The filters were air dried before the addition of LS cocktail and radioactivity measurement with a scintillation counter (N=1) (**A**). The CPM values for the pellet fractions only are shown (**B**).

6.02 Production of the protein A-SDF2L1 #7 Cell Line

This section will briefly outline the procedure for the production of the pA-SDF2L1 #7 cell line, which was used to produce protein-A tagged SDF2L1 fusion protein. A previous graduate student, Taila Hartley, cloned rat SDF2L1 (without signal sequence and without HDEL) cDNA into the pA-IRES vector obtained from Dr. James Rini, University of Toronto, Canada) (**Figure 6.3**).

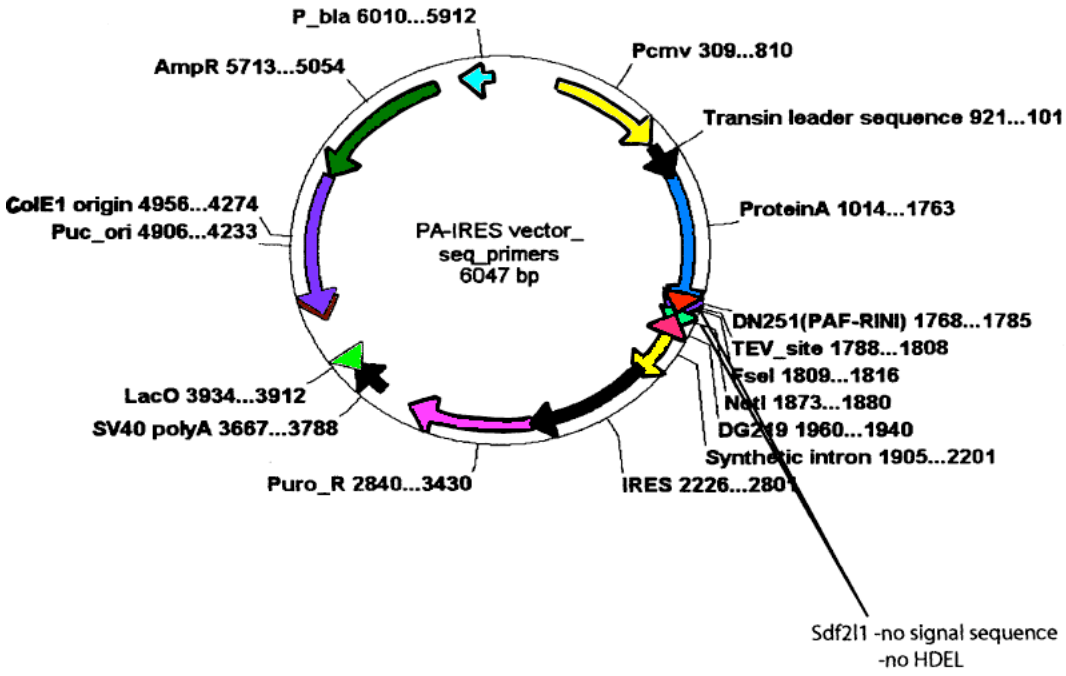

Figure 6.3: protein A-IRES vector obtained from Dr. J. Rini. Rat SDF2L1 (without a signal sequence and without the C-terminal HDEL endoplasmic reticulum retrieval signal) was cloned downstream and in frame with Protein A, which contains a transin signal sequence that allows for targeting to the secretory pathway. A Tev protease site is present between the protein A and SDF2L1.

HEK293 cells were transiently transfected with pA-IRES-SDF2L1 (without signal sequence or HDEL retention sequence) vector to confirm expression of the fusion protein in these cells. Following transfection, cells lysates were immunoblotted with antibodies to SDF2L1 and protein A and a prominent band was detected (**Figure 6.4**). To generate stably expressing lines HEK293 cells were transfected with pA-IRES-SDF2L1 via electroporation and cell lines were selected with 10 μg/μl puromycin. The total pool and individual clones were selected and analyzed by western blot using α-Protein A antibody (**Figure 6.5A**). Stable clones #7 and #4 were compared to the puramycin resistant pool and clone #7 was chosen for future studies since the pool also showed a band of unknown identity migrating at a higher MW (**Figure 6.5B**).

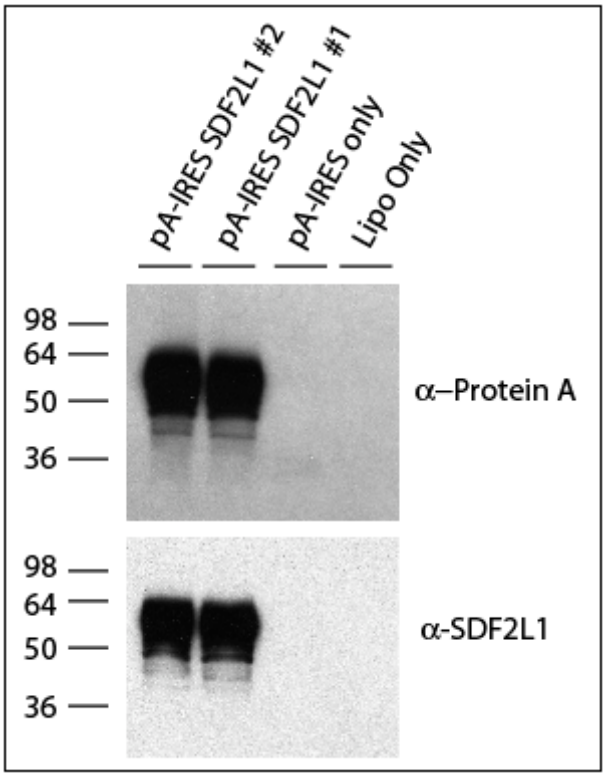

Figure 6.4: Testing transfection of pA-IRES-SDF2L1 vector in HEK293 cells. HEK293 cells were transiently transfected with pA-IRES-SDF2L1, control pA-IRES vector or with lipofectamine only as described in Methods 2.03. Following transfection, the cells were washed with PBS, lysed, and 10 μg of protein was resolved on SDS-PAGE and immunoblotted with α-protein A and α-SDF2L1 antibodies.

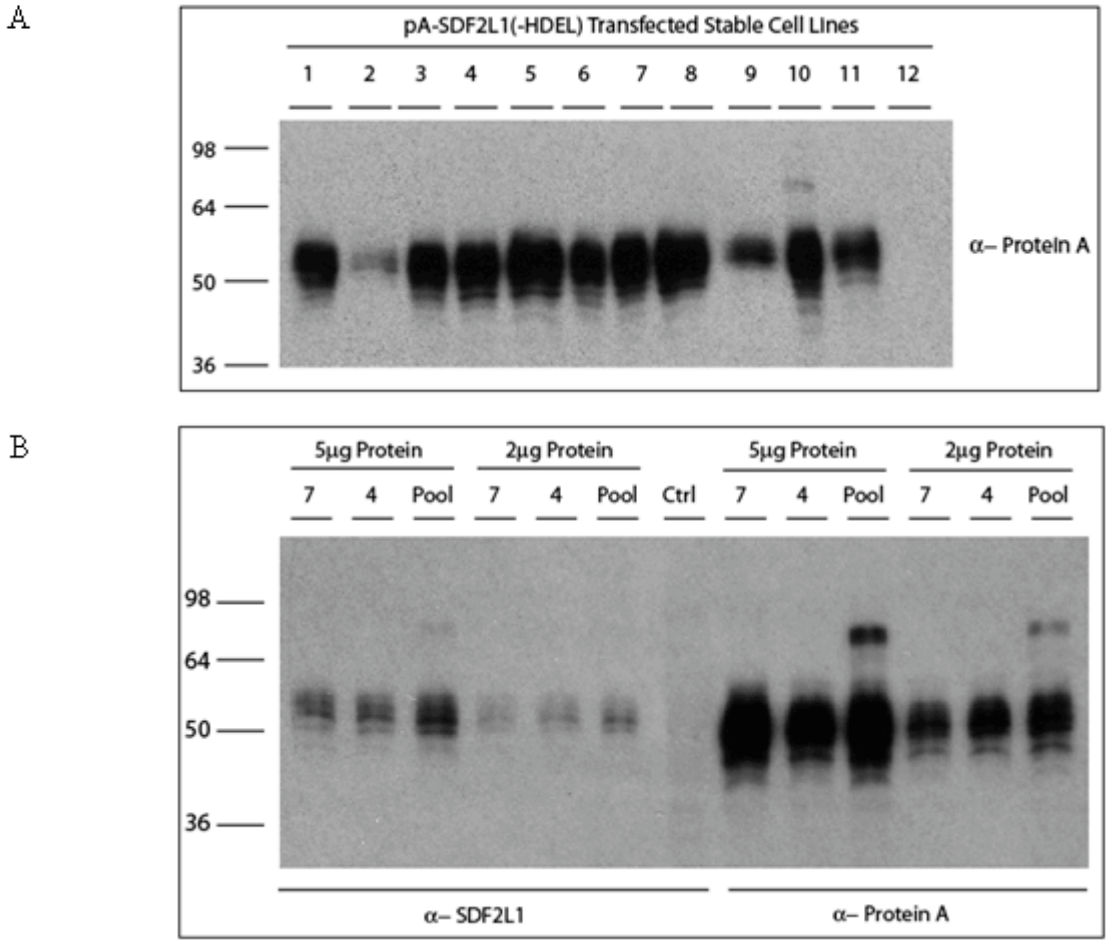

Figure 6.5: Generation of stable pA-SDF2L1 expressing HEK293 clonal cells. HEK293 cells were transfected with pA-IRES-SDF2L1#2 via electroporation. Stable clones were selected using 10 µg/µl puromycin, lysed, and equal amount of cell lysate were resolved by SDS-PAGE and immunoblotted with the α-Protein A antibody (**A**). The stable clones #7and #4 were compared with the puromycin-resistant pool. The clones #7, #4 and pool colonies were washed with PBS, lysed, and 5 µg and 2 µg protein was resolved by SDS-PAGE and immunoblotted with α-SDF2L1 and α-Protein A antibodies (**B**).

The SDF2L1 insert lacks an HDEL sequence, theoretically allowing SDF2L1 protein to be secreted from the cells. To test this pA-SDF2L1#7 cells were washed with PBS then incubated with KRBH buffer for 2 h. The media (SN) was subjected to tricholoacetic acid (TCA) protein precipitation. The TCA precipitates were boiled in 25 µl of 2X Laemmli sample buffer. Simultaneously, the cells were lysed and all the samples were resolved on SDS-PAGE and

immunoblotted for SDF2L1 and GM130 (**Figure 6.6A**). pA-SDF2L1 was detected in the media (SN) indicating that it is being secreted by the cells. Indeed, secretion of pA-SDF2L1 was very efficient, comparable to the secretion of some proteins that have crystallized by the Rini lab (protein A-tagged aminopeptidase N (APN) and protein A-tagged POFUT1) (results not shown).

Since the pA-SDF2L1 bands appeared as a smear I tested whether this was due to glycosylation of the pA-SDF2L1 fusion protein. To test this pA-SDF2L1#7 cells were treated with Tm (which inhibits N-linked glycosylation). As shown in **Figure 6.6 B**, when the cells are treated with Tm with both the SDF2L1 and the Protein A antibodies the band appears smaller in size and sharper. It is likely that the fusion protein is glycosylated on the protein A, since this protein has sites for N-linked glysosylation, which are not present in SDF2L1.

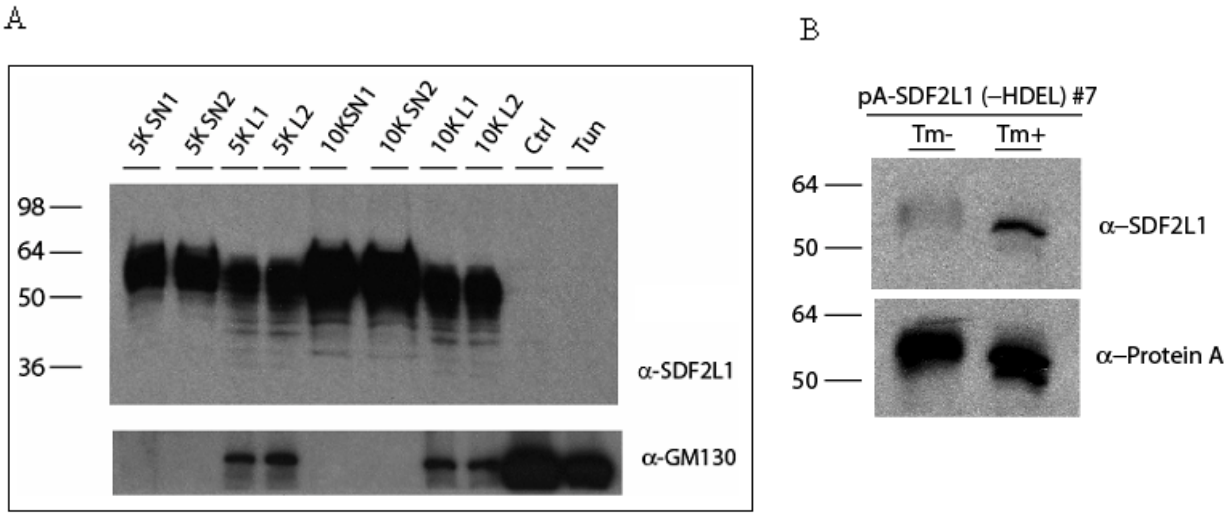

Figure 6.6: Protein A-tagged SDF2L1 production by pA-SDF2L1#7 cells. pA-SDF2L1#7 (5,000 or 10,000) cells were seeded in 12-well plates in duplicates. The cells were incubated with KRBH buffer for 2 h. The supernatant (SN) was subjected to TCA precipitation and the cells were lysed (L). The samples were resolved by 12% SDS-PAGE and immunoblotted with α-SDF2L1 and α-GM130 antibodies (**A**). pA-SDF2L1#7 cells were treated with 2μg/ml Tm for 16 h. Following treatment the cells were washed with PBS, lysed, and equal amounts of protein was resolved on 12% SDS-PAGE and immunoblotted for α-SDF2L1 and α-protein A antibodies (**B**).

It was important to determine if the protein-A tagged SDF2L1 can be efficiently immunoprecipitated for use in interaction studies. pA-SDF2L1#7 cell lysates were prepared and incubated overnight with Rabbit-IgG agarose or Protein A-agarose (control) beads and pellet and supernatant fractions were analyzed by Western blot using Protein-A antibody (**Figure 6.7 A**). The rabbit IgG pellet samples showed significant amount of protein-A tagged SDF2L1 immunoprecipitation as compared to control samples. This technique was further used to conduct binding assays discussed in section **4.02**.

Finally, also determined if SDF2L1 can be separated from the protein A using the TEV protease. pA-SDF2L1 was purified from media using rabbit IgG beads. The beads were then incubated overnight with TEV protease. The samples were then resolved on SDS-PAGE and immunoblotted for SDF2L1 and protein A (**Figure 6.7 B**). Liberated SDF2L1 was detected in the SN fractions, while protein A could only be detected in the pellet fractions. This cell line will be sent to Dr. J. Rini for structural analysis using small scale and large scale crystallography.

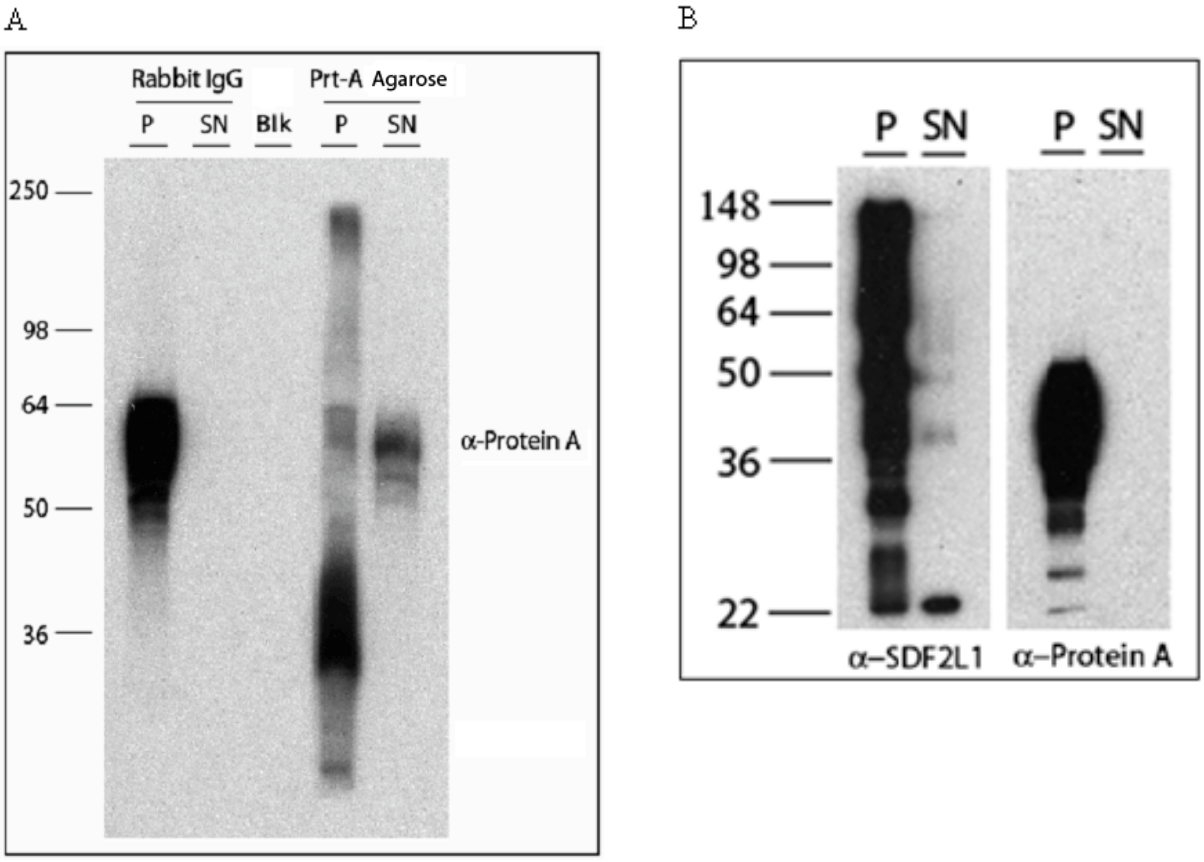

Figure 6.7: Immunoprecipitation of pA-SDF2L1. pA SDF2L1 (-HDEL) #7 cells were lysed and incubated overnight with Rabbit-IgG agarose or Protein A-agarose beads. Pellet and supernatant samples were analyzed with western blot using Protein-A antibody (**A**). Media from pA-SDF2L1 #7 cells was incubated overnight with 20 µL α-rabbit IgG-beads. The beads were then incubated with 20 µL of 0.3 mg/mL TEV in 50 mM Tris pH 8.0 and 50 mM NaCl + 0.3µL Aprotinin overnight. Samples were analyzed via western blot. Liberated SDF2L1 was detected in SN fraction (**B**).

6.03 Mass Spectrometry Data

To identify proteins that may be interacting with SDF2L1, a binding assay was conducted using liver tissue lysate and the samples were resolved on SDS-PAGE and Coomassie stained (**Methods 2.06**). The gel was then examined for bands present in the pA-SDF2L1 pellet and not in the protein A control pellet. Specific bands were excised from the gel and subjected to mass spectrometry (Advanced Protein Technology Centre SickKids). The excised bands can be

visualized in **Figure 6.8**. The mass spectrometry data was analyzed based on the number of unique peptides, protein identification probability and percent coverage. The mass spectrometry data can be made available upon request. No significant information was obtained regarding the bottom band (Black box). However, the top band (red box) showed a few ER related proteins that could potentially be interacting with the pA-SDF2L1 fusion protein. One of the proteins with high percentage coverage (the percentage of the band that corresponds to the suggested protein) was p97/VCP (**Figure 6.9**). As previously discussed, p97/VCP is member of the ERAD family, responsible for extraction of proteins from the ER membrane to the cytosol for proteosomal degradation. The interaction between SDF2L1 and the ERAD component was analyzed in Chapter 4.

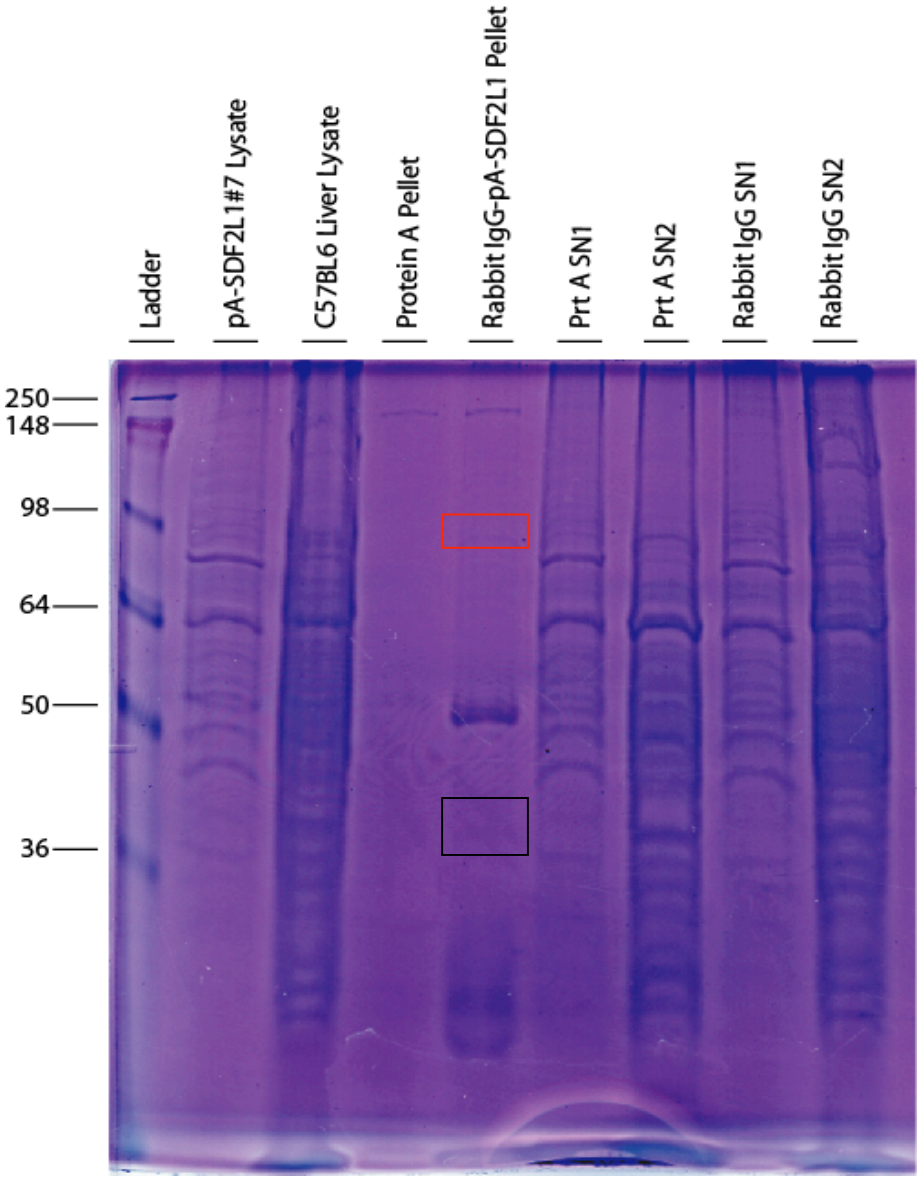

Figure 6.8: Mass Spectrometry Analysis of pA-SDF2L1 interacting proteins. pA-SDF2L1 was precipitated with rabbit IgG agarose beads. These beads or protein A agarose control beads were incubated with 200 µg protein lysate from mouse liver tissue. The pellet (P) and supernatant (SN) fractions were resolved by 12% SDS-PAGE and Coomassie Blue stained. The boxed bands were excised and sent for mass spectrometry analysis.

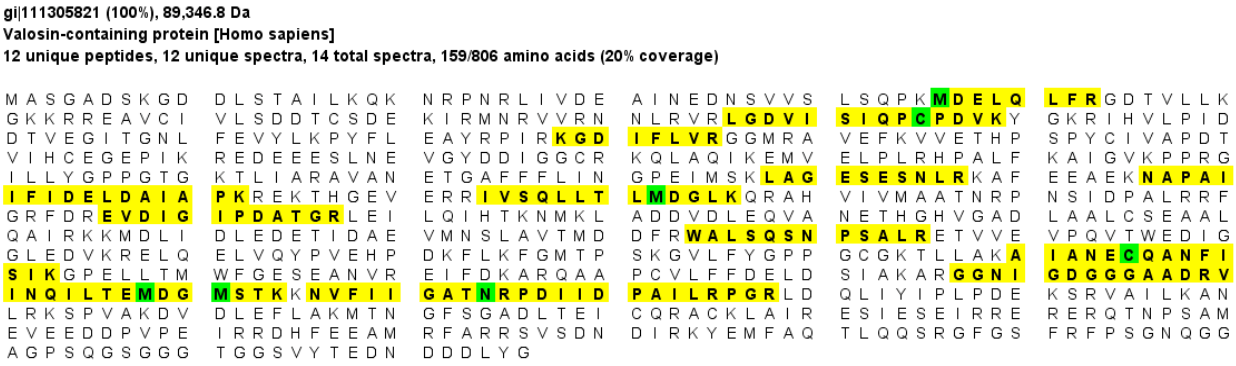

Figure 6.9: p97/VCP identified as potential SDF2L1-interacting protein. The mass spectrometry was analyzed for percentage coverage, protein identification probability and number of unique peptides, and p97/VCP was identified as a possible interacting protein with SDF2L1. The highlighted regions indicate the regions overlapping between the p97/VCP protein sequence and the sequence of the band present in the excised top band.